7. Nonlinear Heterodyne Detection

M. C. Teich

With 24 Figures

7.1 Two-Frequency Single-Photon Heterodyne Detection

Conventional heterodyne detection is useful in a number of configurations, including the detection of scattered or reflected radiation from a moving target (Doppler radar), communications, spectroscopy, and radiometry. Its use has been demonstrated in many regions of the electromagnetic spectrum including the radiowave, microwave, infrared, and optical. Its advantages as a detection technique are well known: high sensitivity, frequency selectivity, and strong directivity. For radar applications, it provides a major method of recovering desired signals and removing clutter. The significant improvement in sensitivity that it provides over direct detection arises from knowledge of the Doppler frequency (also called the heterodyne frequency or the intermediate frequency (IF)) which permits a narrow receiver bandwidth centered about the IF. In such applications, obtaining a reasonably high signal-to-noise ratio (SNR) requires 1) a good knowledge of the velocity of the source or target, 2) a stable yet tunable local oscillator, 3) a target or source which presents a minimum of frequency broadening and 4) at least several photons per measurement interval. These conditions are frequently not adhered to by actual systems, particularly in the infrared and optical, giving rise to detection capabilities which are well below optimum. In this chapter, we study the performance and requirements of a number of alternative heterodyne receiver configurations. In particular, we consider two basic systems which are intrinsically nonlinear, the first by virtue of the multiple-quantum detection process itself, and the second by virtue of the mixing configuration and the electronics following the detector.

After briefly reviewing conventional optical and infrared heterodyne detection, we examine the behavior of a multiphoton absorption heterodyne receiver. Expressions are obtained for the detector response, signal-to-noise ratio, and minimum detectable power for a number of cases of interest. Receiver performance is found to depend on the higher-order correlation functions of the radiation field and on the local oscillator irradiance. This technique may be useful in regions of the spectrum where high quantum efficiency detectors are not available since performance similar to that of the conventional unity quantum efficiency heterodyne receiver can theoretically be achieved. Practical problems which may make this difficult are discussed. A physical interpretation of the process in terms of the absorption of monochromatic and nonmonochromatic photons is given. The double-quantum case is treated in particular detail; the results of a preliminary experiment are presented and

M. C. Teich, "Nonlinear Heterodyne Detection," in Topics in Applied Physics, vol. 19, Optical and Infrared Detectors, edited by R. J. Keyes (Springer-Verlag, New York, 1st ed.: 1977; 2nd ed.: 1980), ch. 7, pp. 229-300.

suggestions for future experiments to ascertain the usefulness of the technique are provided.

We then investigate the operation and performance of a three-frequency nonlinear heterodyne system which eliminates some of the stringent conditions required for conventional heterodyne detection while maintaining its near-ideal SNR. The technique is similar to heterodyne radiometry, but carefully takes into consideration the effects of Doppler shift and signal statistics. It makes use of a two-frequency transmitter and a nonlinear second detector, and is particularly useful for signal acquisition; for signals of unknown Doppler shift, in fact, performance is generally superior to that of the conventional system because of a reduction in the effective noise bandwidth. While primary emphasis is on the infrared and optical because of the large Doppler shifts encountered there, application of the principle in the microwave and radiowave is also discussed. For cw radar and analog communications, the signal-to-noise, power spectral density, and minimum detectable power are obtained and compared with the standard configuration. Both sinewave and Gaussian input signals are treated. A variety of specific cases is discussed including the optimum performance case, the typical radar case, and the AM and FM communications case. The technique is shown to have similar advantages for pulsed radar and digital communications applications, both in the absence and in the presence of the lognormal atmospheric channel. Computer-generated error probability curves as a function of the input signal-to-noise ratio are presented for a variety of binary receiver parameters and configurations, and for various levels of atmospheric turbulence. Orthogonal and nonorthogonal signaling schemes, as well as dependent and independent fading, are considered.

In the last part of the chapter, we extend three-frequency nonlinear heterodyne mixing to n frequencies and examine the performance of a Doppler-insensitive radiometer that detects the radiation from known species moving with unknown velocities. Expressions for the signal-to-noise ratio and the minimum detectable total power are obtained for sinusoidal signals and for Gaussian signals with both Gaussian and Lorentzian spectra. In distinction to conventional heterodyning, knowledge of absolute line rest frequencies and a stable, tunable local oscillator are not required. This configuration may find use in the detection of certain remote species such as interstellar molecules and pollutants. A number of potential applications are examined. Finally, attention is drawn to a recently proposed variation of the technique, called heterodyne correlation radiometry, that incorporates a radiating sample of the species to be detected as part of the laboratory receiver. This configuration should be useful for the sensitive detection of species whose radiated energy is distributed over a large number of lines, with frequencies that are not necessarily known, when the Doppler shift is given.

M. C. Teich, "Nonlinear Heterodyne Detection," in Topics in Applied Physics, vol. 19, Optical and Infrared Detectors, edited by R. J. Keyes (Springer-Verlag, New York, 1st ed.: 1977; 2nd ed.: 1980), ch. 7, pp. 229-300.

Conventional photomixing in the infrared and optical is a useful detection technique for applications such as optical communications, spectroscopy, and radiometry, and it has been studied in great detail. The effect was first observed by *Forrester* et al. [7.1] in a classic experiment using two Zeeman components of a visible (incoherent) spectral line. With the development of the laser, photomixing became considerably easier to observe and was studied by *Javan* et al. [7.2] at 1.15 μm using a He–Ne laser, and by *Siegman* et al. [7.3] at 6943 Å with a ruby laser. Extending this work into the middle infrared, *Teich* et al. used a CO_2 laser at 10.6 μm in conjunction with a copper-doped germanium photoconductive detector operated at 4 K [7.4], and subsequently with a lead-tin selenide photovoltaic detector operated at 77 K [7.5].

The observed signal-to-noise power ratio for these experiments was found to behave in accordance with the theoretical expression obtained for parallel, plane-polarized beams incident on a quantum-noise-limited detector under ideal conditions [7.4–7], i.e.,

$$\mathrm{SNR}^{(1)} = \eta_1 P_1 / h\nu \Delta f. \tag{7.1}$$

Here, η_1 is the detector quantum efficiency (electrons/photon), P_1 is the received signal radiation power, $h\nu$ is the photon energy, and Δf is the receiver bandwidth. Heterodyne detection which is Johnson-noise rather than quantum-noise limited will be considered in Section 7.4.3. For radiation beams which are not parallel to within an angle $\theta = \lambda/d$, with d the detector aperture and λ the radiation wavelength, the SNR is reduced below the value given in (7.1) by spatial averaging of the mixing signal over the detector aperture. This effect was studied in detail by *Siegman* [7.7], and is often referred to as "washboarding". Similar calculations have been effected for focused radiation beams, first considered by *Read* and *Fried* [7.8]. Other factors must also be accounted for in a real system [7.8a]. Furthermore, it is clear that the signal-to-noise ratio is useful as a criterion only under certain conditions. *Jakeman* et al. [7.8b] have recently examined homodyne detection for signal detection and estimation experiments in which performance is more naturally linked to other measures such as error probability or various estimators.

Other experimental and theoretical studies focused on the statistical nature of the heterodyne signal resulting from the beating of a coherent wave with a Gaussian (scattered) wave [7.9, 10]. Although the stochastic nature of this signal was found to depend in detail on the irradiance statistics, the SNR turned out to be essentially independent of the higher-order correlation functions of the field [7.9, 10]. Furthermore, using the first-order coherent field results of *Titulaer* and *Glauber* [7.11] for absorption detectors, an explicit calculation for the case of two-beam photomixing showed that sum- and double-frequency components did not appear in the detected current, and that the heterodyne process could be interpreted in terms of the annihilation of a single (nonmonochromatic) photon

M. C. Teich, "Nonlinear Heterodyne Detection," in Topics in Applied Physics, vol. 19, Optical and Infrared Detectors, edited by R. J. Keyes (Springer-Verlag, New York, 1st ed.: 1977; 2nd ed.: 1980), ch. 7, pp. 229-300.

[7.12, 13] as was qualitatively appreciated by *Forrester* et al. [7.1]. A concise review of the basic theoretical and experimental aspects of heterodyne detection in the infrared and optical, as well as a partial review of the literature, was prepared by *Teich* in 1970 [7.14]. Recently, *Mandel* and *Wolf* [7.15] used geometrical and statistical arguments to show that an optimum receiver area exists for conventional heterodyne detection; this result complements *Siegman*'s antenna theorem [7.7], according to which the product of the receiver area and the angular field of view is of the order of the wavelength λ squared. A number of authors have also examined the photon counting statistics of the superposition of coherent and chaotic signal components, with the same or different mean frequencies [7.15a–15f]. In short, conventional optical heterodyne detection is well understood both theoretically and experimentally, and is a highly useful technique from a practical point of view.

7.2 Two-Frequency Multiphoton Heterodyne Detection

Since multiple-quantum optical direct detection has also been studied in great detail, it seems natural to investigate the behavior of such a detector in the presence of more than one frequency [7.16]. In this section, we obtain the response and the signal-to-noise power ratio (SNR) for a multiple-quantum absorption heterodyne receiver, with particular attention devoted to the simplest case, i.e., the mixing of two waves in a double-quantum infrared or optical device.

After briefly considering the relevant results pertinent to multiple-quantum direct detection (Sec. 7.2.1), we derive the combination device response for the general multiple-quantum photomixing process (including the important two-quantum case) in Section 7.2.2. In Section 7.2.3, we obtain the SNR for a receiver using a multiphoton optical heterodyne device, and compare it with the SNR for conventional optical heterodyne detection. The results of a two-photon experiment are presented in Section 7.2.4, while a suggested setup for future experiments, as well as the applicability of the scheme in general, is reserved for Section 7.2.5.

7.2.1 Multiple-Quantum Direct Detection

The ordinary photoeffect was discovered by *Hertz* in 1887 and explained in terms of the absorption of a single quantum of light by *Einstein* in his now famous work published in 1905 [7.17]. It was not until 1959, however, that the relationship between the statistics of an arbitrary incident radiation field and the emitted photoelectrons was firmly established by *Mandel* [7.18]. Consideration of the general photodetection process in terms of quantum-electrodynamic coherent states of the radiation field was undertaken by *Glauber* [7.19] in 1963, and by *Kelley* and *Kleiner* [7.20] in 1964, and provides a convenient starting point for calculations involving multiple-photon as well as single-photon absorptions.

Multiple-quantum photoemission, being a higher-order effect, is most easily observed in the absence of ordinary (first-order) photoemission. For the two-

M. C. Teich, "Nonlinear Heterodyne Detection," in Topics in Applied Physics, vol. 19, Optical and Infrared Detectors, edited by R. J. Keyes (Springer-Verlag, New York, 1st ed.: 1977; 2nd ed.: 1980), ch. 7, pp. 229-300.

quantum case, it becomes important when

$$\tfrac{1}{2}H < h\nu < H, \tag{7.2}$$

where $h\nu$ is the photon energy of the incident radiation, and H is the work function of the material under consideration. (Even when (7.2) is satisfied, however, it should be kept in mind that small amounts of single-quantum photoemission can arise from excited electrons in the Fermi tail [7.21].) The two-quantum photoeffect was first experimentally observed in 1964. Using a GaAs laser, *Teich* et al. [7.22] observed the effect in sodium metal, while *Sonnenberg* et al. [7.23] induced it in Cs_3Sb with a Nd-doped glass laser. Since that time, there have been a number of experimental measurements of second- and higher-order photoelectric yields in a variety of materials [7.24–28].

Theoretical work has focused on two aspects of the problem: perturbation theory and other calculations of the transition probabilities in the material, and the effect on the transition probability of the statistical nature of the radiation field. *Makinson* and *Buckingham* [7.29] were the first to predict the second-order effect and calculate its magnitude based on a surface model of photoemission; this work was expanded by *Smith* [7.30], *Bowers* [7.31], and *Adawi* [7.32]. The analogous volume calculation was performed by *Bloch* [7.33] and later corrected by *Teich* and *Wolga* [7.24, 25].

All of the models predict a two-quantum dc photocurrent $W_{dc}^{(2)}$ (expressed in amperes) proportional to the square of the incident radiation power P and inversely proportional to the irradiated area A. Using the results of a number of authors [7.24, 25, 30–33], we can therefore write the double-quantum dc photocurrent as

$$W_{dc}^{(2)} = \Lambda^{(2)}(\lambda, T)P \propto IP. \tag{7.3}$$

Here $\Lambda^{(2)}$ is the two-quantum yield expressed in amperes/watt [7.8], λ is the radiation wavelength, T is the sample temperature, P is the radiation power expressed in watts, and I is the irradiance at the detector expressed in watts/cm^2. The two-quantum efficiency (electrons/photon) is denoted by η_2, and is related to the two-quantum yield by the relationship

$$\Lambda^{(2)} = (e/h\nu)\eta_2 \propto I. \tag{7.4}$$

Here, the quantity $(h\nu/e)$ is the incident photon energy expressed in eV and is of order unity. For the k-photon process, defining $W_{dc}^{(k)}$, $\Lambda^{(k)}$, and η_k as the k-photon analogs of the quantities defined above, the following generalized results are obtained:

$$W_{dc}^{(k)} = \Lambda^{(k)}(\lambda, T)P \propto I^{k-1}P \tag{7.5}$$

and

$$\Lambda^{(k)} = (e/h\nu)\eta_k \propto I^{k-1}. \tag{7.6}$$

Typical numerical values for the two-quantum yield are [7.25] $\Lambda_{Na}^{(2)}$ (8450 Å, 300 K) $\sim 8 \times 10^{-16} I$ and $\Lambda_{Cs_3Sb}^{(2)}$ (10600 Å, 300 K) $\sim 5 \times 10^{-11} I$ amperes/watt. Again I represents the irradiance at the detector in watts/cm^2. These values, even

M. C. Teich, "Nonlinear Heterodyne Detection," in Topics in Applied Physics, vol. 19, Optical and Infrared Detectors, edited by R. J. Keyes (Springer-Verlag, New York, 1st ed.: 1977; 2nd ed.: 1980), ch. 7, pp. 229-300.

when precisely measured, can vary by a factor (usually $\leqq 2$) depending on the coherence properties of the inducing radiation, as we now consider.

Theoretical work relating to multiple-quantum statistical effects began in 1966 with an examination of the higher-order field correlation functions by *Teich* and *Wolga* [7.34] and by *Lambropoulos* et al. [7.35]. This was followed by more detailed calculations by *Mollow* [7.36] and by *Agarwal* [7.37]. All of these studies predicted a factor of $k!$ enhancement for the magnitude of certain k-quantum processes induced by chaotic (rather than coherent) sources. This enhancement was later observed in the two-quantum photoeffect by *Shiga* and *Imamura* [7.26], and in second harmonic generation (SHG) by *Teich* et al. [7.38]. The theoretical relationship between two-quantum photocurrent spectra and the incident radiation statistics was then obtained by *Diament* and *Teich* [7.39], and compared with the analogous single-quantum results previously given by *Freed* and *Haus* [7.40]. In 1969, two-quantum photocounting distributions were calculated for amplitude-stabilized, chaotic, and generalized laser sources by *Teich* and *Diament* [7.41]. This work was extended to higher-order photocounting distributions by *Barashev* in 1970 [7.42], who also wrote a comprehensive review article on multiple-quantum photoemission and photostatistics in 1972 [7.43]. Detailed calculations of the generalized higher-order photocounting statistics have also been reported by *Peřina* et al. [7.15e].

7.2.2 Theory of Multiphoton Photomixing

We begin this section by considering a two-quantum absorption detector initially in the ground state. The detector response $W^{(2)}$ at the space-time point $x_a = r_a, t_a$ may be written in terms of the second-order correlation function $G^{(2)}$ [7.19, 34, 36, 41], and is given by

$$W^{(2)} \propto \mathrm{tr}\{\varrho E^-(x_a)E^-(x_a)E^+(x_a)E^+(x_a)\} \equiv G^{(2)}(x_a x_a x_a x_a). \tag{7.7}$$

Here, ϱ is the density operator for the field, and E^- and E^+ represent the negative- and positive-frequency portions of the electric field operator E, respectively. We assume that the final state of the detector is much broader than the bandwidth of the incident radiation, and that a broad band of final states is accessible [7.36, 37].

If we specifically consider the mixing of two single-mode, amplitude-stabilized, first-order coherent waves, both of which are well collimated, parallel, plane polarized along a common unit vector, and normally incident onto a photosensitive material, we may write the positive portion of the electric field operator E^+ as the superposition of two scalar fields

$$E^+ = \varepsilon_1^0 e^{-i\omega_1 t} + \varepsilon_2^0 e^{-i\omega_2 t} \tag{7.8}$$

with angular frequencies ω_1 and ω_2. This is equivalent to assuming a semiclassical approach which makes use of the analytic signal [7.44]. The complex wave amplitude ε_i^0 can be expressed in terms of its absolute magnitude

M. C. Teich, "Nonlinear Heterodyne Detection," in Topics in Applied Physics, vol. 19, Optical and Infrared Detectors, edited by R. J. Keyes (Springer-Verlag, New York, 1st ed.: 1977; 2nd ed.: 1980), ch. 7, pp. 229-300.

$|\varepsilon_i^0|$ and a phase factor $\exp(i\alpha_i)$ such that

$$\begin{aligned}\varepsilon_i^0 &= |\varepsilon_1^0|\, e^{i\alpha} \\ \varepsilon_2^0 &= |\varepsilon_2^0|\, e^{i\beta}.\end{aligned} \tag{7.9}$$

Under these conditions, the quantum-statistical detector responses can be written in terms of the fields as

$$\mathrm{tr}\{\varrho E^- E^+\} \Rightarrow |\varepsilon_1^0|^2 + |\varepsilon_2^0|^2 + 2|\varepsilon_1^0|\,|\varepsilon_2^0| \cos[(\omega_1 - \omega_2)t + (\beta - \alpha)] \tag{7.10}$$

and

$$\begin{aligned}&\mathrm{tr}\{\varrho E^- E^- E^+ E^+\} \\ &\quad \Rightarrow \{|\varepsilon_1^0|^2 + |\varepsilon_2^0|^2 + 2|\varepsilon_1^0|\,|\varepsilon_2^0| \cos[(\omega_1 - \omega_2)t + (\beta - \alpha)]\}^2 .\end{aligned} \tag{7.11}$$

These expressions are scalar quantities and contain no spatial dependence because of the assumptions of plane polarization, parallel beams, and normal incidence.

Generalizing these results to sinusoidal beam photomixing in which the k-photon detector response is the normally ordered product [7.19]

$$W^{(k)} \propto \mathrm{tr}\{\varrho[E^-(x_a)]^k [E^+(x_a)]^k\}, \tag{7.12}$$

and using the binomial theorem leads to a heterodyne signal given by

$$\begin{aligned}W^{(k)} = \zeta_k \{ &\{|\varepsilon_1^0|^2 + |\varepsilon_2^0|^2\}^k \\ &+ \binom{k}{1}\{|\varepsilon_1^0|^2 + |\varepsilon_2^0|^2\}^{k-1}\{2|\varepsilon_1^0|\,|\varepsilon_2^0| \cos[(\omega_1 - \omega_2)t + (\beta - \alpha)]\} \\ &+ \binom{k}{2}\{|\varepsilon_1^0|^2 + |\varepsilon_2^0|^2\}^{k-2}\{2|\varepsilon_1^0|\,|\varepsilon_2^0| \cos[(\omega_1 - \omega_2)t + (\beta - \alpha)]\}^2 + \ldots + \\ &+ \binom{k}{r}\{|\varepsilon_1^0|^2 + |\varepsilon_2^0|^2\}^{k-r}\{2|\varepsilon_1^0|\,|\varepsilon_2^0| \cos[(\omega_1 - \omega_2)t + (\beta - \alpha)]\}^r + \ldots + \\ &+ \{2|\varepsilon_1^0|\,|\varepsilon_2^0| \cos[(\omega_1 - \omega_2)t + (\beta - \alpha)]\}^k \}.\end{aligned} \tag{7.13}$$

Here ζ_k represents a proportionality constant for the k-photon process. The leading dc terms are proportional to $|\varepsilon_1^0|^{2k}$ and $|\varepsilon_2^0|^{2k}$, and may be associated with the absorption of k monochromatic photons, each of which arises from a given beam (1 and 2, respectively). The highest frequency current component is proportional to $|\varepsilon_1^0|^k |\varepsilon_2^0|^k \cos[k(\omega_1 - \omega_2)t + \phi]$, and corresponds to the absorption of k nonmonochromatic photons, each of which must be associated with both of the beams. It is evident from the above that multiple- and sum-frequency terms do not appear in the k-photon absorption heterodyne detector output, in analogy with the result for the one-quantum case [7.12–14].

Inserting the constants ζ for the one- and two-quantum cases in (7.13) above, the detector responses for coherent signal mixing are, respectively,

$$W^{(1)} = \zeta_1 \{|\varepsilon_1^0|^2 + |\varepsilon_2^0|^2 + 2|\varepsilon_1^0|\,|\varepsilon_2^0| \cos[(\omega_1 - \omega_2)t + (\beta - \alpha)]\} \tag{7.14}$$

and

$$\begin{aligned}W^{(2)} = \zeta_2 \{ &|\varepsilon_1^0|^4 + |\varepsilon_2^0|^4 + 2|\varepsilon_1^0|^2\,|\varepsilon_2^0|^2 + 4|\varepsilon_1^0|^3\,|\varepsilon_2^0| \cos[(\omega_1 - \omega_2)t + (\beta - \alpha)] \\ &+ 4|\varepsilon_1^0|\,|\varepsilon_2^0|^3 \cos[(\omega_1 - \omega_2)t + (\beta - \alpha)] \\ &+ 4|\varepsilon_1^0|^2\,|\varepsilon_2^0|^2 \cos^2[(\omega_1 - \omega_2)t + (\beta - \alpha)]\}.\end{aligned} \tag{7.15}$$

M. C. Teich, "Nonlinear Heterodyne Detection," in Topics in Applied Physics, vol. 19, Optical and Infrared Detectors, edited by R. J. Keyes (Springer-Verlag, New York, 1st ed.: 1977; 2nd ed.: 1980), ch. 7, pp. 229-300.

Using the double-angle formula for the last term in (7.15), $W^{(2)}$ may also be written as

$$W^{(2)} = \zeta_2\{|\varepsilon_1^0|^4 + |\varepsilon_2^0|^4 + 4|\varepsilon_1^0|^2\,|\varepsilon_2^0|^2 + 4|\varepsilon_1^0|^3\,|\varepsilon_2^0|\cos[(\omega_1-\omega_2)t+(\beta-\alpha)] + 4|\varepsilon_1^0|\,|\varepsilon_2^0|^3\cos[(\omega_1-\omega_2)t+(\beta-\alpha)] + 2|\varepsilon_1^0|^2\,|\varepsilon_2^0|^2\cos[2(\omega_1-\omega_2)t+2(\beta-\alpha)]\}, \tag{7.16}$$

when this $\cos^2$ term is present. As noted previously, double- and sum-frequency terms are absent.

It is not difficult to associate various second-order correlation functions $G^{(2)}(x_a x_b x_c x_d) \equiv [abcd]$ with (7.15). (When two beams are present, we must consider a space-time point for each of the beams so that the index in $G^{(2)}$ takes on two values [7.34].) Thus, the first term, $|\varepsilon_1^0|^4$, may be associated with [1111], the second with [2222], the third with [1221] and [2112], the fourth with the four permutations of [1112], the fifth with the four permutations of [2221], and the sixth with the four permutations of [1212], with $b \neq c$. The coefficient of each term in (7.15) is therefore equal to the number of permutations in the appropriate form of the correlation function for that term. The physical interpretation follows immediately: the first two dc terms in (7.15) arise from the absorption of two monochromatic photons, both from the same beam. The third dc term, which exists in two permutations with $b=c$, arises from the two ways in which two single monochromatic photons can be absorbed, one from each beam. The fourth and fifth terms correspond to the absorption of a single monochromatic photon from one of the beams plus a single nonmonochromatic photon which must be associated with both beams. These terms therefore contribute currents at the difference frequency $(\omega_1-\omega_2)$, in analogy with the single-quantum heterodyne interference term [7.12–14]. The final term corresponds to the absorption of two nonmonochromatic photons, and therefore varies at double the difference frequency, i.e., at $2(\omega_1-\omega_2)$; clearly there is no analogous process possible in the one-quantum case.

We note that the absorption of two nonmonochromatic photons imparts an additional dc value to the double-difference-frequency term, as may be seen by comparing (7.15) and (7.16). This additional term, of magnitude $2|\varepsilon_1^0|^2\,|\varepsilon_2^0|^2$, appears in the presence of double-quantum photomixing; in the absence of such photomixing, we must obtain $W^{(2)}$ from (7.15) and *not* from (7.16). In this latter case, the detector response reduces to the previously obtained result [7.34]

$$W^{(2)}(\text{mixing absent}) = \zeta_2(|\varepsilon_1^0|^4 + |\varepsilon_2^0|^4 + 2|\varepsilon_1^0|^2\,|\varepsilon_2^0|^2) = \zeta_2'(I_1+I_2)^2, \tag{7.17}$$

where I_i represents the intensity of the ith beam and ζ_2' is a new proportionality constant.

The results presented above can be expanded to modulated, noncoherent, and nonparallel beam mixing. As an example, we consider two ideal amplitude-stabilized nonparallel $(\theta > \lambda/d)$ plane traveling waves impinging on a two-quantum detector, so that washboarding can occur. In contrast to the one-quantum case, the detector responds to the *square* of this spatiotemporal

M. C. Teich, "Nonlinear Heterodyne Detection," in Topics in Applied Physics, vol. 19, Optical and Infrared Detectors, edited by R. J. Keyes (Springer-Verlag, New York, 1st ed.: 1977; 2nd ed.: 1980), ch. 7, pp. 229-300.

intensity variation, resulting in a factor of 2 enhancement in the dc cross term, as obtained with pure temporal mixing. Thus, the two-quantum dc photocurrent will in general be enhanced due to spatiotemporal intensity variations (interference fringes); the magnitude of this enhancement depends on the system configuration. Experimental evidence for two-quantum enhancement due to spatial variations has, in fact, been provided by *Shiga* and *Imamura* [7.26] and by *Teich* et al. [7.38].

As a final example, we consider mixing due to radiation which is nonsinusoidal (i.e., not coherent to all orders). We consider two parallel, plane-polarized normally incident superimposed beams of radiation from the same chaotic source, one of which is a time-delayed version of the other (delay τ_δ) entering one double-quantum detector. This was previously shown to be equivalent to a self-integrating Hanbury-Brown–Twiss device [7.34]. For a thermal source in the absence of a beat signal, we find

$$W^{(2)}(\text{mixing absent}) = 2\zeta_2'(I_1^2 + 2I_1I_2 + I_2^2),\ \tau_\delta < \tau_c \tag{7.18}$$

and

$$W^{(2)}(\text{mixing absent}) = 2\zeta_2'(I_1^2 + I_1I_2 + I_2^2),\ \tau_\delta > \tau_c, \tag{7.19}$$

where τ_c is the coherence time of the source. For $\tau_\delta < \tau_c$, (7.18) represents the enhancement of both the single-beam and the mixed-beam counting rates, arising from the tendency of these photons to arrive in correlated pairs (assuming that the detector intermediate state lifetime $\tau_1 \ll \tau_c$). For $\tau_\delta > \tau_c$, however, there is no correlation between the arrival time of a photon from one beam and the arrival time of a photon from the other. Thus, the absorption of two photons from a single beam is enhanced by a factor of 2 relative to the absorption of one photon from each beam, leading to a cross term of 1. This can also be qualitatively understood from the point of view of additive Gaussian fields; the sum of two fully correlated Gaussian random processes ($\tau_\delta < \tau_c$) has a greater variance than that of two independent Gaussian random processes ($\tau_\delta > \tau_c$) leading to an enhanced value for the cross term when $\tau_\delta < \tau_c$. An arrangement to observe spatial effects of a similar type has also been proposed [7.44a].

From the foregoing, it is clear that the double-quantum current can be calculated for a variety of configurations involving different relative time scales, angular separations, polarization properties, and statistical characteristics. Some additional examples are treated in [7.34]. Clearly, the second-order correlation functions of the field play an important role in determining the magnitude of the signal, in distinction to the one-quantum case.

7.2.3 Signal-to-Noise Ratio and Minimum Detectable Number of Photons

We now follow the usual procedure used for the single-quantum case [7.4–6, 10] to calculate the approximate SNR for k-photon sinusoidal heterodyne detection. We begin with two-quantum photomixing, neglecting the double-difference-frequency component and assuming that the ac signal is at the fundamental-

M. C. Teich, "Nonlinear Heterodyne Detection," in Topics in Applied Physics, vol. 19, Optical and Infrared Detectors, edited by R. J. Keyes (Springer-Verlag, New York, 1st ed.: 1977; 2nd ed.: 1980), ch. 7, pp. 229-300.

difference-frequency (IF) between the two waves. Thus, considering the mixing of two parallel, coherent waves as described earlier, (7.16) yields

$$W_{\mathrm{IF}}^{(2)} = 4\zeta_2(|\varepsilon_1^0|^3\,|\varepsilon_2^0| + |\varepsilon_1^0|\,|\varepsilon_2^0|^3)\cos[(\omega_1-\omega_2)t+(\beta-\alpha)] \tag{7.20}$$

and

$$W_{\mathrm{dc}}^{(2)} = \zeta_2(|\varepsilon_1^0|^4 + |\varepsilon_2^0|^4 + 4|\varepsilon_1^0|^2\,|\varepsilon_2^0|^2), \tag{7.21}$$

so that

$$W^{(2)} = \left\{1 + \frac{4(|\varepsilon_1^0|^3\,|\varepsilon_2^0| + |\varepsilon_1^0|\,|\varepsilon_2^0|^3)\cos[(\omega_1-\omega_2)t+(\beta-\alpha)]}{|\varepsilon_1^0|^4 + |\varepsilon_2^0|^4 + 4|\varepsilon_1^0|^2\,|\varepsilon_2^0|^2}\right\} W_{\mathrm{dc}}^{(2)}. \tag{7.22}$$

We now assume that one of the waves (which we call the local oscillator or LO) is strong, i.e., $E_2 \gg E_1$, in which case

$$W_{\mathrm{IF}}^{(2)} \simeq 4(|\varepsilon_1^0|/|\varepsilon_2^0|)W_{\mathrm{dc}}^{(2)}\cos[(\omega_1-\omega_2)t+(\beta-\alpha)] \tag{7.23}$$

and

$$\langle[W_{\mathrm{IF}}^{(2)}]^2\rangle \simeq 8(|\varepsilon_1^0|^2/|\varepsilon_2^0|^2)[W_{\mathrm{dc}}^{(2)}]^2. \tag{7.24}$$

The noise power can be obtained from the two-quantum photocurrent spectrum [7.39] which, in turn, is related to the stochastic nature of the radiation source. For a coherent and strong LO, however, the k-quantum counting statistics will be Poisson [7.41, 42], and the two-quantum (shot) noise power is then

$$\langle[W_{\mathrm{n}}^{(2)}]^2\rangle = 2e[W_{\mathrm{dc}}^{(2)}]\Delta f. \tag{7.25}$$

Thus, using (7.3), (7.24), and (7.25), the two-quantum SNR can be written as

$$\mathrm{SNR}^{(2)} \simeq \frac{4P_1}{e\Delta f}\left[\frac{W_{\mathrm{dc}}^{(2)}}{P_2}\right] = \frac{4P_1}{e\Delta f}\Lambda^{(2)}. \tag{7.26}$$

Using the relationship between the two-quantum yield $\Lambda^{(2)}$ and the two-quantum efficiency η_2 given in (7.4), we finally obtain

$$\mathrm{SNR}^{(2)} \simeq 4\eta_2 P_1/h\nu\Delta f. \tag{7.27}$$

We recall from (7.4) that η_2 is itself proportional to the irradiance of the LO, and we must have $4\eta_2 < 1$. The result is therefore similar to that for the single-quantum heterodyne detector given in (7.1); in that case, however, η_1 is independent of the LO. The two-quantum minimum detectable power (MDP) [7.4, 5] therefore becomes

$$\mathrm{MDP}^{(2)} \simeq h\nu\Delta f/4\eta_2. \tag{7.28}$$

This corresponds to a minimum number of photons $\mathcal{N}_{\mathrm{min}}^{(2)}$, detectable in the resolution time of the receiver $[\tau_r \sim (\Delta f)^{-1}]$, given by

$$\mathcal{N}_{\mathrm{min}}^{(2)} \simeq (4\eta_2)^{-1}. \tag{7.29}$$

In contradistinction to the single-quantum case, performance is not limited by the detector (single) quantum efficiency since η_2 may be increased by increasing

M. C. Teich, "Nonlinear Heterodyne Detection," in Topics in Applied Physics, vol. 19, Optical and Infrared Detectors, edited by R. J. Keyes (Springer-Verlag, New York, 1st ed.: 1977; 2nd ed.: 1980), ch. 7, pp. 229-300.

the LO irradiance. This technique may therefore be useful in regions of the electromagnetic spectrum where detectors with high (single) quantum efficiency are not available.

We note that the SNR at the double-difference-frequency, corresponding to the absorption of two nonmonochromatic photons, is reduced by the factor (P_1/P_2). Clearly, using methods similar to those presented above and in [7.34] and [7.10], we can obtain analogous SNR expressions for photomixing with nonsinusoidal beams.

The SNR at the fundamental-difference-frequency $(\omega_1 - \omega_2)$ may also be obtained for coherent beam mixing in the k-photon absorption heterodyne detector. Following a series of steps similar to those given above, we find

$$\mathrm{SNR}^{(k)} \simeq c_k \eta_k P_1 / h\nu \Delta f , \tag{7.30}$$

$$\mathrm{MDP}^{(k)} \simeq h\nu \Delta f / c_k \eta_k , \tag{7.31}$$

and

$$\mathscr{N}_{\min}^{(k)} \simeq (c_k \eta_k)^{-1} , \tag{7.32}$$

where c_k is a constant (dependent on k), and η_k is proportional to I^{k-1}, where I is the LO irradiance [see (7.6)]. Here $c_k \eta_k < 1$.

7.2.4 Experiment

In this section we describe a preliminary set of experiments in which double-quantum photoemission was observed from a sodium surface simultaneously illuminated by two superimposed beams of laser radiation. While ac photomixing terms were not observed in these experiments, the measurements are consistent with the theoretical calculations given in Section 7.2.2.

The apparatus used for the experimental measurement of two-quantum photomixing is shown in the block diagram of Fig. 7.1. The radiation source was a pulsed GaAs multimode semiconductor injection laser operated at 77 K and emitting a peak radiation power of 400 mW at about 8450 Å. Mode shifts due to laser heating occurred during the pulse duration, which was about 35 μs. The radiation was collimated by a 10-cm focal length lens, passed through an iris and then through a configuration of dielectric beam splitters and antireflection coated prisms resembling a Mach-Zender interferometer. The beam splitters were approximately 2/3 transmitting and were flat only to about 1 wavelength; the optical phase across the beam could therefore be considered to vary. The purpose of the interferometer configuration was to allow the irradiance of each beam (denoted as 1 and 2) to be independently controlled by means of calibrated attenuating filters. Beam 1 could also be time delayed with respect to beam 2 by means of a sliding prism (see Fig. 7.1), but this capability was not important in these experiments where τ_s was always greater than τ_c due to the very small value of τ_c. After passing through a second iris and a (6-cm focal length) focusing lens, the radiation was allowed to impinge on a specially constructed Na-surface photomultiplier tube, which has been described previously [7.22, 24, 25]. A Polaroid type HN-7 sheet polarizer was almost always placed at the front face of the photomultiplier as shown in Fig. 7.1 (the one exception will be noted later). The electron-multiplied current was passed through a 1-MΩ load resistor which fed a Princeton Applied Research (PAR) low-noise preamplifier followed by a PAR lock-in amplifier. Phase-sensitive detection was performed as 2.2 kHz, which is the fundamental repetition frequency of the pulsed

M. C. Teich, "Nonlinear Heterodyne Detection," in Topics in Applied Physics, vol. 19, Optical and Infrared Detectors, edited by R. J. Keyes (Springer-Verlag, New York, 1st ed.: 1977; 2nd ed.: 1980), ch. 7, pp. 229-300.

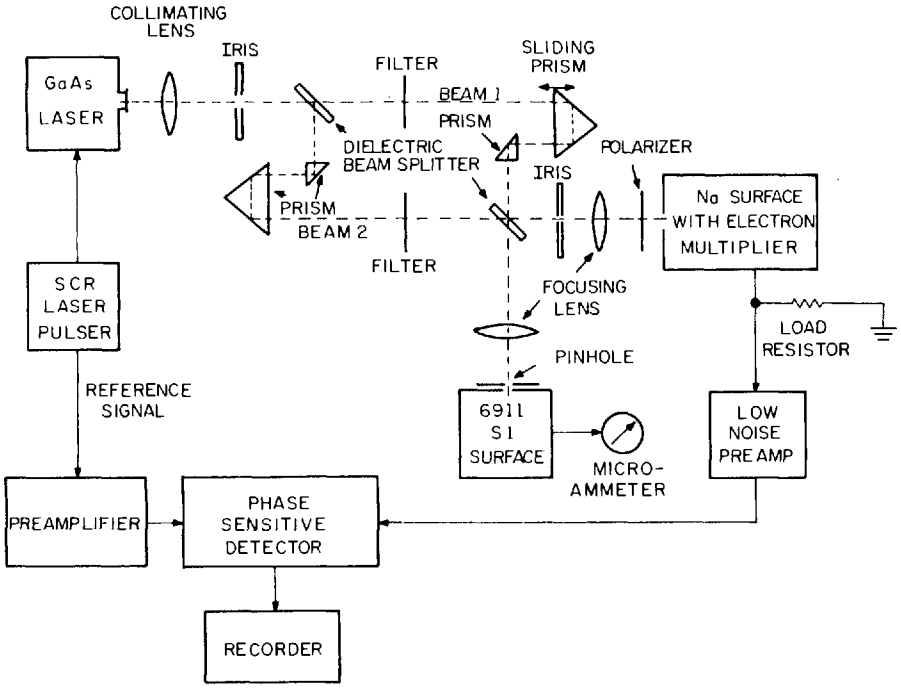

Fig. 7.1. Block diagram of the double-quantum photomixing experimental arrangement

laser output. Large integration times were used so that only the dc or average value of this current component was measured. The reference signal for the lock-in amplifier was obtained directly from the silicon-controlled-rectifier power supply [7.45] used to drive the laser.

Radiation from the other leg of the interferometer was focused onto a 25-μm diameter pinhole which acted as an aperture stop at the face of a standard Dumont 6911 type S–1 photomultiplier. This provided a relatively accurate method for superimposing the two beams [7.24]. This is critical since the double-quantum response is inversely proportional to the illuminated area A. The beams were adjusted to achieve maximum output from the 6911 photomultiplier tube, a procedure which was often difficult and required a great deal of care.

The following procedure was used in making a measurement: 1) The beams were aligned to provide maximum current from the 6911 photomultiplier. 2) Beam 1 was blocked and the double-quantum current $\overline{W_2^{(2)}}$ from beam 2 was maximized by imaging the laser junction on the sodium surface, and then recorded. Using a calibrated attenuating filter, it was ascertained that pure two-quantum emission was occurring, i.e., that $\overline{W_2^{(2)}} \propto I_2^2$, where I_2 represents the irradiance of beam 2. 3) Beam 2 was blocked and the double-quantum current from beam 1 was recorded, after verifying that it was $\propto I_1^2$. (The constant of proportionality was taken to be the same in both cases.) 4) Both beams were then unblocked and, after once again verifying that pure double-quantum emission was occurring, the total average double-quantum current $\overline{W^{(2)}}$ (at the fundamental repetition frequency of 2.2 kHz) was recorded.

Experiments were performed with different values of I_1/I_2, obtained by attenuating one of the beams relative to the other by means of thin gelatin (Kodak Wratten) filters. Ordinary glass filters could not be used to provide the decrements of light intensity because refraction in the glass caused the imaged spot size and position to change thus altering the two-quantum current in an unpredictable way.

M. C. Teich, "Nonlinear Heterodyne Detection," in Topics in Applied Physics, vol. 19, Optical and Infrared Detectors, edited by R. J. Keyes (Springer-Verlag, New York, 1st ed.: 1977; 2nd ed.: 1980), ch. 7, pp. 229-300.

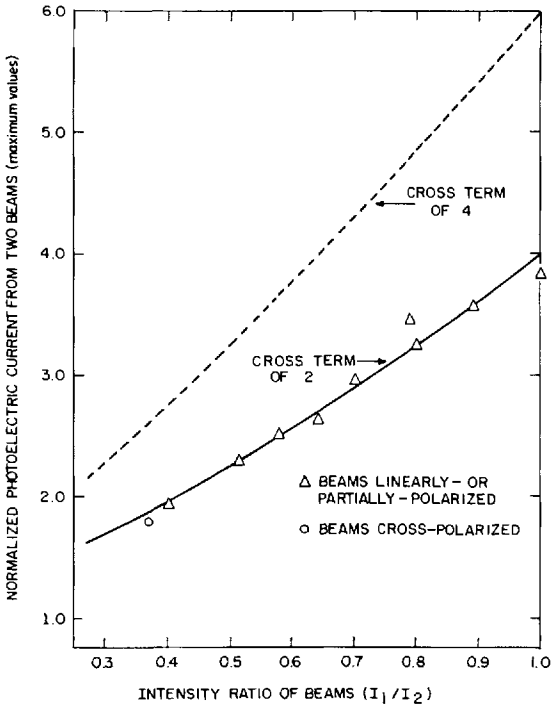

Fig. 7.2. The average double-quantum photocurrent from two beams (maximum values) vs the intensity ratio of the beams

The total average fundamental-repetition-frequency two-quantum photoelectric current $\overline{W^{(2)}}$, for different intensity ratios of the two constituent beams (I_1/I_2), is presented in Fig. 7.2. The solid curve represents the equation $W^{(2)} \propto (I_1 + I_2)^2$ which is simply the parabola $(1 + I_1/I_2)^2$ when the intensity I_2 is normalized to unity. This represents a cross term of $2I_1I_2$, and is so labeled. The cross term of $4I_1I_2$, on the other hand, is shown by the dashed line in Fig. 7.2. Only the highest observed values of $\overline{W^{(2)}}$ are plotted in Fig. 7.2, many more points having been found to lie below the curves. This has been attributed to the difficulty in obtaining precise alignment of the two radiation beams, and therefore superposition of the focused spots on the sodium surface.

The triangles in Fig. 7.2 represent data for linearly or partially polarized radiation, while the circle is for cross-polarized radiation (this is the one exception mentioned previously). The experimental measurements are consistent with the following interpretation. The laser output consists of a number of more-or-less independent Fabry-Perot modes which are changing during the pulse width due to heating of the laser junction [7.24]. The radiation may therefore be considered to behave as a Gaussian source with a coherence time $\tau_c \sim (\Delta\nu)^{-1} \sim 10^{-13}$ s. Since the intermediate-state lifetime for the double-quantum sodium photodetector is much shorter than the radiation coherence time, the irradiance fluctuations result in a factor of 2 enhancement of the single-beam photocurrents. As far as the irradiance cross-term is concerned,

M. C. Teich, "Nonlinear Heterodyne Detection," in Topics in Applied Physics, vol. 19, Optical and Infrared Detectors, edited by R. J. Keyes (Springer-Verlag, New York, 1st ed.: 1977; 2nd ed.: 1980), ch. 7, pp. 229-300.

the two-quantum current will also be enhanced by a factor of 2 owing to the random spatial irradiance fluctuations across the detector for the superimposed beams. Thus, we obtain a relative cross term of 2, i.e., $\overline{W^{(2)}} \propto I_1^2 + 2I_1 I_2 + I_2^2$, in agreement with the data.

7.2.5 Discussion

From the foregoing, it is clear that multiple-quantum heterodyne detection is somewhat more complex than the analogous single-quantum process. In particular, the average detector response and the SNR are found to depend on the higher-order correlation functions of the radiation field and on the LO irradiance. From a physical point of view, it has been possible to associate various terms in the detected current with specific kinds of photon absorptions. Calculations of the SNR and MDP for a number of cases have been carried out. The results of a preliminary two-quantum photomixing experiment are in agreement with the theory.

Although it appears that the k-photon heterodyne detector can be made to perform as well as or better than the single-photon heterodyne detector by simply increasing the LO intensity, a number of practical problems would likely make this difficult. In as much as the transition probabilities decrease rapidly as k is increased, and are furthermore proportional to A^{1-k}, it appears that very high LO intensities would be required to place η_k anywhere in the vicinity of 0.1 for $k > 2$. Aside from alignment problems, these high intensities could result in thermionic emission from cathode heating, or possibly cathode damage.

The two-quantum case is therefore likely to be the most interesting, and also the easiest to examine experimentally. A possible arrangement for studying the effect in a more detailed and controlled fashion is the following. The radiation from a 0.5 mW He-Ne laser, operating at a wavelength of 1.15 μm, is passed through an acoustooptic modulator (which splits it into two frequencies) and a focusing lens. A 5 μm focused spot size, corresponding to an area of 2.5×10^{-7} cm^2, would then provide an incident irradiance $I \sim 2 \times 10^3$ W/cm^2. Using a Cs_3Sb photocathode with a work function ~ 2.05 eV and a yield [7.23] $\sim 5 \times 10^{-11}\, I$ amperes/watt, a two-quantum current $\sim 5 \times 10^{-11}$ amperes may then be obtained. An experiment of this nature would allow the validity of (7.15), (7.16), and (7.27) to be examined. A YAG:Nd laser could be substituted for the He-Ne laser for an even simpler experimental configuration, since focusing would not then be required.

Although the emphasis in this section has been on linearly polarized incident radiation, considerable enhancement of the k-quantum photocurrent may occur for circularly (or elliptically) polarized radiation, as recently discussed by a number of authors [7.46]. We note that information relating to the intermediate-state lifetime of the detector (τ_1) can be obtained by measuring the two-quantum detector output for various values of τ_c.

M. C. Teich, "Nonlinear Heterodyne Detection," in Topics in Applied Physics, vol. 19, Optical and Infrared Detectors, edited by R. J. Keyes (Springer-Verlag, New York, 1st ed.: 1977; 2nd ed.: 1980), ch. 7, pp. 229-300.

Finally, we observe that the use of a two-quantum photomixer in a three-frequency nonlinear heterodyne detection receiver would result in a reduction of the SNR by the factor (P_1/P_2), corresponding to the absorption of 2 nonmonochromatic photons as discussed earlier. It therefore does not appear to be suitable for this application. The next section is devoted to a discussion of the three-frequency technique, but using a single-photon detector, in which case the nonlinearity is derived from a circuit element rather than from a multiphoton process and the (undesirable) reduction factor does not appear.

7.3 Three-Frequency Single-Photon Heterodyne Detection Using a Nonlinear Device

The extension of conventional microwave heterodyne techniques into the infrared and visible, and the attendant increase in the Doppler shift by many orders of magnitude for a target of a given velocity, has provided improved target resolution capabilities [7.47], but there have been attendant difficulties as indicated previously. If the radial velocity of a target or the frequency difference between the transmitter and LO in a communications system has not been established, for example, then the heterodyne frequency is not known and it may be very difficult indeed to acquire a weak signal using the standard single- or multiphoton heterodyne technique. An unknown IF necessitates the use of broad bandwidth detection and electronics, resulting in a degraded signal-to-noise ratio, or perhaps the use of frequency scanning of the receiver or of the LO. The rate of such scanning is of course limited by the time response of the system. In order that the heterodyne signal remain within the electrical passband of the system, furthermore, the LO frequency must be relatively stable with reference to the signal frequency, and yet tunable so that it can track the Doppler shift, which varies in time. These various difficulties are more acute in the infrared and optical where large values of the IF are encountered (Doppler shift is proportional to the radiation frequency).

In this section we discuss the operation of a three-frequency single-photon nonlinear heterodyne detection scheme useful for cw and pulsed radar, and for analog and digital communications. The concept, which is similar to heterodyne radiometry, was first proposed in 1969 by *Teich* [7.48], and experimentally examined in 1972 by *Abrams* and *White* [7.49]. Applications for the system have since been studied in detail from a theoretical point of view [7.50–52]. The system appears to provide the near-ideal SNR offered by conventional heterodyne detection, while eliminating some of the difficulties discussed above. It often obviates the need for high-frequency electronics, improving impedance matching, system noise figure, and range of operation over the conventional case.

The usual frequency scanning is eliminated as is the necessity for a stable LO. And, it allows targets to be continuously observed with Doppler shifts of

M. C. Teich, "Nonlinear Heterodyne Detection," in Topics in Applied Physics, vol. 19, Optical and Infrared Detectors, edited by R. J. Keyes (Springer-Verlag, New York, 1st ed.: 1977; 2nd ed.: 1980), ch. 7, pp. 229-300.

considerably greater magnitude and range than previously possible. This is particularly important in the infrared and optical, where Doppler shifts are generally large [7.47], and the importance of this technique is expected to be emphasized in these regions. Furthermore, it is possible for the three-frequency system to have a higher output SNR than the conventional system by providing a reduced noise bandwidth, as we will show later.

As defined by our usage in this section, the designation "nonlinear" refers to the electronics following the detector, and not to the process itself, which could be referred to as nonlinear in any case since it involves mixing or multiplication. This is again a different kind of nonlinearity than that discussed previously in Section 7.2. In this system, two signals of a small, but well-known difference frequency $\Delta\nu$ are transmitted. With the LO frequency f_L, we then have a three-frequency mixing system. Aside from the heterodyne mixer, a nonlinear element such as a square-law device is included to provide an output signal at a frequency very close to $\Delta\nu$ regardless of the Doppler shift of the transmitted signals.

The over-all system configuration is presented in Section 7.3.1. In Sections 7.3.2, 7.3.3, and 7.3.4, we consider applications of the system to a cw radar with sinewave, Gaussian/Gaussian, and Gaussian/Lorentzian input signals, respectively. Section 7.3.5 deals with its use in an analog communications system, whereas Section 7.3.6 is concerned with low-frequency applications of the technique. A numerical example in Section 7.3.7 is followed by evaluations of system performance for binary communications and pulsed radar in the vacuum channel (Sec. 7.3.8) and in the lognormal atmospheric channel (Sec. 7.3.9). A discussion is presented in Section 7.3.10. The main results are expressed as the output SNR for the system in terms of the input SNR.

7.3.1 System Configuration

In Fig. 7.3, we present a block diagram for a radar version of the system. A transmitter emits two waves of frequencies f_1 and f_2 whose difference $f_c = |f_1 - f_2| = \Delta\nu$ is known to high accuracy. (This is particularly easy to accomplish if the transmitter is a two-mode laser, since the modes tend to drift together keeping f_c constant, or if it is a single-frequency laser modulated into two frequency components.) The waves are Doppler shifted by the moving target, the nature of which is unimportant. Thus, a wave of frequency f will return with a frequency f' given by the standard nonrelativistic Doppler-shift formula

$$f' = f(1 \pm 2v_{||}/c), \tag{7.33}$$

where $v_{||}$ is the radial velocity of the target and c is the speed of light. Therefore, after scattering from the target, and choosing $f_1 > f_2$, the new frequency difference between the two waves f_c' is given by

$$f_c' = |f_1' - f_2'| = f_c \pm (2v_{||}/c) f_c . \tag{7.34}$$

M. C. Teich, "Nonlinear Heterodyne Detection," in Topics in Applied Physics, vol. 19, Optical and Infrared Detectors, edited by R. J. Keyes (Springer-Verlag, New York, 1st ed.: 1977; 2nd ed.: 1980), ch. 7, pp. 229-300.

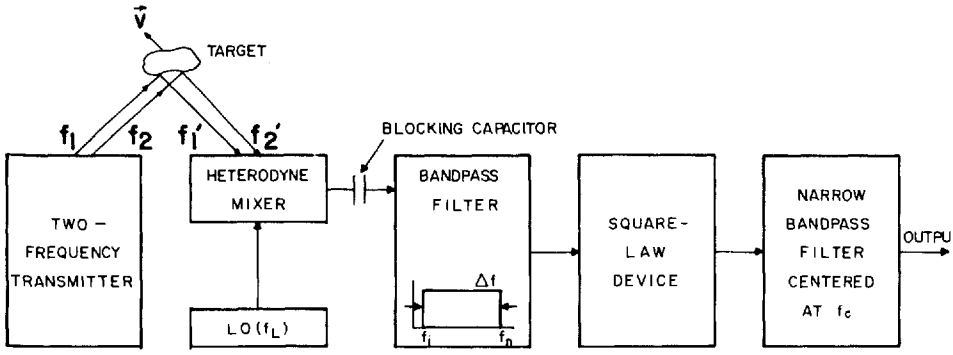

Fig. 7.3. Block diagram of the three-frequency nonlinear heterodyne system for radar application

Aside from the frequency shift which results from the Doppler effect, there may be a frequency broadening of each wave associated with the scattering by a moving target in a typical radar configuration. For a rotating target, this broadening is of the order $4R\omega_\perp/\lambda$, where R is the "radius" of the target, $\omega_\perp$ is its component of angular velocity perpendicular to the beam direction, and λ is the wavelength of the transmitted signal [7.9]. For practical systems, as will be shown later, the difference $f_c' - f_c$ may be made much smaller than the broadening effects and thereby neglected. We can therefore choose $f_c' = f_c$ with high accuracy.

The receiver includes a heterodyne mixer with an LO followed by a blocking capacitor and a bandpass filter with bandwidth $\Delta f = f_n - f_i$. Here f_n and f_i are the upper and lower cutoffs, respectively, of the bandpass filter. When Doppler information is poor (in which case the three-frequency system is particularly useful), Δf will be large so that it will cover a wide frequency range. In the following, we therefore pay particular attention to the case where $f_i \to 0$ so that $\Delta f = f_n$. The noise arising from the strong LO is assumed to be shot noise which, in the high current limit, becomes Gaussian as illustrated by *Davenport* and *Root* [7.53]. To good approximation, the spectrum may be taken to be white. The latter part of the receiver is a square-law (or other nonlinear) device and a narrow bandpass filter centered at frequency $f_c = |f_1 - f_2|$. The details of the system are given below.

The mixer consists of a photodetector and a local oscillator. We are interested in determining the signal-to-noise ratio at the output of the photodetector. The input electric field consists of three plane, parallel, coincident electromagnetic waves, which are assumed to be polarized and to impinge normally on the photodetector. Spatial first-order coherence is assumed over the detector aperture. The total incident electric field E_t may therefore be written as

$$E_t = A_1 \cos(\omega_1 t + \phi_1) + A_2 \cos(\omega_2 t + \phi_2) + A_L \cos(\omega_L t + \phi_L). \tag{7.35}$$

Here ω_1 and ω_2 are the angular frequencies of the two incoming signals (we have omitted the primes for simplicity), ϕ_1 and ϕ_2 are their phases, and ω_L is the

M. C. Teich, "Nonlinear Heterodyne Detection," in Topics in Applied Physics, vol. 19, Optical and Infrared Detectors, edited by R. J. Keyes (Springer-Verlag, New York, 1st ed.: 1977; 2nd ed.: 1980), ch. 7, pp. 229-300.

angular frequency of the LO beam. The quantities A_1, A_2, and A_L are the amplitudes of the three waves, all of which are assumed to have the same plane polarization. In the infrared and optical, the output of a photodetector or mixer is proportional to the total intensity of the incoming waves. Taking into account the quantum electrodynamics of photon absorption by optical and infrared detectors [7.10, 12–14], the output signal r consists only of difference-frequency terms and dc terms. Thus, for $f_L < f_1', f_2'$ or $f_L > f_1', f_2'$,

$$\begin{aligned} r = \beta\{&A_1^2 + A_2^2 + A_L^2 + 2A_1A_L\cos[(\omega_1 - \omega_L)t + (\phi_1 - \phi_L)] \\ &+ 2A_2A_L\cos[(\omega_2 - \omega_L)t + (\phi_2 - \phi_L)] \\ &+ 2A_1A_2\cos[(\omega_1 - \omega_2)t + (\phi_1 - \phi_2)]\}, \end{aligned} \tag{7.36}$$

where β is a proportionality constant containing the detector quantum efficiency. If the incident waves are not spatially first-order coherent and/or polarized in the same direction, the usual decrease in r will occur [7.5–8, 15].

Since the LO beam may be made much stronger than the two signal beams, i.e., $A_L \gg A_1, A_2$, we can write

$$\begin{aligned} r \simeq \beta A_L^2 \Bigg\{ &1 + \frac{2A_1}{A_L}\cos[(\omega_1 - \omega_L)t + (\phi_1 - \phi_L)] \\ &+ \frac{2A_2}{A_L}\cos[(\omega_2 - \omega_L)t + (\phi_2 - \phi_L)] \Bigg\}. \end{aligned} \tag{7.37}$$

The term containing $\omega_1 - \omega_2$ has been neglected because of its relatively small amplitude. We now define

$$r_{dc} \equiv \beta(A_1^2 + A_2^2 + A_L^2) \simeq \beta A_L^2, \tag{7.38a}$$

and

$$\begin{aligned} r_{IF} &\equiv 2\beta A_1A_L\cos[(\omega_1 - \omega_L)t + (\phi_1 - \phi_L)] \\ &\quad + 2\beta A_2A_L\cos[(\omega_2 - \omega_L)t + (\phi_2 - \phi_L)] \\ &= r_{dc}\Bigg\{\frac{2A_1}{A_L}\cos[(\omega_1 - \omega_L)t + (\phi_1 - \phi_L)] \\ &\quad + \frac{2A_2}{A_L}\cos[(\omega_2 - \omega_L)t + (\phi_2 - \phi_L)]\Bigg\}. \end{aligned} \tag{7.38b}$$

The mean-square photodetector response is then given by

$$\langle r_{IF}^2 \rangle = \left(\frac{2A_1^2}{A_L^2} + \frac{2A_2^2}{A_L^2}\right) r_{dc}^2 = 2r_{dc}^2 \frac{P_1 + P_2}{P_L}, \tag{7.39}$$

where P_1, P_2, and P_L are the radiation powers in the two signal beams and in the LO beam, respectively.

M. C. Teich, "Nonlinear Heterodyne Detection," in Topics in Applied Physics, vol. 19, Optical and Infrared Detectors, edited by R. J. Keyes (Springer-Verlag, New York, 1st ed.: 1977; 2nd ed.: 1980), ch. 7, pp. 229-300.

If we consider the noise response r_n of the detector as arising from shot noise, which is the case for the photoemitter and the ideal reverse-biased photodiode [7.5, 10, 14], the mean-square noise response is given by the well-known shot-noise formula [7.5, 54]

$$\langle r_n^2 \rangle = 2er_{dc}\Delta f, \tag{7.40}$$

in which Δf is the noise response bandwidth and is determined by the Doppler uncertainty, and e is the electronic charge. For a comparatively strong LO, we have

$$r_{dc} = \frac{\eta e}{hf_L} P_L, \tag{7.41}$$

where $\eta \equiv \eta_1$ is the quantum efficiency and h is Planck's constant.

From (7.39), (7.40), and (7.41), the signal-to-noise power ratio $(\mathrm{SNR})_{\mathrm{power}} \equiv \mathrm{SNR}^{(1)}$ is given by

$$(\mathrm{SNR})_{\mathrm{power}} = \frac{\langle r_{IF}^2 \rangle}{\langle r_n^2 \rangle} = \frac{\eta(P_1 + P_2)}{hf_L \Delta f}, \tag{7.42a}$$

which is seen to be independent of P_L. If we define $P_r \equiv P_1 + P_2$, and let $\nu = f_L \approx f_1 \approx f_2$, and $(\mathrm{SNR})_i = (\mathrm{SNR})_{\mathrm{power}}$, we obtain

$$(\mathrm{SNR})_i = \frac{\eta P_r}{h\nu \Delta f}. \tag{7.42b}$$

This is similar to (7.1), except that now P_r is the total input signal power. $(\mathrm{SNR})_i$ is referred to as the input signal-to-noise ratio to the square-law device following the photodetector.

By use of a blocking capacitor, the dc part of the photodetector response r_{dc} can be filtered out. The signal, which then has zero mean, is sent to a full-wave square-law device. If we let $s_a(t) = 2\beta A_1 A_L \cos[(\omega_1 - \omega_L)t + (\phi_1 - \phi_L)]$ and $s_b(t) = 2\beta A_2 A_L \cos[(\omega_2 - \omega_L)t + (\phi_2 - \phi_L)]$, and let $n(t)$ be the noise, then using a generalization of the "direct method" of *Davenport* and *Root* [7.55] for the sum of three signals, we can write the input to the square-law device $x(t)$ as

$$x(t) = s_a(t) + s_b(t) + n(t). \tag{7.43}$$

The output of the square-law device $y(t)$ is then given by

$$\begin{aligned} y(t) &= \alpha x^2(t) \\ &= \alpha[s_a^2(t) + s_b^2(t) + n^2(t) + 2s_a(t)s_b(t) \\ &\quad + 2s_a(t)n(t) + 2s_b(t)n(t)], \end{aligned} \tag{7.44}$$

M. C. Teich, "Nonlinear Heterodyne Detection," in Topics in Applied Physics, vol. 19, Optical and Infrared Detectors, edited by R. J. Keyes (Springer-Verlag, New York, 1st ed.: 1977; 2nd ed.: 1980), ch. 7, pp. 229-300.

where α is a scaling constant. For a stationary random process, the expectation value of $y(t)$ is

$$\begin{aligned} E(y) &= \alpha[E(s_a^2) + E(s_b^2) + E(n^2)] \\ &= \alpha(\sigma_a^2 + \sigma_b^2 + \sigma_n^2) \end{aligned} \tag{7.45}$$

for all t, where E denotes the expectation value. In (7.45), we have set $\sigma_a^2 = E(s_a^2)$, $\sigma_b^2 = E(s_b^2)$, and $\sigma_n^2 = E(n^2)$. Furthermore,

$$y^2(t) = \alpha^2[s_a(t) + s_b(t) + n(t)]^4, \tag{7.46}$$

from which the mean-square value of $y(t)$ is evaluated to be

$$\begin{aligned} E(y^2) = \alpha^2[&E(s_a^4) + E(s_b^4) + E(n^4) \\ &+ 6\sigma_a^2\sigma_b^2 + 6\sigma_a^2\sigma_n^2 + 6\sigma_b^2\sigma_n^2]. \end{aligned} \tag{7.47}$$

In obtaining (7.45) and (7.47), we have assumed that $s_a(t)$, $s_b(t)$, and $n(t)$ are all independent of each other, and that $E(s_a) = E(s_b) = E(n) = 0$.

The autocorrelation function of the output of the square-law device is

$$R_y(t_1, t_2) = E(y_1 y_2) = \alpha^2 E[(s_{a1} + s_{b1} + n_1)^2 (s_{a2} + s_{b2} + n_2)^2]. \tag{7.48}$$

For stationary processes, setting $\tau = t_1 - t_2$, we obtain

$$\begin{aligned} R_y(\tau) = &R_{a\times a}(\tau) + R_{b\times b}(\tau) + R_{n\times n}(\tau) + R_{a\times b}(\tau) \\ &+ R_{a\times n}(\tau) + R_{b\times n}(\tau), \end{aligned} \tag{7.49}$$

in which

$$R_{a\times a}(\tau) = \alpha^2 R_{a^2}(\tau), \tag{7.50a}$$

$$R_{b\times b}(\tau) = \alpha^2 R_{b^2}(\tau), \tag{7.50b}$$

$$R_{n\times n}(\tau) = \alpha^2 R_{n^2}(\tau), \tag{7.50c}$$

$$R_{a\times b}(\tau) = 4\alpha^2 R_a(\tau) R_b(\tau) + 2\alpha^2\sigma_a^2\sigma_b^2, \tag{7.50d}$$

$$R_{a\times n}(\tau) = 4\alpha^2 R_a(\tau) R_n(\tau) + 2\alpha^2\sigma_a^2\sigma_n^2, \tag{7.50e}$$

$$R_{b\times n}(\tau) = 4\alpha^2 R_b(\tau) R_n(\tau) + 2\alpha^2\sigma_b^2\sigma_n^2, \tag{7.50f}$$

with $R_{a^2}(\tau) = E(s_{a1}^2 s_{a2}^2)$, $R_a(\tau) = E(s_{a1} s_{a2})$, etc.

If we know the exact forms of these correlation functions, we can use the Fourier transform to obtain the power spectral density of the output which will, in turn, enable us to evaluate the final output signal-to-noise power ratio for the three-frequency system.

M. C. Teich, "Nonlinear Heterodyne Detection," in Topics in Applied Physics, vol. 19, Optical and Infrared Detectors, edited by R. J. Keyes (Springer-Verlag, New York, 1st ed.: 1977; 2nd ed.: 1980), ch. 7, pp. 229-300.

7.3.2 Application to cw Radar with Sinewave Input Signals

We now assume that the two inputs to the photodetector are pure sinusoidal waves with constant phase over the spatial extent of the photodetector. This would be the case, for example, when the combining beam splitting mirror is optically flat and all broadening effects may be neglected. We let $A_a = 2\beta A_1 A_L$, $A_b = 2\beta A_2 A_L$, $\omega_a = \omega_1 - \omega_L$, $\omega_b = \omega_2 - \omega_L$, $\phi_a = \phi_1 - \phi_L$, and $\phi_b = \phi_2 - \phi_L$. The signal input to the square-law device is then

$$\begin{aligned} s(t) &= s_a(t) + s_b(t) \\ &= A_a \cos(\omega_a t + \phi_a) + A_b \cos(\omega_b t + \phi_b) . \end{aligned} \tag{7.51}$$

The amplitudes A_a and A_b are in this case constant, and the phases ϕ_a and ϕ_b are taken to be random variables uniformly distributed over the interval $(0, 2\pi)$ and independent of each other. We easily obtain

$$\begin{aligned} R_a(\tau) &= E(s_{a1} s_{a2}) = A_a^2 E[\cos(\omega_a t_1 + \phi_a)\cos(\omega_a t_2 + \phi_a)] \\ &= \tfrac{1}{2} A_a^2 \cos\omega_a \tau , \end{aligned} \tag{7.52}$$

with $\tau = t_1 - t_2$. Similarly

$$R_b(\tau) = E(s_{b1} s_{b2}) = \tfrac{1}{2} A_b^2 \cos\omega_b \tau . \tag{7.53}$$

The total correlation function of the input signal $R_s(\tau)$ is the sum of the individual correlation functions

$$R_s(\tau) = R_a(\tau) + R_b(\tau) = \tfrac{1}{2} A_a^2 \cos\omega_a \tau + \tfrac{1}{2} A_b^2 \cos\omega_b \tau . \tag{7.54}$$

Taking the Fourier transform, we obtain the power spectral density for the input signal:

$$S_s(f) = \frac{A_a^2}{4}[\delta(f - f_a) + \delta(f + f_a)] + \frac{A_b^2}{4}[\delta(f - f_b) + \delta(f + f_b)] , \tag{7.55}$$

where $f_a = \omega_a/2\pi = f_1 - f_L$ and $f_b = \omega_b/2\pi = f_2 - f_L$. The shot noise arising from the strong LO is taken to be white Gaussian over the frequency band $[0, f_n]$. Thus, the noise spectrum is

$$S_n(f) = \begin{cases} N, & \text{for } 0 < |f| < f_n , \\ 0, & \text{elsewhere.} \end{cases} \tag{7.56}$$

The total input power spectral density $S_x(f)$ including the noise is shown in Fig. 7.4. We arbitrarily assume that $f_1 > f_2$ or $f_a > f_b$, and $A_b > A_a$.

M. C. Teich, "Nonlinear Heterodyne Detection," in Topics in Applied Physics, vol. 19, Optical and Infrared Detectors, edited by R. J. Keyes (Springer-Verlag, New York, 1st ed.: 1977; 2nd ed.: 1980), ch. 7, pp. 229-300.

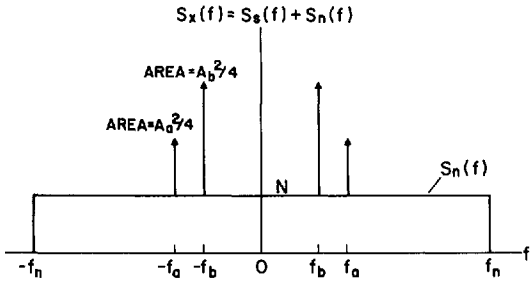

Fig. 7.4. The power spectral density seen at the input to the square-law device for the sine-wave case. If $A_a \neq A_b$, we arbitrarily choose $A_b > A_a$ as shown

From (7.50), we obtain

$$R_{a\times a}(\tau)=\alpha^2 E(s_{a1}^2 s_{a2}^2)=\alpha^2 E[A_a^4\cos^2(\omega_a t_1+\phi_a)\cos^2(\omega_a t_2+\phi_a)]$$

$$=\frac{\alpha^2}{4}A_a^4+\frac{\alpha^2}{8}A_a^4\cos 2\omega_a\tau\,. \tag{7.57a}$$

Similarly

$$R_{b\times b}(\tau)=\frac{\alpha^2}{4}A_b^4+\frac{\alpha^2}{8}A_b^4\cos 2\omega_b\tau\,. \tag{7.57b}$$

Also

$$R_{a\times b}(\tau)=4\alpha^2 E(s_{a1}s_{a2})E(s_{b1}s_{b2})+2\alpha^2\sigma_a^2\sigma_b^2$$

$$=\frac{\alpha^2}{2}A_a^2A_b^2\cos(\omega_a-\omega_b)\tau+\frac{\alpha^2}{2}A_a^2A_b^2\cos(\omega_a+\omega_b)\tau$$

$$+\frac{\alpha^2}{2}A_a^2A_b^2\,. \tag{7.57c}$$

We note that because of the zero means,

$$\sigma_a^2=R_a(0)=\frac{A_a^2}{2}\quad\text{and}\quad\sigma_b^2=R_b(0)=\frac{A_b^2}{2}. \tag{7.58}$$

The total signal-by-signal correlation function $R_{s\times s}(\tau)$ is therefore given by

$$R_{s\times s}(\tau)=R_{a\times a}(\tau)+R_{b\times b}(\tau)+R_{a\times b}(\tau)$$

$$=\frac{\alpha^2}{4}(A_a^2+A_b^2)^2+\frac{\alpha^2}{8}A_a^4\cos 2\omega_a\tau+\frac{\alpha^2}{8}A_b^4\cos 2\omega_b\tau$$

$$+\frac{\alpha^2}{2}A_a^2A_b^2\cos(\omega_a-\omega_b)\tau+\frac{\alpha^2}{2}A_a^2A_b^2\cos(\omega_a+\omega_b)\tau\,. \tag{7.59}$$

M. C. Teich, "Nonlinear Heterodyne Detection," in Topics in Applied Physics, vol. 19, Optical and Infrared Detectors, edited by R. J. Keyes (Springer-Verlag, New York, 1st ed.: 1977; 2nd ed.: 1980), ch. 7, pp. 229-300.

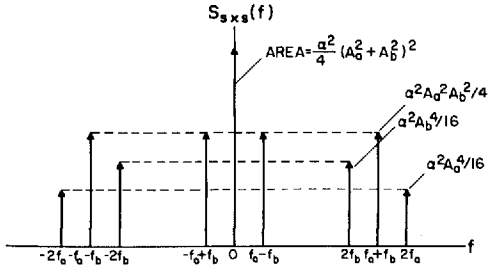

Fig. 7.5. The signal-by-signal power spectral density at the output of the square-law device (sinewave case)

The signal-by-signal part of the power spectral density $S_{s\times s}(f)$ is then, by taking the Fourier transform of $R_{s\times s}(\tau)$,

$$\begin{aligned}S_{s\times s}(f)&=\frac{\alpha^2}{4}(A_a^2+A_b^2)^2\delta(f)\\&+\frac{\alpha^2A_a^4}{16}[\delta(f-2f_a)+\delta(f+2f_a)]\\&+\frac{\alpha^2A_b^4}{16}[\delta(f-2f_b)+\delta(f+2f_b)]\\&+\frac{\alpha^2A_a^2A_b^2}{4}[\delta(f-f_a+f_b)+\delta(f+f_a-f_b)]\\&+\frac{\alpha^2A_a^2A_b^2}{4}[\delta(f-f_a-f_b)+\delta(f+f_a+f_b)]\,.\end{aligned}\tag{7.60}$$

Equation (7.60) is shown in Fig. 7.5.

For the signal-by-noise part, we have from (7.50e) and (7.50f) that

$$\begin{aligned}R_{s\times n}(\tau)&=R_{a\times n}(\tau)+R_{b\times n}(\tau)\\&=4\alpha^2R_n(\tau)[R_a(\tau)+R_b(\tau)]+2\alpha^2\sigma_n^2(\sigma_a^2+\sigma_b^2)\\&=2\alpha^2A_a^2R_n(\tau)\cos\omega_a\tau+2\alpha^2A_b^2R_n(\tau)\cos\omega_b\tau\\&+\alpha^2(A_a^2+A_b^2)\sigma_n^2\,.\end{aligned}\tag{7.61}$$

The corresponding power spectral density is then

$$\begin{aligned}S_{s\times n}(f)&=\alpha^2A_a^2[S_n(f-f_a)+S_n(f+f_a)]\\&+\alpha^2A_b^2[S_n(f-f_b)+S_n(f+f_b)]+\alpha^2(A_a^2+A_b^2)\sigma_n^2\delta(f)\,,\end{aligned}\tag{7.62}$$

where $S_n(f-f_0)$ indicates that f_0 replaces 0 as the center frequency. This spectral density is plotted in Fig. 7.6.

M. C. Teich, "Nonlinear Heterodyne Detection," in Topics in Applied Physics, vol. 19, Optical and Infrared Detectors, edited by R. J. Keyes (Springer-Verlag, New York, 1st ed.: 1977; 2nd ed.: 1980), ch. 7, pp. 229-300.

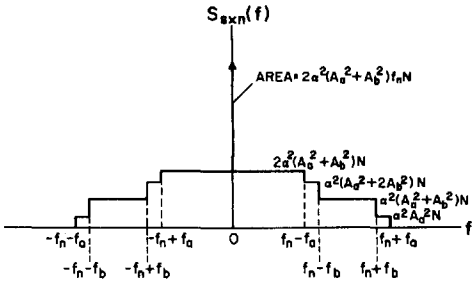

Fig. 7.6. The signal-by-noise power spectral density at the output of the square-law device (sinewave case)

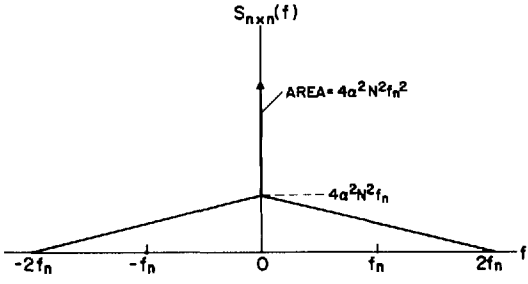

Fig. 7.7. The noise-by-noise power spectral density at the output of the square-law device

Since $R_{n^2}(\tau)=2R_n^2(\tau)+\sigma_n^4$ for Gaussian noise [7.56], (7.50c) for the noise-by-noise part becomes

$$R_{n\times n}(\tau)=2\alpha^2R_n^2(\tau)+\alpha^2\sigma_n^4, \tag{7.63}$$

whence

$$S_{n\times n}(f)=2\alpha^2\int_{-\infty}^{\infty}S_n(f')S_n(f-f')df'+\alpha^2\sigma_n^4\delta(f). \tag{7.64}$$

For the input noise spectrum described by (7.56), we have

$$\sigma_n^2=\int_{-\infty}^{\infty}S_n(f)df=2f_nN. \tag{7.65}$$

Equation (7.64) can therefore be simplified to

$$S_{n\times n}(f)=4\alpha^2f_n^2N^2\delta(f)+\begin{cases}2\alpha^2N^2(2f_n-|f|), & \text{for } |f|<2f_n,\\ 0, & \text{elsewhere},\end{cases} \tag{7.66}$$

which is shown in Fig. 7.7.

The total output power spectral density $S_y(f)$ is the sum of $S_{s\times s}(f)$, $S_{s\times n}(f)$, and $S_{n\times n}(f)$ and is plotted in Fig. 7.8, where we have assumed that $f_c=f_a-f_b=f_1-f_2$ lies in the region between the origin and f_n-f_a. In fact, f_c could be anywhere over the band f_n. We will consider two extreme cases: (a) $0<f_c<f_n-f_a$ and (b) $f_n-f_b<f_c<f_n$.

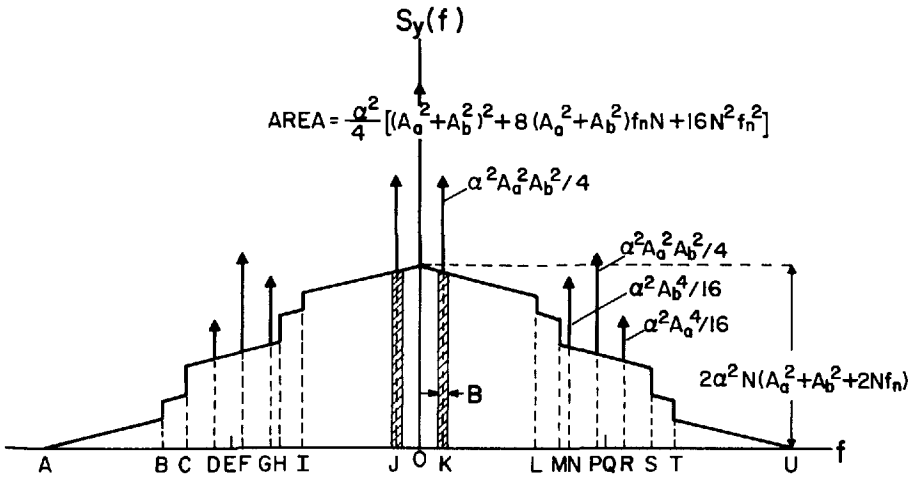

Fig. 7.8. The total power spectral density at the output of the square-law device for the sinewave case (not to scale). Correspondence between letters in figure and abscissa frequencies are: (A) $-2f_n$ (B) $-f_n-f_a$ (C) $-f_n-f_b$ (D) $-2f_a$ (E) $-f_n$ (F) $-f_a-f_b$ (G) $-2f_b$ (H) $-f_n+f_b$ (I) $-f_n+f_a$ (J) $-f_a+f_b$ (K) f_a-f_b (L) f_n-f_a (M) f_n-f_b (N) $2f_b$ (P) f_a+f_b (Q) f_n (R) $2f_a$ (S) f_n+f_b (T) f_n+f_a (U) $2f_n$. The cross-hatched area represents the final bandpass filter, of bandwidth B

Since $f_c=f_a-f_b$ is known with great accuracy we can place a bandpass filter, with center frequency f_c, after the square-law device and obtain an output signal at this frequency. We wish to obtain the output signal-to-noise ratio $(\mathrm{SNR})_0$ in terms of the input signal-to-noise ratio $(\mathrm{SNR})_i=(\mathrm{SNR})_{\mathrm{power}}$ for the two extreme cases indicated in the previous section.

From (7.60) along with Fig. 7.5 (or Fig. 7.8), we see that the output signal power S_0 at the frequency f_c is

$$S_0=\frac{\alpha^2A_a^2A_b^2}{2}. \tag{7.67}$$

For a bandpass filter with bandwidth B, and for $0<f_c<f_n-f_a$, the output noise power is the area under the power spectral density curve enclosed by B (see Figs. 7.6–8), which we choose to be rectangular for simplicity. Although strictly speaking, the rectangular function B (as well as Δf) is not realizable, this is not critical since it is the integrated area under the curve which is important rather than the detailed shape. The result is

$$N_0=4\alpha^2NB(A_a^2+A_b^2)+4\alpha^2N^2B(2f_n-f_a+f_b), \qquad 0<f_c<f_n-f_a. \tag{7.68}$$

The first term is due to the s × n interaction, while the second term is due to the n × n interaction. Equation (7.68) can also be obtained from (7.62–66).

M. C. Teich, "Nonlinear Heterodyne Detection," in Topics in Applied Physics, vol. 19, Optical and Infrared Detectors, edited by R. J. Keyes (Springer-Verlag, New York, 1st ed.: 1977; 2nd ed.: 1980), ch. 7, pp. 229-300.

The final signal-to-noise ratio at the output of the bandpass filter for this first case is therefore given by

$$(\mathrm{SNR})_0 = \frac{S_0}{N_0} = \frac{A_a^2 A_b^2}{8NB[(A_a^2 + A_b^2) + N(2f_n - f_a + f_b)]}, \qquad 0 < f_c < f_n - f_a. \tag{7.69}$$

The input signal power S_i and noise power N_i are, from Fig. 7.4,

$$S_i = R_s(0) = \tfrac{1}{2}(A_a^2 + A_b^2), \tag{7.70a}$$

$$N_i = \sigma_n^2 = 2f_n N. \tag{7.70b}$$

Thus, in terms of the input signal-to-noise ratio $(\mathrm{SNR})_i = S_i/N_i = (A_a^2 + A_b^2)/4f_n N$, (7.69) can be written as

$$(\mathrm{SNR})_0 = \frac{k_P(\mathrm{SNR})_i^2}{\left(1 - \dfrac{f_a - f_b}{2f_n}\right) + 2(\mathrm{SNR})_i}, \qquad 0 < f_c < f_n - f_a, \tag{7.71}$$

with

$$k_P = \frac{f_n A_a^2 A_b^2}{B(A_a^2 + A_b^2)^2} = \frac{f_n A_1^2 A_2^2}{B(A_1^2 + A_2^2)^2} = \frac{f_n}{B}\left\{\frac{\xi_P}{(1 + \xi_P)^2}\right\}, \tag{7.72}$$

where ξ_P represents the ratio of the signal power levels in the two beams, i.e., $\xi_P = A_2^2/A_1^2$.

The output signal-to-noise ratio is therefore inversely proportional to B, indicating that a small value for the final bandwidth is desired. Actually, B should be chosen much smaller than f_n in order that the above results be exactly correct, although results for an arbitrary value of B can easily be obtained from Fig. 7.8 and its associated equations.

If $f_c = f_a - f_b \to 0$, the minimum value for $(\mathrm{SNR})_0$ is obtained:

$$(\mathrm{SNR})_0^{\min} = \frac{k_P(\mathrm{SNR})_i^2}{1 + 2(\mathrm{SNR})_i}. \tag{7.73}$$

A log plot of (7.73) is shown in Fig. 7.9. Since $(\mathrm{SNR})_0$ will increase as f_c increases, the curve will be shifted up as f_c increases from zero. The degenerate case $f_a \equiv f_b$ should be avoided in practice because of additional noise contributions.

We now consider the second case, where $f_n - f_b < f_c < f_n$. Following the same procedure as above, we obtain

$$N_0 = 2\alpha^2 NB(A_a^2 + A_b^2) + 4\alpha^2 N^2 B(2f_n - f_a + f_b), \quad f_n - f_b < f_c < f_n, \tag{7.74}$$

M. C. Teich, "Nonlinear Heterodyne Detection," in Topics in Applied Physics, vol. 19, Optical and Infrared Detectors, edited by R. J. Keyes (Springer-Verlag, New York, 1st ed.: 1977; 2nd ed.: 1980), ch. 7, pp. 229-300.

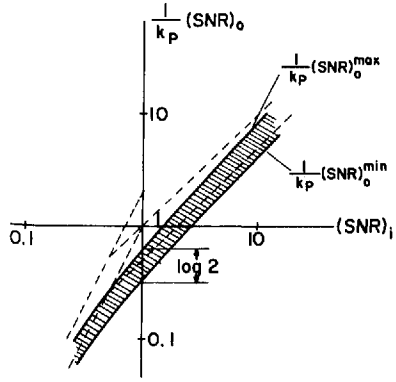

Fig. 7.9. The $(1/k_P)$ $(SNR)_0$ vs. $(SNR)_i$ curve. The actual signal-to-noise ratio depends upon the relative values of $(f_a - f_b)$ and f_n, and lies in the shaded region. This curve also applies to the Gaussian signal case, provided that the quantity k_P is replaced by k_G or k_L, for Gaussian and Lorentzian spectra, respectively (see text)

so that

$$(SNR)_0 = \frac{k_P(SNR)_i^2}{\left(1 - \frac{f_a - f_b}{2f_n}\right) + (SNR)_i}, \quad f_n - f_b < f_c < f_n. \tag{7.75}$$

If we choose $f_c = f_a - f_b = f_n$, a maximum value for the $(SNR)_0$ is obtained:

$$(SNR)_0^{max} = \frac{2k_P(SNR)_i^2}{1 + 2(SNR)_i}. \tag{7.76}$$

The log plot of (7.76) is also given in Fig. 7.9; the result is the $(SNR)_0^{min}$ curve shifted vertically upward by log2. It now becomes clear that, for intermediate cases, i.e., $0 < f_c < f_n$, the $(SNR)_0$ curve will lie in between the curves $(SNR)_0^{min}$ and $(SNR)_0^{max}$. Thus, from a signal-to-noise ratio point of view, it is preferable to maintain the known difference frequency $\Delta\nu$ at a maximum value close to f_n. For all cases, decreasing B will always yield improvement.

We can easily show that equal received power in each beam leads to optimum operation. From (7.72), we see that $k_P \propto A_a^2 A_b^2/(A_a^2 + A_b^2)^2$. Because of the symmetry between A_a and A_b, we maximize k_P by calculating the derivative $(\partial k_P/\partial A_a)|_{A_b = \text{const.}} = 0$. This leads to the relation $A_a = A_b$.

From (7.73) and (7.76) the output signal-to-noise ratio $(SNR)_0$ is seen to be bounded as follows:

$$\frac{k_P(SNR)_i^2}{1 + 2(SNR)_i} \leqq (SNR)_0 \leqq \frac{2k_P(SNR)_i^2}{1 + 2(SNR)_i}, \tag{7.77}$$

again assuming $f_L < f_1', f_2'$ or $f_L > f_1', f_2'$. For LO frequencies between the two signal frequencies, however, the output of the square-law device at $|f_1' - f_2'|$ arises from the sum-frequency rather than the difference-frequency term and therefore falls in a region of lower noise. This, then, is the most desirable configuration

M. C. Teich, "Nonlinear Heterodyne Detection," in Topics in Applied Physics, vol. 19, Optical and Infrared Detectors, edited by R. J. Keyes (Springer-Verlag, New York, 1st ed.: 1977; 2nd ed.: 1980), ch. 7, pp. 229-300.

from an SNR point of view, and allows us to comfortably realize the upper bound. (We recall, however, that the degenerate case should be avoided.) Nevertheless, we proceed under the more conservative assumption that the LO frequency is either greater than or less than both received signal frequencies. If we examine the specific (and optimum) case of $A_a = A_b$ so that $k_P = f_n/4B$, with $(\mathrm{SNR})_i = \eta P_r/h\nu f_n$ as given by (7.42b), we obtain

$$\frac{f_n}{4B}\left[\frac{(\eta P_r/h\nu f_n)^2}{1+2\eta P_r/h\nu f_n}\right] \leqq (\mathrm{SNR})_0 \leqq \frac{f_n}{2B}\left[\frac{(\eta P_r/h\nu f_n)^2}{1+2\eta P_r/h\nu f_n}\right]. \tag{7.78}$$

This yields an approximate average value given by

$$(\mathrm{SNR})_0 \simeq \frac{f_n}{3B}\left[\frac{(\eta P_r/h\nu f_n)^2}{1+2\eta P_r/h\nu f_n}\right]. \tag{7.79}$$

The case where $A_a \neq A_b$ will be considered in Section 7.4.

To obtain the minimum detectable total power $(\mathrm{MDP})_0$ for this three-frequency system, we set $(\mathrm{SNR})_0 = 1$ and solve for P_r. Thus,

$$\eta\frac{(\mathrm{MDP})_0}{h\nu f_n} = \frac{3B}{f_n} + \left[\frac{3B}{f_n}\left(1+\frac{3B}{f_n}\right)\right]^{1/2}. \tag{7.80a}$$

Since $B \ll f_n$,

$$\eta\frac{(\mathrm{MDP})_0}{h\nu f_n} \simeq \frac{3B}{f_n} + \left(\frac{3B}{f_n}\right)^{1/2}\left(1+\frac{3B}{2f_n}\right) \simeq \left(\frac{3B}{f_n}\right)^{1/2} \tag{7.80b}$$

and therefore

$$(\mathrm{MDP})_0 \simeq \sqrt{3Bf_n}(h\nu/\eta) = \sqrt{\frac{3B}{f_n}}\,P_r(\mathrm{min}), \tag{7.81}$$

with $P_r(\mathrm{min}) = f_n h\nu/\eta$ as the standard minimum detectable power for the conventional heterodyne system with Doppler uncertainty f_n [7.4, 5]. By choosing $B \ll f_n$, therefore, it is possible to achieve a reduced minimum detectable power

$$(\mathrm{MDP})_0 \ll P_r(\mathrm{min}), \qquad B \ll f_n \tag{7.82}$$

using three-frequency nonlinear heterodyne detection. *Equations (7.77–82) represent the key results obtained in this analysis.*

In the limit of large $(\mathrm{SNR})_i$ (strong input signals and/or small Doppler uncertainty), $P_r/f_n \gg h\nu/\eta$, and (7.78) yields the relationship

$$\frac{\eta P_r}{8h\nu B} \leqq (\mathrm{SNR})_0 \leqq \frac{\eta P_r}{4h\nu B}. \tag{7.83}$$

M. C. Teich, "Nonlinear Heterodyne Detection," in Topics in Applied Physics, vol. 19, Optical and Infrared Detectors, edited by R. J. Keyes (Springer-Verlag, New York, 1st ed.: 1977; 2nd ed.: 1980), ch. 7, pp. 229-300.

This can be approximated, then, as

$$(\mathrm{SNR})_0 \simeq \frac{\eta P_r}{6h\nu B} = \frac{f_n}{6B}\left(\frac{\eta P_r}{h\nu f_n}\right)$$
$$= \frac{f_n}{6B}(\mathrm{SNR})_{\mathrm{power}}, \tag{7.84}$$

where $(\mathrm{SNR})_{\mathrm{power}} = \eta P_r / h\nu f_n$ is the signal-to-noise ratio for the conventional heterodyne system as given in (7.42b). Again, we can provide that

$$(\mathrm{SNR})_0 \gg (\mathrm{SNR})_{\mathrm{power}} \tag{7.85}$$

by choosing $B \ll f_n$.

7.3.3 Application to cw Radar with Gaussian Input Signals (Gaussian Spectra)

The sinusoidal signal assumption is, in many cases, an idealization which provides simple physical and mathematical insights into a problem. In most real situations, however, the heterodyne signal will have a narrowband character [7.2, 5, 9, 10, 14]. This may be due to the surface roughness of a scattering target in a radar system, or due to the modulation imposed on the carrier in a communications system. For a scatterer returning Gaussian radiation, experiments show that the power spectral density is also frequently in the form of a Gaussian [7.9, 14, 57, 58]. It is the purpose of this section to investigate this case.

We assume that the two signal inputs to the photodetector, $E_1(t)$ and $E_2(t)$, take the form of narrowband Gaussian processes:

$$E_1(t) = A_1(t)\cos(\omega_1 t + \phi_1), \tag{7.86a}$$

$$E_2(t) = A_2(t)\cos(\omega_2 t + \phi_2), \tag{7.86b}$$

where, for any given t, the two independent amplitudes $A_1(t)$ and $A_2(t)$ are random variables with Rayleigh distributions, and the two independent phases ϕ_1 and ϕ_2 are uniformly distributed over the interval $(0, 2\pi)$. It should be pointed out that the independent amplitude case considered here is appropriate only for a sufficiently large value of $\Delta\nu$ and for sufficiently large targets. After mixing with a stable LO and filtering out the dc portion, the signal input to the square-law device is easily found to be [7.9, 10, 14]

$$s(t) = 2\beta A_L A_1(t)\cos[(\omega_1 - \omega_L)t + (\phi_1 - \phi_L)]$$
$$+ 2\beta A_L A_2(t)\cos[(\omega_2 - \omega_L)t + (\phi_2 - \phi_L)]. \tag{7.87}$$

Since β and A_L are constant, the new amplitudes $A_a(t) = 2\beta A_L A_1(t)$ and $A_b(t) = 2\beta A_L A_2(t)$ remain Rayleigh distributed. Similarly, the new phases $\phi_a = \phi_1 - \phi_L$

M. C. Teich, "Nonlinear Heterodyne Detection," in Topics in Applied Physics, vol. 19, Optical and Infrared Detectors, edited by R. J. Keyes (Springer-Verlag, New York, 1st ed.: 1977; 2nd ed.: 1980), ch. 7, pp. 229-300.

and $\phi_b = \phi_2 - \phi_L$ can be easily shown to possess uniform distributions over $(0, 2\pi)$. Therefore the narrowband Gaussian nature of the signals is preserved, provided that the envelope variations are slower than the intermediate frequencies $\omega_1 - \omega_L$ and $\omega_2 - \omega_L$ [7.9, 10, 14] and we write

$$s(t) = A_a(t)\cos(\omega_a t + \phi_a) + A_b(t)\cos(\omega_b t + \phi_b). \tag{7.88}$$

The power spectral densities for the narrowband Gaussian inputs are also taken to be Gaussian. Thus

$$S_s(f) = S_a(f) + S_b(f), \tag{7.89a}$$

with

$$S_a(f) = P_a \exp\left[-\frac{(f-f_a)^2}{2\gamma_a^2}\right] + P_a \exp\left[-\frac{(f+f_a)^2}{2\gamma_a^2}\right], \tag{7.89b}$$

$$S_b(f) = P_b \exp\left[-\frac{(f-f_b)^2}{2\gamma_b^2}\right] + P_b \exp\left[-\frac{(f+f_b)^2}{2\gamma_b^2}\right], \tag{7.89c}$$

where P_a and P_b represent the peak values of the Gaussian distributions, and γ_a and γ_b are their standard deviations. The signal powers are then given by

$$\sigma_a^2 = \int_{-\infty}^{\infty} S_a(f)df = 2\sqrt{2\pi}\gamma_a P_a = \frac{\langle A_a^2 \rangle}{2}, \tag{7.90a}$$

$$\sigma_b^2 = \int_{-\infty}^{\infty} S_b(f)df = 2\sqrt{2\pi}\gamma_b P_b = \frac{\langle A_b^2 \rangle}{2}. \tag{7.90b}$$

The noise input once again is assumed to be white Gaussian over the real frequency band $[0, f_n]$, and therefore has the same spectral density as the sinewave input case. The total power spectral density at the input to the square-law device is presented in Fig. 7.10 (compare with Fig. 7.4 for the sinewave case).

Because the signals are stationary Gaussian processes, the signal-by-signal correlation functions at the output of the square-law device are given by [see (7.63)]

$$R_{a\times a}(\tau) = 2\alpha^2 R_a^2(\tau) + \alpha^2\sigma_a^4, \tag{7.91a}$$

$$R_{b\times b}(\tau) = 2\alpha^2 R_b^2(\tau) + \alpha^2\sigma_b^4. \tag{7.91b}$$

From (7.64), the Fourier transform of $R_{a\times a}(\tau)$ is

$$\begin{aligned} S_{a\times a}(f) &= 2\alpha^2 \int_{-\infty}^{\infty} S_a(f')S_a(f-f')df' + \alpha^2\sigma_a^4\delta(f) \\ &= 2\sqrt{\pi}\alpha^2\gamma_a P_a^2 \left[e^{-(f-2f_a)^2/4\gamma_a^2} + e^{-(f-2f_a)^2/4\gamma_a^2} + 2e^{-f^2/4\gamma_a^2}\right] \\ &\quad + \alpha^2\sigma_a^4\delta(f), \end{aligned} \tag{7.92}$$

M. C. Teich, "Nonlinear Heterodyne Detection," in Topics in Applied Physics, vol. 19, Optical and Infrared Detectors, edited by R. J. Keyes (Springer-Verlag, New York, 1st ed.: 1977; 2nd ed.: 1980), ch. 7, pp. 229-300.

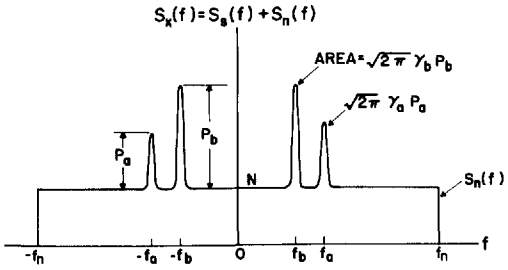

Fig. 7.10. The power spectral density at the input to the square-law device for the Gaussian signal case. We arbitrarily choose $P_b > P_a$

with the identical result for $S_{b\times b}(f)$ (b replaces a). Furthermore, using (7.50d) we obtain

$$S_{a\times b}(f)=4\sqrt{2\pi}\alpha^2\frac{(\gamma_a P_a)(\gamma_b P_b)}{\sqrt{\gamma_a^2+\gamma_b^2}}\left(\exp\left\{-\frac{[f-(f_a+f_b)]^2}{2(\gamma_a^2+\gamma_b^2)}\right\}\right.$$
$$+\exp\left\{-\frac{[f+(f_a+f_b)]^2}{2(\gamma_a^2+\gamma_b^2)}\right\}+\exp\left\{-\frac{[f-(f_a-f_b)]^2}{2(\gamma_a^2+\gamma_b^2)}\right\}$$
$$\left.+\exp\left\{-\frac{[f+(f_a-f_b)]^2}{2(\gamma_a^2+\gamma_b^2)}\right\}\right)+2\alpha^2\sigma_a^2\sigma_b^2\delta(f). \tag{7.93}$$

The total signal-by-signal power spectral density $S_{s\times s}(f)$ is, of course, given by

$$S_{s\times s}(f)=S_{a\times a}(f)+S_{b\times b}(f)+S_{a\times b}(f), \tag{7.94}$$

and is shown in Fig. 7.11 (compare with Fig. 7.5 for the sinewave case).

For the signal-by-noise part, we have

$$R_{s\times n}(\tau)=R_{a\times n}(\tau)+R_{b\times n}(\tau), \tag{7.95}$$

and, from (7.50e), we write

$$R_{a\times n}(\tau)=4\alpha^2R_a(\tau)R_n(\tau)+2\alpha^2\sigma_a^2\sigma_n^2, \tag{7.96}$$

which Fourier transforms to

$$S_{a\times n}(f)=4\alpha^2\int_{-\infty}^{\infty}S_a(f')S_n(f-f')df+2\alpha^2\sigma_a^2\sigma_n^2\delta(f). \tag{7.97}$$

This can be readily evaluated to yield

$$S_{a\times n}(f)=4\sqrt{2\pi}\alpha^2NP_a\gamma_a\left[\Phi\left(\frac{f+f_n-f_a}{\gamma_a}\right)-\Phi\left(\frac{f-f_n-f_a}{\gamma_a}\right)\right.$$
$$\left.+\Phi\left(\frac{f+f_n+f_a}{\gamma_a}\right)-\Phi\left(\frac{f-f_n+f_a}{\gamma_a}\right)\right]+2\alpha^2\sigma_a^2\sigma_n^2\delta(f), \tag{7.98}$$

M. C. Teich, "Nonlinear Heterodyne Detection," in Topics in Applied Physics, vol. 19, Optical and Infrared Detectors, edited by R. J. Keyes (Springer-Verlag, New York, 1st ed.: 1977; 2nd ed.: 1980), ch. 7, pp. 229-300.

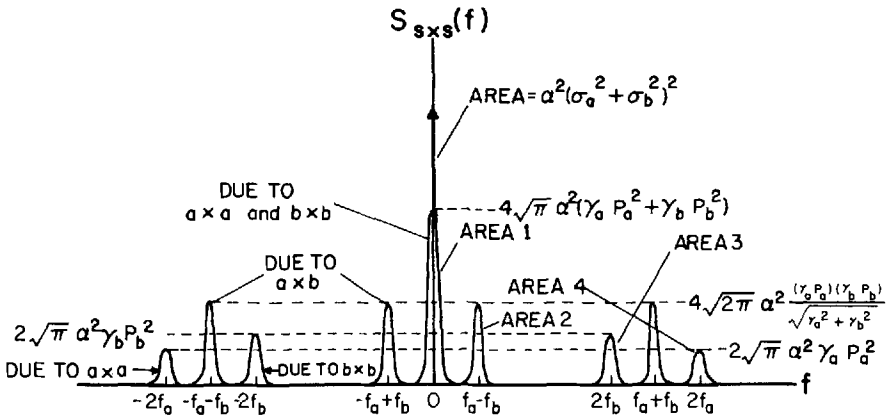

Fig. 7.11. The signal-by-signal power spectral density at the output of the square-law device (Gaussian signal case). Areas under curves: AREA $1=8\pi\alpha^2(\gamma_a^2P_a^2+\gamma_b^2P_b^2)$; AREA 2 $=8\pi\alpha^2(\gamma_aP_a)(\gamma_bP_b)$; AREA $3=4\pi\alpha^2\gamma_b^2P_b^2$; AREA $4=4\pi\alpha^2\gamma_a^2P_a^2$

where $\Phi(x)$ is the normal distribution function

$$\Phi(x)=\frac{1}{\sqrt{2\pi}}\int_{-\infty}^{x}e^{-x'^2/2}dx'. \tag{7.99}$$

Similarly, we obtain the identical result for $S_{b\times n}$ (b replaces a). The total signal-by-noise power spectral density $S_{s\times n}(f)$ is just the sum of $S_{a\times n}(f)$ and $S_{b\times n}(f)$, or

$$S_{s\times n}(f)=S_{a\times n}(f)+S_{b\times n}(f). \tag{7.100}$$

A sketch of $S_{s\times n}(f)$ is given in Fig. 7.12. Assuming that the standard deviations γ_a and γ_b are small in comparison with the width of the plateau regions in Fig. 7.6, the plot will be very similar to that of the sinewave case. The only notable difference is the rounding of sharp corners. Small values of γ_a and γ_b also guard against spectrum overlap which would make the solution of the problem more difficult.

The noise-by-noise power spectral density is the same as that for the pure sinewave case (Fig. 7.7). The total output power spectral density $S_y(f)$ is plotted in Fig. 7.13 where we arbitrarily have assumed that $f_a>f_b$ and $f_a-f_b<f_n-f_a<f_n$.

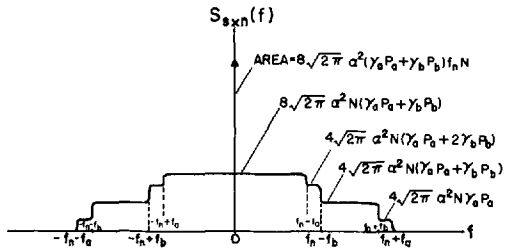

Fig. 7.12. The signal-by-noise power spectral density at the output of the square-law device (Gaussian signal case)

M. C. Teich, "Nonlinear Heterodyne Detection," in Topics in Applied Physics, vol. 19, Optical and Infrared Detectors, edited by R. J. Keyes (Springer-Verlag, New York, 1st ed.: 1977; 2nd ed.: 1980), ch. 7, pp. 229-300.

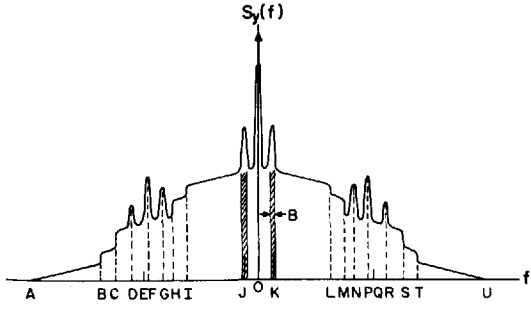

Fig. 7.13. The total power spectral density at the output of the square-law device for the Gaussian signal case. Note the smoothing of all sharp edges. This figure is similar to Fig. 7.6 except that the delta functions are replaced by Gaussians

Here again, we place a bandpass filter of bandwidth B and center frequency $f_c = f_a - f_b$ after the square-law device. Referring to Fig. 7.11 and (7.93), we find

$$S_0 = \frac{8\alpha^2 \sqrt{2\pi}(\gamma_a P_a)(\gamma_b P_b)}{\sqrt{\gamma_a^2 + \gamma_b^2}} \left[\int_{-B/2}^{B/2} e^{-f^2/2(\gamma_a^2+\gamma_b^2)} df\right]$$

$$= 16\pi\alpha^2(\gamma_a P_a)(\gamma_b P_b)\left[2\Phi\left(\frac{B}{2\sqrt{\gamma_a^2+\gamma_b^2}}\right) - 1\right]. \tag{7.101}$$

The input signal power is, from (7.90), given by

$$S_i = 2\sqrt{2\pi}(\gamma_a P_a + \gamma_b P_b). \tag{7.102}$$

The input noise power is the same as for the sinewave case. Referring to Figs. 7.7 and 7.12, the output noise power can be very well approximated by

$$N_0 = 16\sqrt{2\pi}\alpha^2 NB(\gamma_a P_a + \gamma_b P_b) + 4\alpha^2 N^2 B(2f_n - f_a + f_b),$$
$$0 < f_a - f_b < f_n - f_a, \tag{7.103a}$$

$$N_0 = 8\sqrt{2\pi}\alpha^2 NB(\gamma_a P_a + \gamma_b P_b) + 4\alpha^2 N^2 B(2f_n - f_a + f_b),$$
$$f_n - f_b < f_a - f_b < f_n. \tag{7.103b}$$

The input signal-to-noise ratio $(\mathrm{SNR})_i$ is simply

$$(\mathrm{SNR})_i = \frac{\sqrt{2\pi}}{N f_n}(\gamma_a P_a + \gamma_b P_b) \tag{7.104}$$

while the output signal-to-noise ratio $(\mathrm{SNR})_0$ can be easily evaluated:

$$(\mathrm{SNR})_0 = \frac{k_G(\mathrm{SNR})_i^2}{\left(1 - \frac{f_a - f_b}{2f_n}\right) + 2(\mathrm{SNR})_i}, \quad 0 < f_a - f_b < f_n - f_a, \tag{7.105a}$$

$$(\mathrm{SNR})_0 = \frac{k_G(\mathrm{SNR})_i^2}{\left(1 - \frac{f_a - f_b}{2f_n}\right) + (\mathrm{SNR})_i}, \quad f_n - f_b < f_a - f_b < f_n. \tag{7.105b}$$

M. C. Teich, "Nonlinear Heterodyne Detection," in Topics in Applied Physics, vol. 19, Optical and Infrared Detectors, edited by R. J. Keyes (Springer-Verlag, New York, 1st ed.: 1977; 2nd ed.: 1980), ch. 7, pp. 229-300.

These equations are identical to (7.71) and (7.75) with the exception that the factor k_P [(7.72)] has been replaced by the factor k_G given by

$$k_G = \frac{f_n}{2\sqrt{\gamma_a^2+\gamma_b^2}} \frac{(\gamma_a P_a)(\gamma_b P_b)}{(\gamma_a P_a+\gamma_b P_b)^2} \left\{\frac{1}{u}[2\Phi(u)-1]\right\}$$
$$= \frac{f_n}{2\sqrt{\gamma_1^2+\gamma_2^2}} \frac{(\gamma_1 P_1)(\gamma_2 P_2)}{(\gamma_1 P_1+\gamma_2 P_2)^2} \left\{\frac{1}{u}[2\Phi(u)-1]\right\}$$
$$= \frac{f_n}{2\sqrt{\gamma_1^2+\gamma_2^2}} \left\{\frac{\xi_G}{(1+\xi_G)^2}\right\} \left\{\frac{1}{u}[2\Phi(u)-1]\right\}. \tag{7.106a}$$

Here

$$u = \frac{B}{2\sqrt{\gamma_a^2+\gamma_b^2}} = \frac{B}{2\sqrt{\gamma_1^2+\gamma_2^2}} \tag{7.106b}$$

and ξ_G, which is the ratio of the beam powers, is

$$\xi_G = \gamma_2 P_2/\gamma_1 P_1 . \tag{7.106c}$$

Now, if $f_a - f_b \to 0$ in (7.105a) and choosing $f_a - f_b = f_n$ in (7.105b), we obtain the following bounds for $(\mathrm{SNR})_0$

$$(\mathrm{SNR})_0^{\min} = \frac{k_G(\mathrm{SNR})_i^2}{1+2(\mathrm{SNR})_i}, \tag{7.107a}$$

$$(\mathrm{SNR})_0^{\max} = \frac{2k_G(\mathrm{SNR})_i^2}{1+2(\mathrm{SNR})_i}, \tag{7.107b}$$

in analogy with (7.73) and (7.76). Again we note that when the LO frequency is between the received signal frequencies, the upper bound can be safely used. The results presented in Fig. 7.9 are therefore also appropriate to this case with the substitution of k_G for k_P.

Since $(\mathrm{SNR})_i$ is the same for the Gaussian case as it is for the pure sinewave case [7.10], the results presented in Section 7.3.2 apply directly with the simple replacement of k_P by k_G; thus

$$\frac{1}{B} \to \frac{1}{2\sqrt{\gamma_a^2+\gamma_b^2}} \left\{\frac{1}{u}[2\Phi(u)-1]\right\} = \frac{2\Phi(u)-1}{B}, \tag{7.108a}$$

with

$$A_a^2 \to 4\sqrt{2\pi}\gamma_a P_a , \tag{7.108b}$$

$$A_b^2 \to 4\sqrt{2\pi}\gamma_b P_b . \tag{7.108c}$$

M. C. Teich, "Nonlinear Heterodyne Detection," in Topics in Applied Physics, vol. 19, Optical and Infrared Detectors, edited by R. J. Keyes (Springer-Verlag, New York, 1st ed.: 1977; 2nd ed.: 1980), ch. 7, pp. 229-300.

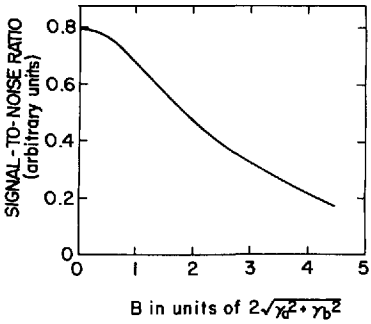

Fig. 7.14. Plot of the function $z(u)$ vs u, which represents the B dependence of the signal-to-noise ratio for Gaussian signals

For equal powers in both beams, therefore, the final signal-to-noise ratio for the Gaussian case is degraded in comparison with the sinewave case by the factor $[2\Phi(u)-1]=[\Phi(u)-\Phi(-u)]<1$. It is clear that the spectral width, as determined by the quantity $\sqrt{\gamma_a^2+\gamma_b^2}$, should be minimized if possible. An expression for the MDP is given in Section 7.4.3.

We now consider the variation of the quantity k_G with the bandwidth B, assuming that the parameters f_n, γ_a, γ_b, P_a, and P_b are fixed. Since $u \propto B$ and $k_G \propto (1/u)[2\Phi(u)-1] \equiv z(u)$, it is sufficient to examine the function $z(u)$ sketched in Fig. 7.14. It is apparent that k_G, and therefore $(\mathrm{SNR})_0$, increases with decreasing B. This evidences the fact that the noise power decreases more rapidly than the signal power as the bandwidth B is narrowed on $f_c = f_a - f_b$. This effect can be observed in Fig. 7.13. For both sinewave and Gaussian signal inputs, therefore, it is desirable to minimize B. The limitation, of course, is provided by the unequal Doppler shifts of the two input signals. For a given bandwidth B, furthermore, it is understood that all of the signal will be detected in the sinewave case, while only a portion of it will be detected in the Gaussian case.

If we let γ_a and $\gamma_b \to 0$ while keeping the power constant (i.e., $\sqrt{2\pi}\gamma_a P_a = A_a^2/4$ and $\sqrt{2\pi}\gamma_b P_b = A_b^2/4$), the Gaussian spectra shrink to delta functions. In this limit, we observe that

$$\lim_{\substack{\gamma_a \to 0 \\ \gamma_b \to 0}} S_0(\text{Gaussian}) = \frac{\alpha^2 A_a^2 A_b^2}{2}[2\Phi(\infty)-1] = \frac{\alpha^2 A_a^2 A_b^2}{2}, \tag{7.109}$$

which is, as expected, the expression obtained for the output power for the sinewave case [(7.67)].

7.3.4 Application to cw Radar with Gaussian Input Signals (Lorentzian Spectra)

In those cases where the narrowband Gaussian signal inputs possess Lorentzian power spectra rather than Gaussian power spectra, the input power spectral

M. C. Teich, "Nonlinear Heterodyne Detection," in Topics in Applied Physics, vol. 19, Optical and Infrared Detectors, edited by R. J. Keyes (Springer-Verlag, New York, 1st ed.: 1977; 2nd ed.: 1980), ch. 7, pp. 229-300.

densities are given by

$$S_a(f)=\frac{D_a\Gamma_a}{2[(f-f_a)^2+\Gamma_a^2]}+\frac{D_a\Gamma_a}{2[(f+f_a)^2+\Gamma_a^2]}, \tag{7.110a}$$

$$S_b(f)=\frac{D_b\Gamma_b}{2[(f-f_b)^2+\Gamma_b^2]}+\frac{D_b\Gamma_b}{2[(f+f_b)^2+\Gamma_b^2]}. \tag{7.110b}$$

Here D_a and D_b are arbitrary constants, while Γ_a and Γ_b are constants reflecting the spectral width. Performing the inverse Fourier transform, the autocorrelation functions are found to be

$$R_a(\tau)=\pi D_a e^{-2\pi\Gamma_a|\tau|}\cos 2\pi f_a\tau, \tag{7.111a}$$

$$R_b(\tau)=\pi D_b e^{-2\pi\Gamma_b|\tau|}\cos 2\pi f_b\tau, \tag{7.111b}$$

whereas the input signal powers are given by

$$\sigma_a^2=\int_{-\infty}^{\infty}S_a(f)df=\pi D_a=\frac{\langle A_a^2\rangle}{2}, \tag{7.112a}$$

$$\sigma_b^2=\int_{-\infty}^{\infty}S_b(f)df=\pi D_b=\frac{\langle A_b^2\rangle}{2}. \tag{7.112b}$$

With the same noise input as considered in the previous section, and making use of (7.50), (7.91), (7.97), and (7.111), the output power spectral densities are

$$S_{a\times a}(f)=\alpha^2\pi D_a^2\left[\frac{2\Gamma_a}{f^2+4\Gamma_a^2}+\frac{\Gamma_a}{(f-2f_a)^2+4\Gamma_a^2}+\frac{\Gamma_a}{(f+2f_a)^2+4\Gamma_a^2}\right]+\alpha^2\sigma_a^4\delta(f), \tag{7.113a}$$

$$S_{b\times b}(f)=S_{a\times a}(f)|_{\text{sub. a}\to\text{sub. b}}, \tag{7.113b}$$

$$S_{a\times b}(f)=\alpha^2\pi D_aD_b\left[\frac{\Gamma_a+\Gamma_b}{(f-f_a-f_b)^2+(\Gamma_a+\Gamma_b)^2}+\frac{\Gamma_a+\Gamma_b}{(f+f_a+f_b)^2+(\Gamma_a+\Gamma_b)^2}+\frac{\Gamma_a+\Gamma_b}{(f-f_a+f_b)^2+(\Gamma_a+\Gamma_b)^2}+\frac{\Gamma_a+\Gamma_b}{(f+f_a-f_b)^2+(\Gamma_a+\Gamma_b)^2}\right]+2\alpha^2\sigma_a^2\sigma_b^2\delta(f), \tag{7.113c}$$

$$S_{a\times n}(f)=2\alpha^2ND_a\tan^{-1}\left\{\frac{4f_n\Gamma_a(f^2+f_a^2+\Gamma_a^2-f_n^2)}{[(f-f_a)^2+\Gamma_a^2-f_n^2][(f+f_a)^2+\Gamma_a^2-f_n^2]-4f_n^2\Gamma_a^2}\right\}+2\alpha^2\sigma_a^2\sigma_n^2\delta(f), \tag{7.113d}$$

$$S_{b\times n}(f)=S_{a\times n}|_{\text{sub. a}\to\text{sub. b}}, \tag{7.113e}$$

M. C. Teich, "Nonlinear Heterodyne Detection," in Topics in Applied Physics, vol. 19, Optical and Infrared Detectors, edited by R. J. Keyes (Springer-Verlag, New York, 1st ed.: 1977; 2nd ed.: 1980), ch. 7, pp. 229-300.

with $0<\tan^{-1}x<\pi$ (negative angles excluded). For narrow spectral widths (Γ_a, Γ_b small), it is clear that the power spectral densities for the Lorentzian case should look just about the same as those for the Gaussian case. We may simply replace $2\sqrt{2\pi}\gamma_a P_a$ and $2\sqrt{2\pi}\gamma_b P_b$, respectively, by πD_a and πD_b [see (7.90) and (7.112)].

We may calculate the output signal and noise to obtain $(\mathrm{SNR})_0$ as follows. Let

$$S_0 = 2\pi\alpha^2 D_a D_b \int_{-B/2}^{B/2} \frac{\Gamma_a+\Gamma_b}{f^2+(\Gamma_a+\Gamma_b)^2}\,df$$
$$= 2\pi\alpha^2 D_a D_b \tan^{-1}\left[\frac{4B(\Gamma_a+\Gamma_b)}{4(\Gamma_a+\Gamma_b)^2-B^2}\right], \tag{7.114}$$

with $0<\tan^{-1}x<\pi$. For small B, the output noise power is

$$N_0 = \int_{f_a-f_b-B/2}^{f_a-f_b+B/2}[S_{a\times n}(f)+S_{b\times n}(f)+S_{n\times n}(f)]df$$
$$+\int_{-f_a+f_b-B/2}^{-f_a+f_b+B/2}[S_{a\times n}(f)+S_{b\times n}(f)+S_{n\times n}(f)]df$$
$$\simeq B[S_{a\times n}(f_a-f_b)+S_{a\times n}(-f_a+f_b)+S_{b\times n}(f_a-f_b)+S_{b\times n}(-f_a+f_b)]$$
$$+4\alpha^2N^2B(2f_n-f_a+f_b). \tag{7.115}$$

As an approximation, we use the replacements $2\sqrt{2\pi}\gamma_a P_a \to \pi D_a$ and $2\sqrt{2\pi}\gamma_b P_b \to \pi D_b$ in Fig. 7.12 to obtain

$$N_0 = 8\pi\alpha^2 NB(D_a+D_b)+4\alpha^2N^2B(2f_n-f_a+f_b),$$
$$0<f_a-f_b<f_n-f_a, \tag{7.116a}$$

$$N_0 = 4\pi\alpha^2 NB(D_a+D_b)+4\alpha^2N^2B(2f_n-f_a+f_b),$$
$$f_n-f_b<f_a-f_b<f_n. \tag{7.116b}$$

Using an input signal-to-noise ratio $(\mathrm{SNR})_i$ [see (7.112)] given by

$$(\mathrm{SNR})_i = \frac{\pi(D_a+D_b)}{2Nf_n}, \tag{7.117}$$

and using (7.114), (7.116), and (7.117), we find the output signal-to-noise ratio $(\mathrm{SNR})_0$ to be

$$(\mathrm{SNR})_0 = \frac{k_L(\mathrm{SNR})_i^2}{\left(1-\frac{f_a-f_b}{2f_n}\right)+2(\mathrm{SNR})_i}, \quad 0<f_a-f_b<f_n-f_a, \tag{7.118a}$$

$$(\mathrm{SNR})_0 = \frac{k_L(\mathrm{SNR})_i^2}{\left(1-\frac{f_a-f_b}{2f_n}\right)+(\mathrm{SNR})_i}, \quad f_n-f_b<f_a-f_b<f_n. \tag{7.118b}$$

M. C. Teich, "Nonlinear Heterodyne Detection," in Topics in Applied Physics, vol. 19, Optical and Infrared Detectors, edited by R. J. Keyes (Springer-Verlag, New York, 1st ed.: 1977; 2nd ed.: 1980), ch. 7, pp. 229-300.

This result is therefore the same as that for both the sinewave case and the Gaussian spectrum case [see (7.71), (7.75), (7.105)] except that we now use the factor k_L given by

$$k_L = \frac{f_n}{\pi(\Gamma_a+\Gamma_b)} \frac{D_a D_b}{(D_a+D_b)^2} \frac{\tan^{-1}\left(\frac{4v}{4-v^2}\right)}{v}$$

$$= \frac{f_n}{\pi(\Gamma_1+\Gamma_2)} \frac{D_1 D_2}{(D_1+D_2)^2} \frac{\tan^{-1}\left(\frac{4v}{4-v^2}\right)}{v}$$

$$= \frac{f_n}{\pi(\Gamma_1+\Gamma_2)} \left\{\frac{\xi_L}{(1+\xi_L)^2}\right\} \frac{\tan^{-1}\left(\frac{4v}{4-v^2}\right)}{v} \tag{7.119a}$$

where

$$v = B/(\Gamma_a+\Gamma_b) = B/(\Gamma_1+\Gamma_2) \tag{7.119b}$$

and

$$\xi_L = D_2/D_1 . \tag{7.119c}$$

Thus the results presented in Fig. 7.9 apply also to this case with k_P replaced by k_L.

For small v (small B), the quantity $4v/(4-v^2) \simeq v$. It is not difficult to show that the behavior of the function $(\tan^{-1} v)/v$ is similar to that of $z(u)$ (see Fig. 7.14). The maximum value occurs at the origin so that in this case too, optimum operation occurs for $B \to 0$.

Furthermore, using the replacements $\pi D_a \to A_a^2/2$ and $\pi D_b \to A_b^2/2$ and letting $\Gamma_a, \Gamma_b \to 0$, (7.119) reduces to

$$k_L = \frac{f_n}{B} \frac{A_a^2 A_b^2}{(A_a^2+A_b^2)^2} \left\{\lim_{\Gamma_a+\Gamma_b \to 0} \frac{1}{\pi} \tan^{-1}\left[\frac{4B(\Gamma_a+\Gamma_b)}{4(\Gamma_a+\Gamma_b)^2 - B^2}\right]\right\}$$

$$= \frac{f_n}{B} \frac{A_a^2 A_b^2}{(A_a^2+A_b^2)^2} = k_P . \tag{7.120}$$

Thus, the present case also reduces to the sinewave case as the spectral width approaches zero with the power fixed. Similarly it is clear from the above that for fixed B the spectral width, as determined by the quantity $(\Gamma_a+\Gamma_b)$, should be minimized if possible.

7.3.5 Application to an Analog Communications System

Use of the three-frequency method for a communications system (in which the transmitter and receiver may be moving relative to each other) is similar to the radar already described, and is indicated in Fig. 7.15. Note, however, that only

M. C. Teich, "Nonlinear Heterodyne Detection," in Topics in Applied Physics, vol. 19, Optical and Infrared Detectors, edited by R. J. Keyes (Springer-Verlag, New York, 1st ed.: 1977; 2nd ed.: 1980), ch. 7, pp. 229-300.

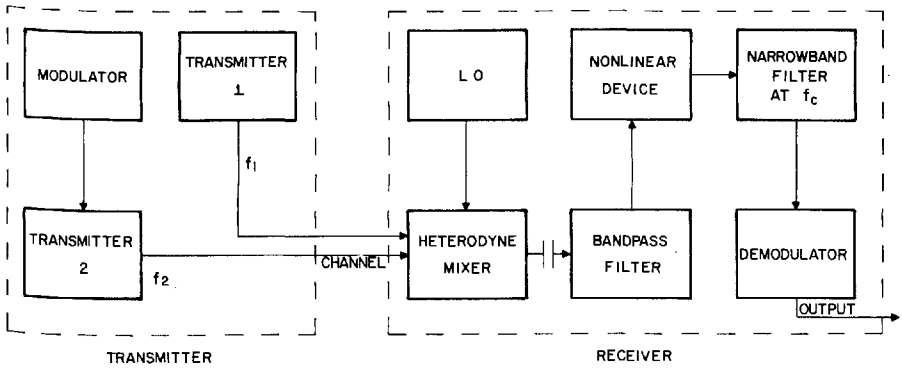

Fig. 7.15. A three-frequency nonlinear heterodyne analog communications system

one of the carrier waves (f_2) is modulated, and that a demodulator is included. By modulating only one of the beams, the $s \times s$ component reaching the demodulator results from the convolution of a delta function (at f_1) with the modulated signal (centered at f_2), which is simply the original undistorted spectral information ready for demodulation by a suitable device such as a mixer, an envelope detector, or a discriminator. The maximum rate at which modulation may be decoded (or the information capacity) of the system will, of course, depend upon the time response of the system which is usually governed by the final bandwidth B. We could, in the alternative, construct an analog FM communication system in which a single frequency laser beam is split into two frequencies by a modulator (e.g., an acoustooptic modulator [7.49]). In that case, the frequency difference f_c will carry the information. In the absence of information (i.e., f_c constant), f_c will be spectrally very pure (it should be as narrow as the spectral width of the modulator drive signal). Thus the three-frequency nonlinear system could provide the advantage of lower deviation and thereby provide bandwidth compression.

7.3.6 Operation at Low Frequencies and in Various Configurations

Thus far, we have been especially concerned with absorption detectors operating in the optical and infrared regions of the electromagnetic spectrum ($h\nu \gg kT$, where k is the Boltzmann constant and T is the detector temperature). In this case, the intensity of the incoming wave is obtained from the analytic signal and excludes double- and sum-frequency components [7.10, 12–14]. Nevertheless, (7.77) is a general result for intensity detection which applies also to the microwave and radiowave regions ($h\nu \ll kT$).

For low frequencies, the intensity is related to the square of the electric field, $I \propto E^2$. For a diode mixer which is either operating in the square-law regime or in

M. C. Teich, "Nonlinear Heterodyne Detection," in Topics in Applied Physics, vol. 19, Optical and Infrared Detectors, edited by R. J. Keyes (Springer-Verlag, New York, 1st ed.: 1977; 2nd ed.: 1980), ch. 7, pp. 229-300.

the linear regime followed by a square-law device, the detector response r for a three-frequency system is then given by the classical expression

$$\begin{aligned} r &= \beta' E_t^2 = \beta'[A_1\cos(\omega_1 t+\phi_1)+A_2\cos(\omega_2 t+\phi_2)+A_L\cos(\omega_L t+\phi_L)]^2 \\ &= \beta'\{A_1^2\cos^2(\omega_1 t+\phi_1)+A_2^2\cos^2(\omega_2 t+\phi_2)+A_L^2\cos^2(\omega_L t+\phi_L) \\ &\quad + A_1A_2\cos[(\omega_1-\omega_2)t+(\varphi_1-\varphi_2)]+A_1A_2\cos[(\omega_1+\omega_2)t+(\varphi_1+\varphi_2)] \\ &\quad + A_1A_L\cos[(\omega_1-\omega_L)t+(\phi_1-\phi_L)]+A_1A_L\cos[(\omega_1+\omega_L)t+(\phi_1+\phi_L)] \\ &\quad + A_2A_L\cos[(\omega_2-\omega_L)t+(\phi_2-\phi_L)]+A_2A_L\cos[(\omega_2+\omega_L)t+(\phi_2+\phi_L)]\}. \end{aligned} \tag{7.121}$$

Note that $A^2\cos^2(\omega t+\phi)=(A^2/2)[1+\cos(2\omega t+2\phi)]$. Now, since the detector generally does not follow the instantaneous intensity at double- and sum-frequencies ($2\omega_1$, $\omega_1+\omega_2$, ...), only dc and difference-frequency terms remain. Hence (7.121) will in practice reduce to (7.36). The calculations leading to (7.121) will remain correct, provided of course, that we insert the proper relation for $(\mathrm{SNR})_i$ in the classical low frequency detection regime. Generally, this is obtained by replacing $h\nu$ by kT and η by $1/F_T$, where F_T is the noise figure of the receiver.

Once the target is ascertained to be present, a wide bandpass filter can be gradually narrowed about $2|f_1'-f_L|$ or $2|f_2'-f_L|$ and thereby used to obtain Doppler information. Alternatively one could, of course, switch to a conventional configuration.

It is of interest to examine the operation of the three-frequency nonlinear heterodyne system in a variety of configurations [7.59] different from those assumed earlier. In this section, we consider the behavior of the system under the following conditions: 1) at zero frequency (dc), 2) without a final bandpass filter, 3) with increased Doppler information, 4) as an optimum system with no uncertainty in Doppler shift, and 5) with a νth law nonlinear device other than square-law. We also consider the consequences of four-frequency nonlinear heterodyne detection; this will be examined in greater detail in Section 7.4.

Assuming that $B\to 0$, a calculation of $(\mathrm{SNR})_0$ for the final filter centered at zero frequency rather than at f_c yields the result given by (7.73) with $k_P=1$, thus independent of f_n, A_a, A_b, and B. The advantageous factor f_n/B therefore does not appear in the equation. For $B>0$, the noise increases while the signal does not so that the above result is optimum for zero frequency. It must be kept in mind, however, that this result has been obtained for a system containing a blocking capacitor (see Fig. 7.3).

If we altogether omit the final bandpass filter, a rather complicated expression for $(\mathrm{SNR})_0$ obtains. Assuming that f_a and f_b are much smaller than f_n, and with $A_a=A_b$, the MDP is calculated to be $(\mathrm{MDP})_0\simeq 2.9h\nu f_n/\eta$, approximately a factor three worse than the conventional system.

We now consider the case in which the bandpass filter barely encompasses f_a and f_b so that $f_i=f_b$ and $f_n=f_a$, with $f_a>f_b$. Clearly, decreasing this bandwidth

M. C. Teich, "Nonlinear Heterodyne Detection," in Topics in Applied Physics, vol. 19, Optical and Infrared Detectors, edited by R. J. Keyes (Springer-Verlag, New York, 1st ed.: 1977; 2nd ed.: 1980), ch. 7, pp. 229-300.

should decrease the overall noise and thereby improve system performance, but this requires knowledge of the Doppler shifts involved. A calculation of the average MDP yields the result $(\mathrm{MDP})_0 \simeq 3h\nu B/\eta$, which is considerably lower than the result given in (7.81), as it should be.

A calculation for the case in which complete Doppler information is available displays clearly the additional noise introduced by the three-frequency system over the conventional system, by virtue of the nonlinear processing. The result for the MDP in this case is $(\mathrm{MDP})_0 \simeq 1.8h\nu B/\eta$, which is a factor of 1.8 greater than the MDP for the conventional heterodyne receiver with bandwidth B.

General considerations [7.60] show that all νth law detectors behave in an essentially similar manner to the full-wave square-law detector in terms of the ratio of $(\mathrm{SNR})_0$ and $(\mathrm{SNR})_i$. For large values of $(\mathrm{SNR})_i$, therefore, $(\mathrm{SNR})_0$ is expected to be directly proportional to $(\mathrm{SNR})_i$. Thus, if a half-wave linear device were used instead of the full-wave square-law device considered previously, we would expect results similar to those obtained earlier. This provides a wide choice for designing a heterodyne-nonlinear detector combination, perhaps in a single package.

Finally, we consider the consequences of four-frequency mixing. This would have the advantage of making the transmitter and LO identical. Assuming that only one of the sidebands of the LO is strong (A_{L1}), the $(\mathrm{SNR})_0$ is still given by (7.73) and (7.76), but in this case

$$ {}^4k_P = \frac{f_n A_a^2 A_b^2}{B(A_a^2 + A_b^2 + A_c^2)^2} = \frac{f_n A_1^2 A_2^2}{B(A_1^2 + A_2^2 + A_{L2}^2)^2}, \tag{7.122} $$

with $A_c/A_a = A_{L2}/A_1$. If $A_1 = A_2 = A_{L2}$, we obtain ${}^4k_P = f_n/9B$ which is to be compared with the value ${}^3k_P = f_n/4B$ for the three-frequency case. Thus a single unit may be used both as transmitter and local oscillator without a great deal of loss, provided that one of the two sidebands of the LO beam is attenuated down to the level of the received signal. From (7.122), it is seen that the LO optimally consists of a single frequency, however.

The worst case, in which the LO consists of two strong frequencies separated by f_c, gives rise to very large s × n terms arising from the beating between the two LO frequencies. Aside from other terms not contained in (7.122), this case would make the A_c^4 term in the denominator of (7.122) very large, leading to a factor $(P_r/P_L)^2$ in $(\mathrm{SNR})_0$ (P_r and P_L are typical signal and LO powers, respectively). Thus, in other than very large input SNR situations, the transmitter cannot be directly used as an LO without attenuation of one of its sidebands.

7.3.7 Numerical Example: A CO_2 Laser Radar

As an example of three-frequency nonlinear heterodyne detection, we consider a CO_2 laser radar operating at 10.6 μm in the infrared [7.14, 61, 62] (see Fig. 7.3). If we assume that we wish to acquire and track a 1-m-radius satellite with a

M. C. Teich, "Nonlinear Heterodyne Detection," in Topics in Applied Physics, vol. 19, Optical and Infrared Detectors, edited by R. J. Keyes (Springer-Verlag, New York, 1st ed.: 1977; 2nd ed.: 1980), ch. 7, pp. 229-300.

rotation rate of 1 rpm, the expected bandwidth (resulting from rotation) of the radar return is of order $4R\omega_\perp/\lambda \sim 40$ kHz [7.9]. We therefore choose a difference frequency f_c at a (convenient) value of 1 MHz, which eliminates spectrum overlap. If the satellite has a radial velocity ~ 10 km/s, the Doppler frequency is ~ 2 GHz, yielding a value $f_c' - f_c = 2v_{||}f_c/c \sim 60$ Hz. This shift is very small indeed compared with general frequency modulations in an ordinary heterodyne system, justifying the assumption that $f_c' - f_c \to 0$. Thus, assuming we have only an upper bound on the satellite velocity, i.e., its velocity may be anywhere in the range 0–10 km/s, we choose $\Delta f = f_n \sim 2$ GHz and $B \sim 20$ kHz. The MDP for this system would, therefore, be $\sim (\sqrt{3}h\nu/\eta)(Bf_n)^{1/2}$ which is equivalent to the MDP obtained from a conventional setup with a bandwidth of approximately 10 MHz. If the Doppler shift is more confined, the MDP is correspondingly reduced. For strong returns, of course, the SNR will show an enhancement commensurate with the bandwidth B. Thus, the advantages of the three-frequency heterodyne system may be secured with such a radar. Similar results would be obtained at other frequencies; in the microwave, for example, f_c may be made as small as tens of Hz. In some cases, it may be possible to reduce clutter by the insertion of an extremely sharp notch filter at exactly f_c.

7.3.8 Application to Binary Communications and Pulsed Radar (Vacuum Channel)

The previous subsections were primarily concerned with the behavior of the three-frequency nonlinear heterodyne system for applications in cw radar and analog communications. As such, a determination of the output signal-to-noise ratio $(\text{SNR})_0$ was adequate to characterize the system. In this subsection, we investigate applications in digital communications and pulsed radar, and therefore examine system performance in terms of the error probability P_e. Evaluation of the probability of error under various conditions requires a decision criterion as well as a knowledge of the signal statistics; we now investigate operation of the three-frequency nonlinear heterodyne scheme in the time domain rather than in the frequency domain.

Because of the added complexity of dealing in the time domain, we limit our investigation to sinewave signals, Gaussian local oscillator (LO) noise, and envelope detection. The configuration of such a receiver is therefore similar to that considered previously, with the addition of an envelope detector (see Figs. 7.3 and 7.15). We therefore examine the case of a particular "square-law envelope detector", consisting of a square-law device, a narrowband filter, and an envelope detector [7.63]. Although envelope detection is generally suboptimum because it is insensitive to phase, it is easy to implement practically and is therefore widely used [7.64].

We begin with an investigation of binary communications and pulsed radar for both nonorthogonal and orthogonal signaling formats in the vacuum channel. In Section 7.3.9, we examine envelope probability distributions and

M. C. Teich, "Nonlinear Heterodyne Detection," in Topics in Applied Physics, vol. 19, Optical and Infrared Detectors, edited by R. J. Keyes (Springer-Verlag, New York, 1st ed.: 1977; 2nd ed.: 1980), ch. 7, pp. 229-300.

binary signaling for sinewave signals in the lognormal channel (clear air turbulent atmosphere). The advantages of the three-frequency nonlinear heterodyne scheme in the digital communications/pulsed radar configuration are similar to those cited for cw radar/analog communications.

We assume here, as previously, that when a signal is present the fields incident on the mixer are parallel, plane polarized, and spatially first-order coherent over the detector aperture. In general, therefore, the input to the square-law device, as previously [see (7.51)], will be two narrowband signals plus white Gaussian noise with zero mean resulting from the LO, over the band $[0, f_n]$. Thus

$$s(t) = A_a \cos(\omega_a t + \phi_a) + A_b \cos(\omega_b t + \phi_b), \tag{7.123}$$

with A_a, A_b, ϕ_a, and ϕ_b stochastic processes. The amplitudes are assumed to be independent of the phases. We first treat the specific case of sinusoidal signals, i.e., A_a and A_b constant and ϕ_a, ϕ_b independent random variables uniformly distributed over $(0, 2\pi)$.

In the time domain, the white Gaussian noise, which arises from the LO, can be expressed as [7.65]

$$n(t) = \sum_{k=1}^{\infty} u_k \cos\omega_k t + \sum_{k=1}^{\infty} v_k \sin\omega_k t. \tag{7.124}$$

Here, $\omega_k = k\omega_0$ with $\omega_0 = 2\pi/2T$. If the input signal is a pulse, the pulse duration is the time interval $(-T, T)$. The coefficients u_k and v_k may therefore be written as

$$u_k = \frac{1}{T}\int_{-T}^{T} n(t)\cos\omega_k t dt, \tag{7.125a}$$

and

$$v_k = \frac{1}{T}\int_{-T}^{T} n(t)\sin\omega_k t dt. \tag{7.125b}$$

(In the alternative, a narrowband representation could be used.) Since u_k and v_k are linear transformations of the Gaussian random variable $n(t)$, they are also Gaussian random variables [7.66]; furthermore it can be shown that for T large, all u_k's and v_k's are uncorrelated and independent of one another [7.67]. Since the mean of $n(t)$ is taken to be zero, we find

$$\langle u_k \rangle = \left\langle \frac{1}{T}\int_{-T}^{T} n(t)\cos\omega_k t dt \right\rangle = 0 \tag{7.126a}$$

and similarly

$$\langle v_k \rangle = 0, \tag{7.126b}$$

M. C. Teich, "Nonlinear Heterodyne Detection," in Topics in Applied Physics, vol. 19, Optical and Infrared Detectors, edited by R. J. Keyes (Springer-Verlag, New York, 1st ed.: 1977; 2nd ed.: 1980), ch. 7, pp. 229-300.

while the variance $\langle u_k^2 \rangle$ is given by

$$\langle u_k^2 \rangle = \frac{1}{T^2} \int_{-T}^{T} \int_{-T}^{T} \langle n(t)n(t') \rangle \cos\omega_k t \cos\omega_k t' dt dt' = \frac{N}{T}. \tag{7.127a}$$

Similarly,

$$\langle v_k^2 \rangle = \frac{N}{T}. \tag{7.127b}$$

In calculating these quantities, we have assumed that the Gaussian noise $n(t)$ is stationary, and that the band $[f_i, f_n]$ is sufficiently large so that the noise can be approximated to be completely white (over an infinite band) leading to an autocorrelation function $R_n(t-t') \simeq N\delta(t-t')$. Here N is the height of the white noise spectrum.

The input $x(t)$ to the square-law device can now be written as

$$\begin{aligned} x(t) &= s(t) + n(t) \\ &= A_a \cos(\omega_a t + \phi_a) + A_b \cos(\omega_b t + \phi_b) \\ &\quad + \textstyle\sum_k u_k \cos\omega_k t + \sum_k v_k \sin\omega_k t. \end{aligned} \tag{7.128}$$

We note that since ω_0 is small, it is always possible to find integers m and n such that $m\omega_0$ and $n\omega_0$ are very close to ω_a and ω_b, respectively. This implies that T is much larger than $2\pi/\omega_a$ and $2\pi/\omega_b$.

By direct substitution, we find the output of the square-law device $y(t)$ to be

$$\begin{aligned} y(t) &= \alpha x^2(t) \\ &= \alpha(\tfrac{1}{2}\textstyle\sum_k u_k^2(1+\cos 2\omega_k t) + \tfrac{1}{2}\sum_k v_k^2(1-\cos 2\omega_k t) \\ &\quad + \textstyle\sum_k u_k v_k \sin 2\omega_k t + \sum\sum_{i>j} u_i u_j[\cos(\omega_i-\omega_j)t + \cos(\omega_i+\omega_j)t] \\ &\quad + \textstyle\sum\sum_{i>j} v_i v_j[\cos(\omega_i-\omega_j)t - \cos(\omega_i+\omega_j)t] \\ &\quad + \textstyle\sum\sum_{i>j} u_i v_j[\sin(\omega_i+\omega_j)t - \sin(\omega_i-\omega_j)t] \\ &\quad + \textstyle\sum\sum_{i<j} u_i v_j[\sin(\omega_i+\omega_j)t + \sin(\omega_j-\omega_i)t] \\ &\quad + \tfrac{1}{2}A_a^2[1+\cos(2\omega_a t + 2\phi_a)] + \tfrac{1}{2}A_b^2[1+\cos(2\omega_b t + 2\phi_b)] \\ &\quad + A_a A_b\{\cos[(\omega_a+\omega_b)t + \phi_a + \phi_b] + \cos[(\omega_a-\omega_b)t + \phi_a - \phi_b]\} \\ &\quad + A_a \textstyle\sum_k u_k\{\cos[(\omega_k+\omega_a)t + \phi_a] + \cos[(\omega_k-\omega_a)t - \phi_a]\} \\ &\quad + A_b \textstyle\sum_k u_k\{\cos[(\omega_k+\omega_b)t + \phi_b] + \cos[(\omega_k-\omega_b)t - \phi_b]\} \\ &\quad + A_a \textstyle\sum_k v_k\{\sin[(\omega_k+\omega_a)t + \phi_a] + \sin[(\omega_k-\omega_a)t - \phi_a]\} \\ &\quad + A_b \textstyle\sum_k v_k\{\sin[(\omega_k+\omega_b)t + \phi_b] + \sin[(\omega_k-\omega_b)t - \phi_b]\}), \end{aligned} \tag{7.129}$$

M. C. Teich, "Nonlinear Heterodyne Detection," in Topics in Applied Physics, vol. 19, Optical and Infrared Detectors, edited by R. J. Keyes (Springer-Verlag, New York, 1st ed.: 1977; 2nd ed.: 1980), ch. 7, pp. 229-300.

where we have used the following symmetrical relations:

$$\tfrac{1}{2}\sum\sum_{i>j} u_i u_j[\cos(\omega_i+\omega_j)t+\cos(\omega_i-\omega_j)t]$$
$$=\tfrac{1}{2}\sum\sum_{i<j} u_i u_j[\cos(\omega_i+\omega_j)t+\cos(\omega_i-\omega_j)t], \tag{7.130a}$$

and

$$\tfrac{1}{2}\sum\sum_{i>j} v_i v_j[\cos(\omega_i+\omega_j)t+\cos(\omega_i-\omega_j)t]$$
$$=\tfrac{1}{2}\sum\sum_{i<j} v_i v_j[\cos(\omega_i+\omega_j)t+\cos(\omega_i-\omega_j)t]. \tag{7.130b}$$

Since it is the effective bandwidth rather than the shape of the final narrowband filter which is important, we choose a realizable impulse response for this filter given by

$$h(t)=2B\cos 2\pi f_c t \qquad 0<t<\frac{1}{B}. \tag{7.131}$$

This choice facilitates the computation in the time domain and provides accord with signal-to-noise ratios calculated previously. Assuming B is very small, the time output from the bandpass filter $z(t)$ is given by

$$z(t)=\int_0^{1/B} h(t-t')y(t')dt$$
$$=A\cos(\omega_c t+\phi)+u\cos\omega_c t+v\sin\omega_c t. \tag{7.132}$$

Here

$$A=\alpha A_a A_b, \tag{7.133a}$$
$$\phi=\phi_a-\phi_b, \tag{7.133b}$$

and after a great deal of calculation, u and v turn out to be the sum of an infinite number of random variables, and therefore Gaussian. The means and variances of u and v are found to be [7.59]

$$\langle u\rangle=\langle v\rangle=0 \tag{7.134}$$

and

$$\langle u^2\rangle=\langle v^2\rangle\simeq 4\alpha^2\frac{N}{T}[2f_n N+(\langle A_a^2\rangle+\langle A_b^2\rangle)], \tag{7.135}$$

assuming $f_0, f_c \ll f_n$. It is also found that

$$\langle uv\rangle=\langle u\rangle\langle v\rangle=0, \tag{7.136}$$

M. C. Teich, "Nonlinear Heterodyne Detection," in Topics in Applied Physics, vol. 19, Optical and Infrared Detectors, edited by R. J. Keyes (Springer-Verlag, New York, 1st ed.: 1977; 2nd ed.: 1980), ch. 7, pp. 229-300.

indicating that u and v are uncorrelated and independent processes. Equations (7.134), (7.135), and (7.136) indicate that the last two terms in (7.132), $u\cos\omega_c t + v\sin\omega_c t$, constitute a narrowband Gaussian random process with zero mean and center frequency ω_c. In fact, (7.135) represents the output noise power N_0.

We can corroborate this rather broad result [7.59] for a specific case by generalizing the results obtained by *Kac* and *Siegert* [7.68] and *Emerson* [7.69], who have treated a related problem. We assume the output of the heterodyne mixer to consist of two sinewave signals plus uncorrelated (white) Gaussian noise. The system, in this case, consists of a realizable IF Gaussian bandpass filter, with arbitrary width Δf and a center frequency around f_a or f_b (which is large in comparison with f_c), the usual square-law device, and a realizable final narrowband filter with bandwidth B. Under the restrictions $f_c \ll f_a, f_b$ and $B \ll f_c \ll \Delta f$, it may be shown that the output of the final narrowband filter will be a sinewave signal plus a Gaussian random process. For noise alone, the output will simply be Gaussian. Thus the envelope distribution for noise will be Rayleigh, while that for signal-plus-noise will be Rician. This is we might add, the same result obtained for conventional two-frequency heterodyne detection, although the means and variances will not have the same relationship in that case.

For $f_c \ll f_n$, as prescribed previously, it is not difficult to verify that the above description in the time domain is in accord with the frequency-domain results presented previously. Since the relationship between the pulse width T and the minimum bandwidth of the final filter is governed by the Fourier transform property $TB \sim 1$ [7.70], (7.135) for the noise power in this regime may be written as

$$\langle u^2\rangle = \langle v^2\rangle = N_0 \simeq 4\alpha^2 NB[2f_n N + (\langle A_a^2\rangle + \langle A_b^2\rangle)]. \tag{7.137}$$

Using (7.133a), we therefore obtain for the output signal-to-noise ratio

$$(\mathrm{SNR})_0 = \frac{S_0}{N_0} = \frac{\langle A^2\rangle}{2\langle u^2\rangle} = \frac{\langle A_a^2 A_b^2\rangle}{8NB[(\langle A_a^2\rangle + \langle A_b^2\rangle)2f_n N]}. \tag{7.138}$$

Using an input signal-to-noise ratio given by

$$(\mathrm{SNR})_i = \frac{\langle A_a^2\rangle + \langle A_b^2\rangle}{4f_n N}, \tag{7.139}$$

we finally obtain

$$(\mathrm{SNR})_0 = \frac{k_Q(\mathrm{SNR})_i^2}{1 + 2(\mathrm{SNR})_i}, \tag{7.140}$$

with

$$k_Q = \frac{f_n\langle A_a^2 A_b^2\rangle}{B(\langle A_a^2\rangle + \langle A_b^2\rangle)^2} = \frac{f_n\langle A_1^2 A_2^2\rangle}{B(\langle A_1^2\rangle + \langle A_2^2\rangle)^2}. \tag{7.141}$$

M. C. Teich, "Nonlinear Heterodyne Detection," in Topics in Applied Physics, vol. 19, Optical and Infrared Detectors, edited by R. J. Keyes (Springer-Verlag, New York, 1st ed.: 1977; 2nd ed.: 1980), ch. 7, pp. 229-300.

These expressions are valid in the regime $f_c \ll f_n$, and are analogous to (7.72) and (7.73) of Section 7.3.2. Our treatment is therefore consistent with that presented previously.

According to (7.132) and the discussion following, in the presence of signal plus noise the output of the narrowband final filter $z(t)$, after being passed through the envelope detector, is given by the Rician distribution [7.71]

$$f_1(r) = \frac{r}{\sigma^2} I_0\left(\frac{Ar}{\sigma^2}\right) \exp\left(-\frac{r^2 + A^2}{2\sigma^2}\right). \tag{7.142}$$

Here, r represents the envelope of $z(t)$, $\sigma^2 = \langle u^2 \rangle = 4\alpha^2 NB[2f_n N + (\langle A_a^2 \rangle + \langle A_b^2 \rangle)]$, and $I_0(x)$ is the modified Bessel function of the first kind and zero order, also expressible as

$$I_0(x) = \frac{1}{2\pi} \int_0^{2\pi} \exp(x \cos\theta) d\theta. \tag{7.143a}$$

We may use the asymptotic expansion for $x \ll 1$ [7.72],

$$I_0(x) = 1 + \frac{x^2}{4} + \ldots \simeq e^{x^2/4}, \tag{7.143b}$$

while for $x \gg 1$,

$$I_0(x) \simeq \frac{e^x}{\sqrt{2\pi x}}. \tag{7.143c}$$

In the presence of noise alone, i.e., for $A_a = A_b = 0$, the probability density function for the envelope $f_0(r)$ is the Rayleigh distribution

$$f_0(r) = \frac{r}{\sigma_0^2} \exp\left(-\frac{r^2}{2\sigma_0^2}\right). \tag{7.144}$$

Here σ_0^2 is the noise power in the absence of signal, i.e.,

$$\sigma_0^2 = \langle u^2 \rangle|_{A_a = A_b = 0} = 8\alpha^2 B f_n N^2. \tag{7.145}$$

We note that in our nonlinear problem $\sigma^2 \neq \sigma_0^2$ because of the presence of s × n terms in σ^2. In the usual linear systems problem, these terms do not appear, and $\sigma^2 = \sigma_0^2$.

Given the probability distributions for the output signals, we can proceed to investigate binary communications and pulsed radar systems performance upon choosing a decision rule. In the following, we consider both orthogonal and nonorthogonal formats for digital signaling.

M. C. Teich, "Nonlinear Heterodyne Detection," in Topics in Applied Physics, vol. 19, Optical and Infrared Detectors, edited by R. J. Keyes (Springer-Verlag, New York, 1st ed.: 1977; 2nd ed.: 1980), ch. 7, pp. 229-300.

Nonorthogonal Signaling Formats

We first consider pulse-code modulation where it is the intensity which is modulated. This simple nonorthogonal scheme is frequently referred to as PCM/IM [7.73]. The signal is considered to be present when a 1 is transmitted, and absent when a 0 is transmitted. To evaluate system performance, we choose the likelihood-ratio criterion [7.72, 73]. If Q represents the *a priori* probability that a 1 is transmitted, the signal is judged to be present if

$$Qf_1(r) \gtrless (1-Q)f_0(r). \tag{7.146}$$

For simplicity, we assume throughout that the different types of errors are equally costly. Since the signals are pulse coded, the value of r chosen is the average value over the pulse width. The decision threshold r_D is the value of r for which the equality in (7.146) holds. Using (7.142), (7.143a), and (7.144) for sinewave signals and Gaussian noise, r_D is therefore the solution to the transcendental equation

$$\frac{1}{2\pi}\int_0^{2\pi} \exp\left(\frac{Ar}{\sigma^2}\cos\theta\right)d\theta = \left(\frac{1-Q}{Q}\right)\frac{\sigma^2}{\sigma_0^2} e^{A^2/2\sigma^2} \exp\left(-\frac{\sigma^2-\sigma_0^2}{2\sigma_0^2\sigma^2}r^2\right). \tag{7.147}$$

Using (7.137) and (7.141), it is clear that

$$\sigma^2 = \sigma_0^2(1+2\sqrt{\xi_0/k_Q}), \tag{7.148}$$

where

$$\xi_0 \equiv \frac{\langle A^2\rangle}{2\sigma_0^2}. \tag{7.149}$$

For sinewave inputs, A, A_a, and A_b are constant and the quantity k_Q is identical with the quantity k_P introduced earlier [see (7.72), Sec. 7.3.2]. Defining $r_0 \equiv r/\sigma_0$, (7.147) can be rewritten as

$$\frac{1}{2\pi}\int_0^{2\pi} \exp\left(\frac{\sqrt{2\xi_0}r_0\cos\theta}{1+2\sqrt{\xi_0/k_P}}\right)d\theta = \left(\frac{1-Q}{Q}\right)\left(1+2\sqrt{\frac{\xi_0}{k_P}}\right)\exp\left(\frac{\xi_0}{1+2\sqrt{\xi_0/k_P}}\right) \cdot \exp\left(-\frac{r_0^2\sqrt{\xi_0/k_P}}{1+2\sqrt{\xi_0/k_P}}\right). \tag{7.150}$$

M. C. Teich, "Nonlinear Heterodyne Detection," in Topics in Applied Physics, vol. 19, Optical and Infrared Detectors, edited by R. J. Keyes (Springer-Verlag, New York, 1st ed.: 1977; 2nd ed.: 1980), ch. 7, pp. 229-300.

Therefore, with k_P and Q fixed, the solution to (7.150) for r_0, which we call $\hat{r}_0$, is a function only of ξ_0. If we further define

$$\xi' \equiv (\mathrm{SNR})_0 = \frac{\langle A^2 \rangle}{2\sigma^2}, \tag{7.151}$$

then the quantity $\xi' = (\sigma_0^2/\sigma^2)\xi_0 = \xi_0/(1+2\sqrt{\xi_0/k_P})$ is also a function only of ξ_0. Thus, $\hat{r}_0$ is a function only of ξ'. The decision threshold $r_D \equiv \sigma_0 \hat{r}_0$ is therefore a function of both ξ' and σ_0.

The probability of a decoding error P_e is given by

$$P_e = Q\int_0^{r_D} f_1(r)dr + (1-Q)\int_{r_D}^{\infty} f_0(r)dr, \tag{7.152}$$

which in the present case, may be written as

$$P_e = Q\int_0^{r_D} \frac{r}{\sigma^2} I_0\left(\frac{Ar}{\sigma^2}\right) e^{-\frac{r^2+A^2}{2\sigma^2}} dr + (1-Q)\int_{r_D}^{\infty} \frac{r}{\sigma_0^2} e^{-\frac{r^2}{2\sigma_0^2}} dr. \tag{7.153}$$

Replacing r/σ by r', we can rewrite the first integral I_1 in (7.152) as follows

$$I_1 = \int_0^{\hat{r}_0\sigma_0/\sigma} r' I_0(\sqrt{2\xi'}r') e^{-\left(\frac{r'^2}{2}+\xi'\right)} dr'. \tag{7.154}$$

Since $\hat{r}_0\sigma_0/\sigma = \hat{r}_0/(1+2\sqrt{\xi_0/k_P})^{1/2}$ is a function only of ξ_0 which, in turn, is a function only of the output signal-to-noise ratio ξ', this integral is a function only of ξ'. The second integral in (7.153) can be easily evaluated as follows:

$$\int_{r_D}^{\infty} \frac{r}{\sigma_0^2} e^{-r^2/2\sigma_0^2} dr = \int_{r_D/\sigma_0}^{\infty} x e^{-x^2/2} dx = -e^{-x^2/2}\Big|_{r_D/\sigma_0}^{\infty} = e^{-r_D^2/2\sigma_0^2} = e^{-\hat{r}_0^2/2}, \tag{7.155}$$

which is also a function only of ξ'.

Therefore, with fixed $k_P(\propto f_n/B)$ and fixed Q, the probability of error P_e is a function only of the output signal-to-noise ratio $\xi' \equiv (\mathrm{SNR})_0$. By use of (7.141), in turn, P_e can be written in terms of $(\mathrm{SNR})_i$. Computer results for the probability of error are presented in Fig. 7.16 [(7.143) has been used for the computer calculation], in which P_e is plotted against $(\mathrm{SNR})_i$ for several values of f_n/B, with the usual choice $Q = 0.5$ and $A_a = A_b$. The solid curves represent this PCM/IM scheme. For fixed f_n, the advantage of using small B is obvious.

Also shown in Fig. 7.16 is the P_e versus SNR curve for the conventional two-frequency heterodyne system in which no square-law device is used and f_n must be narrowed to Δf to provide a detectable signal. The output for this case is again a sinewave signal plus a narrowband (Δf) Gaussian noise [7.73]. Thus the

M. C. Teich, "Nonlinear Heterodyne Detection," in Topics in Applied Physics, vol. 19, Optical and Infrared Detectors, edited by R. J. Keyes (Springer-Verlag, New York, 1st ed.: 1977; 2nd ed.: 1980), ch. 7, pp. 229-300.

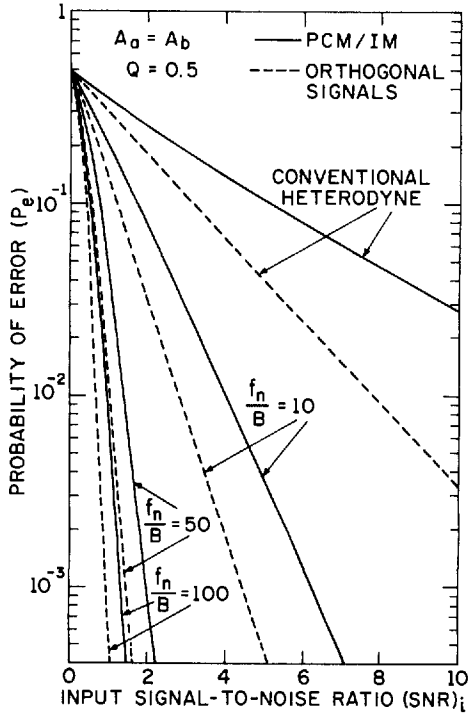

Fig. 7.16a. Probability of error vs $(SNR)_i$ for the three-frequency binary communication system in the vacuum channel. The input signals are assumed to be sinusoidal while the noise is Gaussian. The result for the conventional heterodyne system is shown for comparison (log vs linear plot)

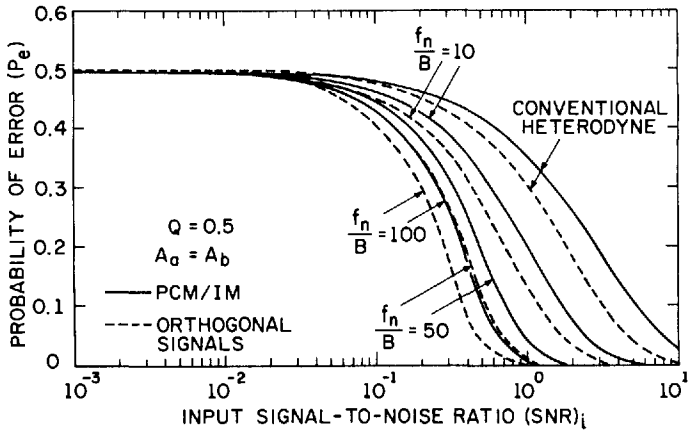

Fig. 7.16b. Same curves as Fig. 7.16a on a linear vs log plot

computation is the same as for the three-frequency heterodyne case with $\sigma^2 = \sigma_0^2$ and $\xi' = \xi_0 = (SNR)_i$. The probability of error at a given signal-to-noise ratio for the ordinary heterodyne system is seen to be higher than for the three-frequency system. This results from the exclusion of noise demanded by the final bandpass filter where $f_n/B > 1$, thus providing higher $(SNR)_0$ and lower P_e for the three-

frequency system. Since the Rician and Rayleigh distributions have been calculated only for $B \ll f_c$ (hence $B \ll f_n$) and for white noise, the optimum three-frequency case considered previously is not shown in Fig. 7.16.

Pulsed Radar Application

The three-frequency nonlinear heterodyne system can also be used for pulsed radar applications. The configuration is similar to that considered previously. Pulses are sent to the target and the maximum-likelihood test is used to determine whether the target is or is not present (reflected or scattered signal deemed present or absent). For a detailed treatment of conventional range-gated pulsed radar applications, the reader is referred to the book by *Davenport* and *Root* [7.74].

Orthogonal Signaling Formats

We consider a number of orthogonal signaling formats—we begin with frequency shift keying (FSK) which is also referred to as PCM/FM. In such a scheme, the frequency of one of the transmitted beams is fixed at the value f_1, while the frequency of the other is caused to shift between two values, f_2 and f_2' (not to be confused with the Doppler shifted f_2' considered earlier). When a 1(0) is transmitted, the second carrier will be at frequency $f_2(f_2')$. The difference frequency will therefore shift between $f_c = f_1 - f_2$ and $f_c' = f_1 - f_2'$ (assuming $f_1 > f_2, f_2'$). The frequencies $|f_1 - f_L|$, $|f_2 - f_L|$, and $|f_2' - f_2|$ will all lie within the band f_n. A block diagram for such a system is shown in Fig. 7.17. Two narrow bandpass final filters with center frequencies at f_c and f_c' (not to be confused with the Doppler shifted f_c' considered earlier) are used. Following each bandpass filter is an envelope detector. If a 1(0) is transmitted, the signal will ideally pass through the top (bottom) narrow bandpass filter along with the noise; only noise will be present at the other filter.

For such an orthogonal format, the optimum single detector receiver chooses the largest signal as the correct one. Let the outputs of the first and second envelope detectors be represented by r_1 and r_2, respectively, while the probability density functions for r_1 and r_2 are $h_1(r_1)$ and $h_2(r_2)$, respectively. If we assume that a 1 is transmitted, we have

$$h_1(r_1) = f_1(r_1), \tag{7.156a}$$

$$h_2(r_2) = f_0(r_2), \tag{7.156b}$$

where $f_1(\cdot)$ and $f_0(\cdot)$ are given by (7.142) and (7.144), respectively. Using the decision rule of the largest, error occurs during times when $r_2 > r_1$. The error probability P_{e_1} is, therefore,

$$P_{e_1} = \int_0^\infty dr_1 [f_1(r_1) \int_{r_1}^\infty dr_2 f_0(r_2)]$$

$$= \frac{\sigma_0^2}{\sigma_0^2 + \sigma^2} e^{-A^2/2(\sigma_0^2 + \sigma^2)}. \tag{7.157}$$

M. C. Teich, "Nonlinear Heterodyne Detection," in Topics in Applied Physics, vol. 19, Optical and Infrared Detectors, edited by R. J. Keyes (Springer-Verlag, New York, 1st ed.: 1977; 2nd ed.: 1980), ch. 7, pp. 229-300.

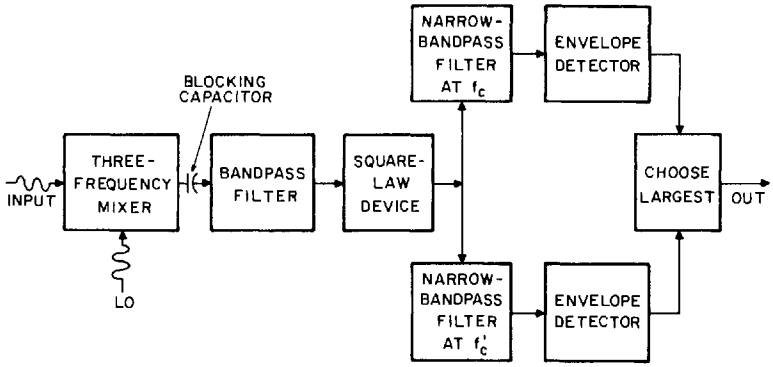

Fig. 7.17. Block diagram for the PCM/FM three-frequency nonlinear heterodyne receiver

This can be readily shown to be a function only of ξ'. In exactly the same manner, the error probability P_{e_0}, when 0 is transmitted, is given by the same expression; thus $P_{e_0}=P_{e_1}$. The overall probability of error P_e is therefore given by

$$P_e=QP_{e_1}+(1-Q)P_{e_0}=P_{e_1}, \tag{7.158}$$

which is presented in Fig. 7.16 in dashed form with the same parameters as for the PCM/IM case. The conventional heterodyne case is also shown [7.73]. The improvement obtained by using the orthogonal PCM/FM signaling format is seen to be substantial.

Another binary orthogonal pulse-code modulation scheme is polarization modulation (PCM/PL). Thus the bit 1(0) is represented by right (left) circular or vertical (horizontal) linear polarization. At the transmitter, a polarization modulator converts the laser beam into one of two polarization states. At the receiver (see Fig. 7.18), the circularly polarized beam may be passed through an optical filter and then be converted to horizontal or vertical linear polarization by a quarter-wave plate. The linear polarization components are spatially separated (e.g., by a Wollaston prism) so that the vertically polarized component will strike the upper photodetector and the horizontally polarized component will strike the lower photodetector. With 100% modulation, when the bit 1 is transmitted, only vertical polarization will appear at the receiver and the radiation will ideally strike only the upper detector. When a 0 is transmitted, only horizontal polarization will appear and a signal will ideally strike only the lower detector. The "choice of largest" decision rule is used for decoding. It is not difficult to see that the results for P_e in this case are identical to those for the PCM/FM system. Depolarization effects of the atmosphere, which are not generally large, will result in a decrease of $(\mathrm{SNR})_i$ and thus $(\mathrm{SNR})_0$ [7.75–78].

The final orthogonal format which we consider is binary pulse-position modulation (PPM/IM). In this scheme, each bit period is divided into two equal subintervals. If a 1(0) is transmitted, the pulse is caused to occur in the first (second) subinterval. A block diagram for one implementation of such a system

M. C. Teich, "Nonlinear Heterodyne Detection," in Topics in Applied Physics, vol. 19, Optical and Infrared Detectors, edited by R. J. Keyes (Springer-Verlag, New York, 1st ed.: 1977; 2nd ed.: 1980), ch. 7, pp. 229-300.

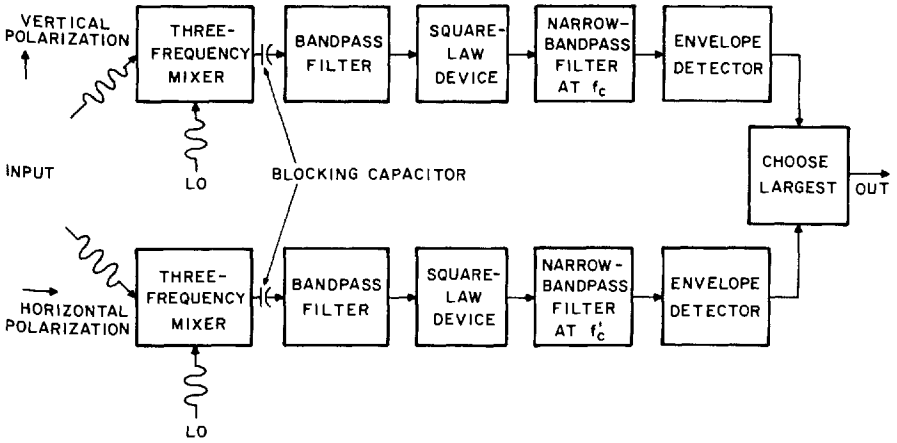

Fig. 7.18. Block diagram for the PCM/PL three-frequency nonlinear heterodyne receiver

is presented in Fig. 7.19. The upper (lower) gate is open for every initial (final) subinterval, and closed for every final (initial) subinterval. A time delay equal to the subinterval length is provided for the signal in the upper gate so that the outputs for both intervals can be compared at the same time. The rule of largest decision is used for decoding. The results for the probability of error are again the same as those for the PCM/FM system.

The input signals for the PCM/FM, PCM/PL, and PPM/IM systems possess the orthogonality property

$$\int_{-T}^{T} S_1(t)S_0(t)dt = 0, \tag{7.159}$$

where $S_1(t)$ is the signal waveform representing a 1 state, and $S_0(t)$ is the signal waveform representing a 0 state. Depending on specific definitions, such orthogonal modulation schemes are generally superior to nonorthogonal

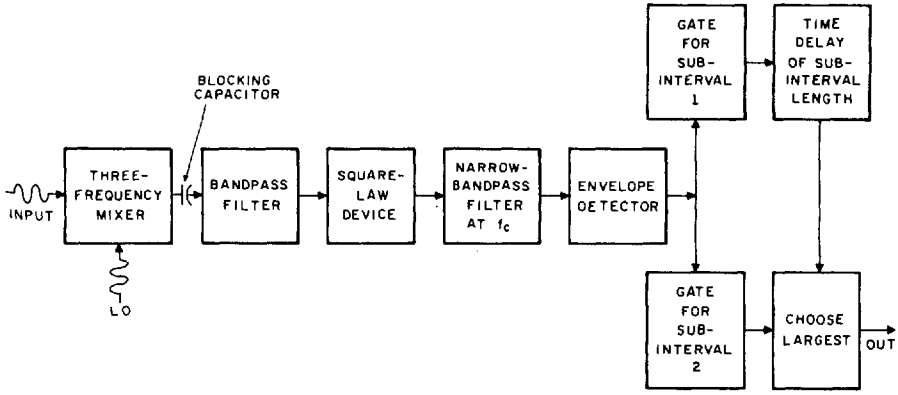

Fig. 7.19. Block diagram for the PPM/IM three-frequency nonlinear heterodyne receiver

M. C. Teich, "Nonlinear Heterodyne Detection," in Topics in Applied Physics, vol. 19, Optical and Infrared Detectors, edited by R. J. Keyes (Springer-Verlag, New York, 1st ed.: 1977; 2nd ed.: 1980), ch. 7, pp. 229-300.

schemes in terms of error probability performance [7.76–78] and have the further advantage of requiring no more than a simple comparison for optimum reception. The M-ary signaling case is a straightforward generalization of the binary case [7.79].

7.3.9 Application to Binary Communications and Pulsed Radar (Lognormal Atmospheric Channel)

Whereas the previous section (7.3.8) was concerned with the calculation of system performance for the vacuum channel, we now turn to the error probabilities for three-frequency nonlinear heterodyne detection for the atmospheric channel. The behavior of the clear-air turbulent atmosphere as a lognormal channel for optical radiation has been well documented both theoretically and experimentally [7.76–78, 80–82]. We therefore choose the amplitudes A_1 and A_2 to be lognormally distributed, and the phases ϕ_1 and ϕ_2 to be uniformly distributed over $(0, 2\pi)$. Since $A_a \propto A_1$ and $A_b \propto A_2$, while $\phi_a = \phi_1 - \phi_L$ and $\phi_b = \phi_2 - \phi_L$, we can write

$$A_a = u_a B_a, \tag{7.160a}$$

$$A_b = u_b B_b, \tag{7.160b}$$

where B_a and B_b are constants, and u_a and u_b have the same lognormal distribution

$$P_N(u_i) = \frac{1}{\sigma_\chi u \sqrt{2\pi}} \exp\left[-\frac{1}{2\sigma_\chi^2}(\ln u_i - m)^2\right], \qquad i = a, b. \tag{7.161}$$

Here σ_χ is the logarithmic-amplitude standard deviation which is related to the logarithmic-irradiance standard deviation σ by the formula $4\sigma_\chi^2 = \sigma^2$ [7.82]. Assuming energy is conserved and that there is no scattering of radiation out of the beam, we choose

$$\langle u_i^2 \rangle = 1 \tag{7.162}$$

which is equivalent to setting $m = -\sigma_\chi^2$.

Using (7.133a) the output amplitude A is given by

$$A = \alpha A_a A_b = \alpha B_a B_b u_a u_b. \tag{7.163}$$

If u_a and u_b are independent, we obtain

$$\langle A^2 \rangle = \alpha^2 B_a^2 B_b^2 \langle u_a^2 \rangle \langle u_b^2 \rangle = \alpha^2 B_a^2 B_b^2, \tag{7.164a}$$

M. C. Teich, "Nonlinear Heterodyne Detection," in Topics in Applied Physics, vol. 19, Optical and Infrared Detectors, edited by R. J. Keyes (Springer-Verlag, New York, 1st ed.: 1977; 2nd ed.: 1980), ch. 7, pp. 229-300.

or

$$\alpha B_a B_b = \sqrt{\langle A^2 \rangle} = \sqrt{\alpha^2 \langle A_a^2 A_b^2 \rangle} \,. \tag{7.164b}$$

Furthermore,

$$\ln A = \ln u_a + \ln u_b + \ln \alpha B_a B_b \,. \tag{7.165}$$

Since the quantities $y_a \equiv \ln u_a$ and $y_b \equiv \ln u_b$ will both be normally distributed as

$$f_N(y_i) = \frac{1}{\sqrt{2\pi}\sigma_\chi} \exp\left[-\frac{1}{2\sigma_\chi^2} (y_i + \sigma_\chi^2)^2 \right], \tag{7.166}$$

if u_a and u_b are independent, the variable $y_L = \ln A$ will have the normal distribution

$$f_L(y_L) = \frac{1}{2\sigma_\chi \sqrt{\pi}} \exp\left[-\frac{1}{4\sigma_\chi^2} (y_L + 2\sigma_\chi^2 - \ln \alpha B_a B_b)^2 \right], \tag{7.167}$$

from which we obtain the probability density for A

$$f_A(A) = \frac{1}{2\sigma_\chi \sqrt{\pi A}} \exp\left[-\frac{1}{4\sigma_\chi^2} \left(\ln \frac{A}{\sqrt{\langle A^2 \rangle}} + 2\sigma_\chi^2 \right)^2 \right], \tag{7.168}$$

u_a, u_b independent, where we have made use of (7.164b).

We also consider the situation $u_a = u_b = u$, which would arise if both incoming signals were sufficiently close in frequency and space such that they suffered precisely the same fluctuations at each instant of time [7.83]. This case is more likely to occur in a practical situation than the independent case. For dependent fluctuations, then,

$$A = \alpha A_a A_b = \alpha B_a B_b u^2 \,, \tag{7.169}$$

whence

$$\langle A \rangle = \alpha \langle A_a A_b \rangle = \alpha B_a B_b \,, \tag{7.170}$$

and

$$\ln A = \ln \langle A \rangle + 2 \ln u \,. \tag{7.171}$$

Since $\ln u$ has the normal distribution $f_L(u)$ as given by (7.166), we find that the variable $y_L = \ln A$ has the normal probability density function

$$f_N(y_L) = \frac{1}{2\sigma_\chi \sqrt{2\pi}} \exp\left[-\frac{1}{8\sigma_\chi^2} (y_L + 2\sigma_\chi^2 - \ln \langle A \rangle)^2 \right]. \tag{7.172}$$

M. C. Teich, "Nonlinear Heterodyne Detection," in Topics in Applied Physics, vol. 19, Optical and Infrared Detectors, edited by R. J. Keyes (Springer-Verlag, New York, 1st ed.: 1977; 2nd ed.: 1980), ch. 7, pp. 229-300.

By variable transformation, we obtain the probability density function for A as

$$f_A(A)=\frac{1}{2\sigma_\chi\sqrt{2\pi A}}\exp\left[-\frac{1}{8\sigma_\chi^2}\left(\ln\frac{A}{\langle A\rangle}+2\sigma_\chi^2\right)^2\right],\qquad u_a=u_b. \tag{7.173}$$

This equation appears similar to (7.168); we note that $\sqrt{\langle A^2\rangle}$ is replaced by $\langle A\rangle$ and the effective variance has been doubled. This results in a flattening and broadening of the probability density for the case of identical disturbance to both beams, $u_a=u_b$.

For atmospheric fluctuations which vary slowly in comparison with the pulse time T (this is the usual case, see [7.76–78, 81–83]) the three-frequency system envelope output will be Rician during each time interval. The over-all envelope distribution in the presence of the atmosphere $f_{1A}(r)$ will therefore be a Rician smeared over all possible values of A,

$$f_{1A}(r)=\int_0^\infty f_1(r|A)f_A(A)dA, \tag{7.174}$$

where $f_1(r|A)$ is given by (7.142). In the absence of signal, the envelope probability density remains as it was before [see (7.144)] since the noise alone arises from the local oscillator which is unaffected by atmospheric fluctuations. Thus,

$$f_{0A}(r)=f_0(r). \tag{7.175}$$

Under the assumptions leading to (7.174), and considering the various modulation schemes discussed previously, the probability of error in the presence of the lognormal turbulent atmosphere is given by

$$P_e(\text{turbulent})=\int_0^\infty P_e(\text{quiescent})\,f_A(A)dA. \tag{7.176}$$

This quantity was calculated using the Columbia University IBM-OS 360 computer, and the results are presented in Figs. 7.20–23. In Figs. 7.20 and 7.21, the quantities A_a and A_b were assumed to be independent with the same signal power $\langle A_a^2\rangle=\langle A_b^2\rangle$. The error probability curves displayed in these figures correspond to two values of the log-amplitude variance, $\sigma_\chi^2=0.25$ and $\sigma_\chi^2=0.57$. These correspond approximately to $\sigma=1$ and $\sigma=1.5$ (saturation value) [7.81, 82]. Other parameters are identical to those for the quiescent atmosphere as shown in Fig. 7.16. Figures 7.22 and 7.23 are analogous to Figs. 7.20 and 7.21, with the exception of the fact that $A_a=A_b$. For all cases, the results for conventional heterodyne operation are also shown in Figs. 7.20 and 7.21. For $\sigma_\chi\to 0$, the results properly reduce to the quiescent atmosphere data presented in Fig. 7.16. Computer results also indicate that the probability of error curves depend only on the signal-to-noise ratio and not on the absolute noise level in the presence of the lognormal channel, as well as in its absence.

From the graphical data presented in Figs. 7.16, 7.20–7.23, it is clear that orthogonal signaling formats yield better performance than nonorthogonal PCM/IM (this is also the case for direct detection [7.76–78]). Error probabilities

M. C. Teich, "Nonlinear Heterodyne Detection," in Topics in Applied Physics, vol. 19, Optical and Infrared Detectors, edited by R. J. Keyes (Springer-Verlag, New York, 1st ed.: 1977; 2nd ed.: 1980), ch. 7, pp. 229-300.

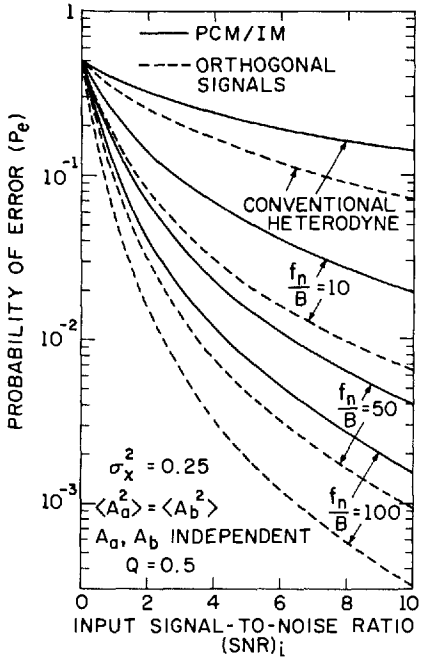

Fig. 7.20. Probability of error vs $(SNR)_i$ for the three-frequency binary communication system with atmospheric turbulence at the level $\sigma_x^2 = 0.25$. The input amplitudes A_a and A_b are assumed to be independent, and the noise is Gaussian. The result for the conventional heterodyne system is shown for comparison

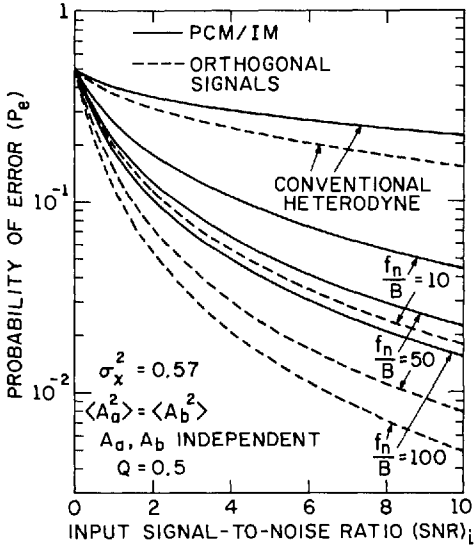

Fig. 7.21. Probability of error vs $(SNR)_i$ for the three-frequency binary communication system with atmospheric turbulence at the level $\sigma_x^2 = 0.57$. The input amplitudes A_a and A_b are assumed to be independent, and the noise is Gaussian. The result for the conventional heterodyne system is shown for comparison

are seen to increase with increasing atmospheric turbulence levels. Independent fluctuations in the two signal beams serve as a kind of diversity and thereby improve receiver performance. In all cases, furthermore, it is evident that three-frequency nonlinear heterodyne detection can provide improved performance over conventional heterodyne detection, particularly as the ratio f_n/B increases.

M. C. Teich, "Nonlinear Heterodyne Detection," in Topics in Applied Physics, vol. 19, Optical and Infrared Detectors, edited by R. J. Keyes (Springer-Verlag, New York, 1st ed.: 1977; 2nd ed.: 1980), ch. 7, pp. 229-300.

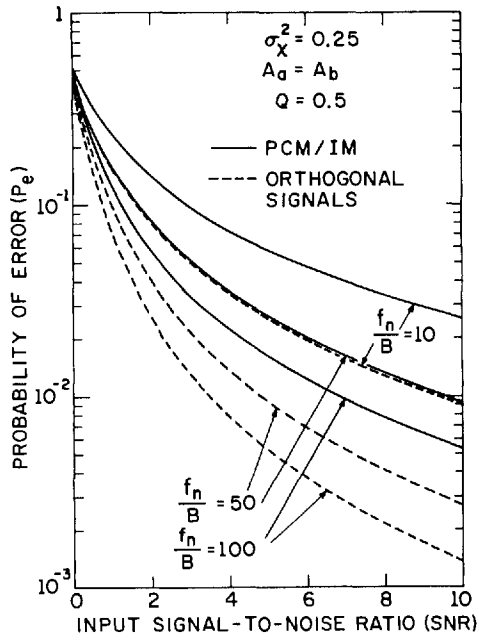

Fig. 7.22. Probability of error vs $(SNR)_i$ for the three-frequency binary communication system with atmospheric turbulence at the level $\sigma_X^2 = 0.25$. We assume $A_a = A_b$

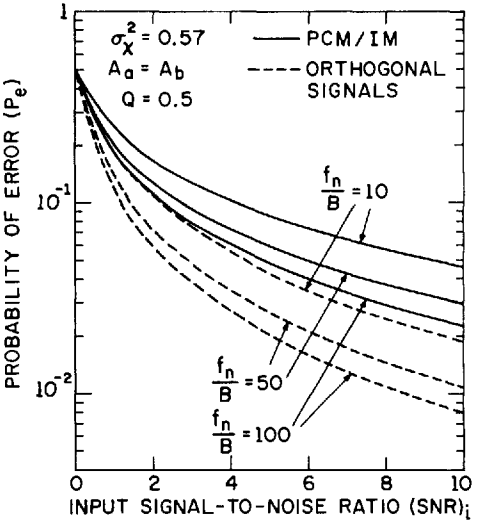

Fig. 7.23. Probability of error vs $(SNR)_i$ for the three-frequency binary communication system with atmospheric turbulence at the level $\sigma_X^2 = 0.57$. We assume $A_a = A_b$

Finally, receiver performance for the cases of phase detection with a maximum-likelihood criterion [7.84] and phase-shift keying (PSK) have also been obtained [7.59]. While PSK is definitely superior to phase detection, neither scheme provides very satisfactory error probabilities.

The next section (7.3.10) presents an over-all discussion of the usefulness of the three-frequency nonlinear heterodyne technique for radar and communications applications.

M. C. Teich, "Nonlinear Heterodyne Detection," in Topics in Applied Physics, vol. 19, Optical and Infrared Detectors, edited by R. J. Keyes (Springer-Verlag, New York, 1st ed.: 1977; 2nd ed.: 1980), ch. 7, pp. 229-300.

7.3.10 Discussion

The three-frequency nonlinear heterodyne detection scheme has certain advantages over the conventional single-photon two-frequency configuration for both analog and digital systems. One advantage is the possibility of increasing the detection sensitivity, and minimizing the probability of error, particularly when little Doppler information is available. It provides an output signal at a well-known difference frequency regardless of the Doppler shift of the transmitted signals. Frequency scanning of the LO or receiver may therefore be eliminated. It allows a target to be continuously observed with Doppler shifts of greater magnitude and range than previously possible. The system is also angle independent in the sense that the Doppler shift is proportional to the radial velocity and therefore is generally a function of angle. A wide bandpass filter following the square-law device can be gradually narrowed about $2|f_1' - f_L|$ or $2|f_2' - f_L|$ in order to obtain Doppler information. If Doppler information is increased, we find that the receiver performance can be improved, in accordance with our expectations.

Since the use of a two-frequency transmitter can be considered as a special case of a modulated single-frequency beam, the system can be thought of as a heterodyne version of signal extraction at a predetermined modulation frequency. Thus, the technique is similar to conventional heterodyne radiometry, but *carefully takes into consideration the effects of Doppler shift and signal statistics.* Since Doppler shift is generally not an important parameter in the usual heterodyne radiometry detection scheme, the final filter bandwidth (associated with the integration time) can almost always be made arbitrarily small; furthermore, it is often possible to maintain a fixed phase relationship between the reference and detected signals, so that an additional factor of 2 (arising from coherent detection) becomes available. These specific benefits are not available for three-frequency nonlinear heterodyne detection.

Under the usual conditions of Doppler uncertainty, optimum operation occurs with the known difference frequency f_c at a maximum value close to f_n, or with the LO frequency between the received signal frequencies, and requires that the radiation power be equally divided between the two received beams. Processing of the dc output from the square-law device was not found to be useful when a blocking capacitor is included in the system. Four-frequency mixing was found to provide acceptable performance only when one of the LO frequencies is substantially attenuated.

Signals of three varieties were considered: a) sinewave input signals, b) Gaussian input signals with Gaussian power spectra, and c) Gaussian input signals with Lorentzian power spectra. Taking the pure sinewave case as a standard, the output signal-to-noise ratio for Gaussian signals is degraded by the factor $[2\Phi(u) - 1] < 1$ (for Gaussian spectra) or by the factor $\{(1/\pi)\tan^{-1}[4v/(4-v^2)]\} < 1$ (for Lorentzian spectra), where u and v are quantities proportional to the bandwidth B of the final narrowband filter. In all cases, decreasing B serves to increase the signal-to-noise ratio and decrease the

M. C. Teich, "Nonlinear Heterodyne Detection," in Topics in Applied Physics, vol. 19, Optical and Infrared Detectors, edited by R. J. Keyes (Springer-Verlag, New York, 1st ed.: 1977; 2nd ed.: 1980), ch. 7, pp. 229-300.

minimum detectable power. In the Gaussian cases, it was found desirable to keep the width of the spectra as small as possible in order to maximize the signal-to-noise ratio.

The digital results, in particular, may be easily extended in a number of directions. Stochastic signals, rather than sinewave signals, could be treated in the binary communication problem. An extensive treatment of M-ary communications is possible, as is the generalization from a single detector to an array of detectors [7.76–78]. Consideration could be given to the optimum matched filter detector rather than the envelope detector discussed earlier. While the present treatment consists of a per-symbol analysis, prediction could be used to estimate the atmospheric turbulence level over a time period from a particular symbol, for example. In short, the usual variations possible with the conventional heterodyne system may be extended and/or modified for application to the three-frequency nonlinear heterodyne technique.

The principle appears to be applicable in all regions of the electromagnetic spectrum where conventional heterodyne detection is useful. In the next section (7.4), we consider two versions of the system useful for the detection of remote species.

7.4 Multifrequency Single-Photon Selective Heterodyne Radiometry for Detection of Remote Species

The radiation from known remote species, such as extraterrestrial molecules and smokestack effluents, is generally shifted as well as broadened in frequency when detected at a receiving station. Shifts in the center frequency can be attributed to a number of effects, including Doppler shift arising from the mass motion of a group of molecules and red shift arising from emission in the presence of a strong gravitational field. The magnitude of the Doppler shift is proportional to velocity and can be quite large, leading to an uncertainty in the appropriate frequency at which to search for a weak signal. This problem is magnified at high frequencies since Doppler shift is also proportional to frequency.

In this section, we consider using a passive version of the three-frequency single-photon heterodyne technique for partially eliminating the effects of Doppler shift in detecting remotely radiating objects. It is useful where a pair (or pairs) of emission lines exists with a definite and well-known frequency separation, such as those produced by two transitions of a given molecular species or by a given transition of two isotopes of that species. If the two radiated frequencies are close to each other, they are Doppler shifted by essentially the same amount (as with the active system) so that the effects of Doppler shift can be made to nearly cancel in the difference frequency. By employing two signal frequencies instead of one, an effective modulation of the source is achieved so that the bandwidth of the receiver can be narrowed about the difference frequency, in a manner similar to that accomplished by using a radiometer. But

M. C. Teich, "Nonlinear Heterodyne Detection," in Topics in Applied Physics, vol. 19, Optical and Infrared Detectors, edited by R. J. Keyes (Springer-Verlag, New York, 1st ed.: 1977; 2nd ed.: 1980), ch. 7, pp. 229-300.

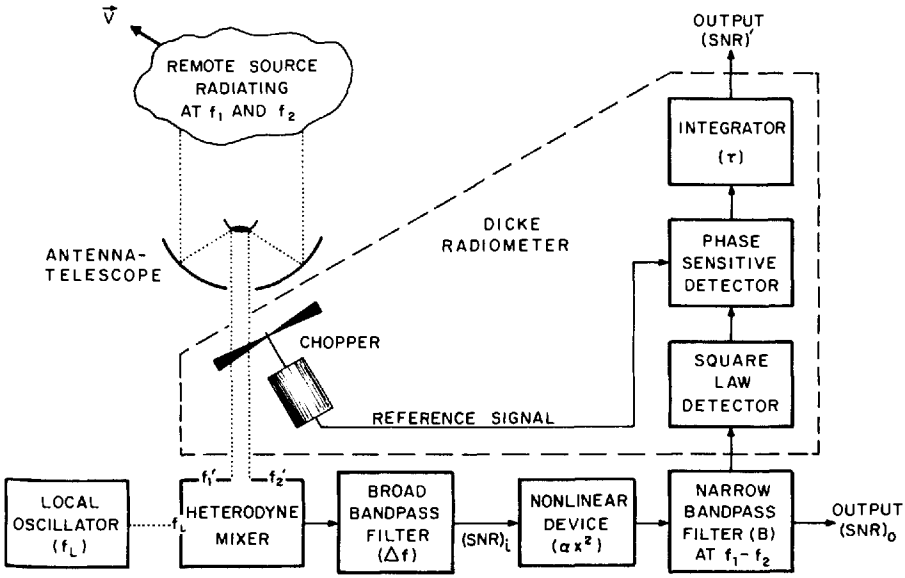

Fig. 7.24. Block diagram for the Doppler-independent three-frequency selective heterodyne radiometer. Dotted lines represent radiation signals, solid lines with arrows represent electrical signals, and dashed lines enclose a Dicke radiometer which can be added to the system if required. For clarity, amplification stages are omitted

whereas the modulation occurs at the detector in the classical radiometer (which is therefore nonspecific), the modulation frequency in the system described here is directly related to the remote species being detected. The system can, furthermore, be coupled with a classical Dicke radiometer [7.85–89] to provide improved performance where warranted. The technique will be most useful in the infrared and optical where the Doppler shifts are large; conventional heterodyne radiometry and spectroscopy have recently begun to find use at these frequencies [7.88–91]. A variation of the system, useful when the Doppler shift is known, is described at the very end of the discussion section (Sec. 7.4.5).

7.4.1 Configuration for Two Received Frequencies

The simplest example of the three-frequency system, useful in the acquisition and tracking of radar and communications signals, has been discussed in Section 7.3. In Fig. 7.24, we show a block diagram for the selective heterodyne radiometry version. The remotely radiating source emits two waves at frequencies f_1 and f_2 whose rest difference frequency $f_c \equiv |f_1 - f_2|$ is known to high accuracy. The waves experience a Doppler shift arising from the mass motion (Doppler feature) of the source. (They are also broadened due to the constituent particle velocity distribution.) Thus, a wave whose center frequency is f is detected at the receiving station with a frequency f'. Assuming that the velocity

M. C. Teich, "Nonlinear Heterodyne Detection," in Topics in Applied Physics, vol. 19, Optical and Infrared Detectors, edited by R. J. Keyes (Springer-Verlag, New York, 1st ed.: 1977; 2nd ed.: 1980), ch. 7, pp. 229-300.

of the cloud is much smaller than the speed of light c, the nonrelativistic Doppler formula provides

$$f' = f(1 \pm v_{||}/c), \tag{7.177}$$

where $v_{||}$ is the radial component of the over-all velocity vector $\boldsymbol{v}$. This expression differs from that given in (7.33) by a factor of 2 in the second term; the radiation in the passive system makes only a one-way trip. The frequency difference between the two received waves f_c' is therefore given by

$$f_c' \equiv |f_1' - f_2'| = f_c \pm (v_{||}/c) f_c \simeq f_c\ ; \tag{7.178}$$

thus, the radiated and received difference frequencies are independent of Doppler shift to good approximation when $v_{||}/c \ll 1$.

The two radiation fields f_1' and f_2' are again mixed in a heterodyne detector with a strong, coherent, and polarized LO signal (at frequency f_L) yielding two electrical beat signals at $|f_1' - f_L|$ and $|f_2' - f_L|$, along with a dc component which is blocked. The third signal at $|f_1' - f_2'|$, arising without benefit of the LO, is weak and may be neglected. The ac output of the heterodyne mixer is then broadband coupled, through a filter of bandwidth Δf, to a nonlinear device. The value chosen for Δf should be as small as possible in order to maximize the signal-to-noise ratio (SNR), but must encompass the (somewhat unknown) difference frequencies generated in the mixer. The nonlinear device, which also has a response over Δf, then generates a component at the frequency

$$f_c' = |f_1' - f_2'|\,. \tag{7.179}$$

Since the output of the nonlinear device is essentially independent of the Doppler shift as well as the LO frequencies, variations in these quantities have little effect on the system output. In many instances, therefore, the necessity for a stable and tunable LO may be eliminated. Again, the reception in this system is angle independent.

The narrowband filter centered at $f_c \simeq f_c'$, and of bandwidth B, placed after the nonlinear device, achieves the low noise bandwidth. Thus, amplifiers and other detection apparatus process electrical signals at (usually) moderate frequencies, which provides ease of matching as well as good receiver noise figure. This, in turn, decreases the LO power necessary for optimum coherent detection. Only the heterodyne mixer and the nonlinear device need have high-frequency response in many instances. For clarity, amplifiers have been eliminated from the block diagram. If warranted, the output of the narrow bandpass filter may be fed into a standard Dicke radiometer (dashed box in Fig. 7.24) consisting of a (third) detector, a phase-sensitive (synchronous) detector, and an integrator with time constant τ. (Although we specify that this detector is square-law in Fig. 7.24, its characteristic is not critical and, in fact, a linear detector will often provide the cleanest signal.) The modulation may be obtained from a chopper as indicated. This technique can sometimes provide improvement in the SNR and has been coupled with a conventional infrared

M. C. Teich, "Nonlinear Heterodyne Detection," in Topics in Applied Physics, vol. 19, Optical and Infrared Detectors, edited by R. J. Keyes (Springer-Verlag, New York, 1st ed.: 1977; 2nd ed.: 1980), ch. 7, pp. 229-300.

heterodyne radiometer in a number of instances [7.88–91]. It may also be advantageous to use a balanced mixer in this configuration [7.89].

The SNR at the output (o) of the three-frequency nonlinear heterodyne system $(\mathrm{SNR})_0$ is given by [see (7.76) and (7.107b)]

$$(\mathrm{SNR})_0 = 2k'(\mathrm{SNR})_i^2/[1+2(\mathrm{SNR})_i], \tag{7.180}$$

assuming the use of an LO which produces no excess noise (and lies between the two signal frequencies), a bandpass filter close to low-pass ($\Delta f \to f_n$), and a square-law nonlinear device for which it is easy to carry out the calculation. Here $(\mathrm{SNR})_i$ represents the SNR at the input (i) to the square-law device (see Fig. 7.24) which will generally be $\ll 1$. The factor k' appearing in (7.180) is discussed in the next section.

7.4.2 n Received Frequencies and the Factor k'

For the system involving two signal frequencies, the quantity k' has been previously shown to depend on the magnitude and on the statistical and spectral nature of the received radiation, as well as on the widths of the two bandpass filters. Inasmuch as the radiation from remote molecular species may contain multiple frequencies, we consider operation of the system in the more general case when $n(\geq 2)$ lines with equal frequency spacing are passed through the broad bandpass filter *and detected.* Again, a number of cases are of interest: sinusoidal signals (P), independent Gaussian signals with Gaussian spectra (G), and independent Gaussian signals with Lorentzian spectra (L). The Gaussian signal case is considered in detail since radiation from astronomical sources is generally Gaussian [7.92]. The effect of multiple lines is included in the parameter k' by generalizing the previously obtained expressions for k [see (7.72), (7.106), and (7.119)]. For the cases considered above, this quantity can be written as

$$k'_P \simeq \frac{f_n}{B}\left\{\frac{\sum_{j=1}^{n-1} A_j^2 A_{j+1}^2}{(\sum_{j=1}^{n} A_j^2)^2}\right\}, \tag{7.181a}$$

$$k'_G \simeq \frac{f_n}{\sqrt{8}\gamma}\left\{\frac{\sum_{j=1}^{n-1}(\gamma P_j)(\gamma P_{j+1})}{(\sum_{j=1}^{n}\gamma P_j)^2}\right\}\left[\frac{2\Phi(B/\sqrt{8}\gamma)-1}{(B/\sqrt{8}\gamma)}\right], \tag{7.181b}$$

and

$$k'_L \simeq \frac{f_n}{2\Gamma}\left\{\frac{\sum_{j=1}^{n-1} D_j D_{j+1}}{(\sum_{j=1}^{n} D_j)^2}\right\} \times \left[\frac{\pi^{-1}\tan^{-1}\{(2B/\Gamma)[4-(B^2/4\Gamma^2)]^{-1}\}}{B/2\Gamma}\right]. \tag{7.181c}$$

Here, A_j represents the amplitude of the jth line in the sinusoidal case, P_j represents the peak value of the Gaussian spectral distribution and γ is its

M. C. Teich, "Nonlinear Heterodyne Detection," in Topics in Applied Physics, vol. 19, Optical and Infrared Detectors, edited by R. J. Keyes (Springer-Verlag, New York, 1st ed.: 1977; 2nd ed.: 1980), ch. 7, pp. 229-300.

standard deviation, whereas D_j and Γ represent the height and width of the Lorentzian spectrum, respectively. The quantity Φ is the error function. It has been assumed for simplicity that all spectral widths are identical, i.e., $\gamma_j = \gamma_{j+1} = \gamma$ and $\Gamma_j = \Gamma_{j+1} = \Gamma$; similar but more complex expressions are obtained when this is not the case.

Inasmuch as the quantities in large square brackets in (7.181b) and (7.181c) above are of order unity for $B \lesssim \gamma(\Gamma)$, it is the *larger* of B and $\gamma(\Gamma)$ which limits k' and therefore the SNR in the Gaussian signal case. In particular, for the Gaussian spectrum case with $B = \sqrt{8}\gamma$, $[2\Phi(1) - 1] = 0.68$ whereas for the Lorentzian spectrum case with $B = 4(\sqrt{2} - 1)\Gamma \simeq 1.66\Gamma$, $\pi^{-1} \tan^{-1} 1 = 1/4$. Thus the SNRs for the Gaussian and Lorentzian cases are reduced below that for the sinewave case (delta-function spectrum), for the same bandwidth B. This is understood to arise from the fact that some signal is being excluded in the Gaussian and Lorentzian cases in comparison with the delta-function case, but the noise is approximately the same. For fixed $\gamma(\Gamma)$, the best SNR for the Gaussian and Lorentzian cases is obtained as $B \to 0$, since the noise decreases faster than the signal, as B decreases, in the approximation $v_{||} \to 0$. Of course, B cannot be decreased below the Doppler shift of the frequency difference $|f_c' - f_c| = (v_{||}/c) f_c$, which is unknown but can generally be estimated. For $B \gg \gamma(\Gamma)$, essentially all of the signal is included, and the results reduce to those obtained in the sinewave case. If possible, therefore, lines should be chosen for which the (Doppler) width and the Doppler shift are minimized, i.e., the lines should be narrow and closely spaced in frequency.

In the case where all such lines are of equal spacing, power, and width ($A_j = A_{j+1}$; $P_j = P_{j+1}$, $\gamma_j = \gamma_{j+1} = \gamma$; $D_j = D_{j+1}$, $\Gamma_j = \Gamma_{j+1} = \Gamma$), the braces in (7.181) can be replaced by

$$\{\cdot\}_{P,G,L} \to (n-1)/n^2, \qquad n = 2, 3, 4, \ldots . \tag{7.182}$$

For fixed input radiation power, the best operation is clearly achieved for $n = 2$ (so that $\{\cdot\}_{P,G,L} = 1/4$), since additional lines increase the (signal-by-noise contribution to the) total noise more than they do the signal. When increased radiation power becomes available by virtue of the additional lines, however (e.g., the detection of more than one Doppler feature), $n > 2$ can be advantageous.

We also consider the case in which n equal-power, equal-width lines are allowed through the broad bandpass filter, these not being equally spaced, however, so that only one pair of lines contributes to the output signal. In this case, the braces in (7.181) must be replaced by

$$\{\cdot\}_{P,G,L} \to 1/n^2, \qquad n = 2, 3, 4, \ldots . \tag{7.183}$$

Performance in this case is degraded for $n > 2$ since the additional lines contribute only to the noise.

M. C. Teich, "Nonlinear Heterodyne Detection," in Topics in Applied Physics, vol. 19, Optical and Infrared Detectors, edited by R. J. Keyes (Springer-Verlag, New York, 1st ed.: 1977; 2nd ed.: 1980), ch. 7, pp. 229-300.

Finally, we consider the case in which only two lines ($n=2$) of arbitrary width are received and detected. Recalling that ξ represents the ratio of received power in these two lines, i.e., $\xi_P = A_2^2/A_1^2$, $\xi_G = \gamma_2 P_2/\gamma_1 P_1$, and $\xi_L = D_2/D_1$, the expressions in braces in (7.181) become

$$\{\cdot\}_{P,G,L} = \xi(1+\xi)^{-2}, \tag{7.184}$$

which is again equal to 1/4 for equal-power received signals ($\xi = 1$).

7.4.3 SNR and MDP for Two Gaussian Signals

The expression for the SNR at the output of the three-frequency system $(\mathrm{SNR})_0$ for two Gaussian signals with Gaussian spectra (standard deviations γ_1 and γ_2) is obtained by using (7.180), (7.181b), (7.184), and (7.106). To good approximation, assuming $(\mathrm{SNR})_i \ll 1$, this is given by

$$(\mathrm{SNR})_0 \simeq \frac{f_n}{(\gamma_1^2+\gamma_2^2)^{1/2}} \left\{\frac{\xi_G}{(1+\xi_G)^2}\right\} \cdot \left[\frac{2\Phi\{B/[2(\gamma_1^2+\gamma_2^2)^{1/2}]\}-1}{B/[2(\gamma_1^2+\gamma_2^2)^{1/2}]}\right](\mathrm{SNR})_i^2 . \tag{7.185}$$

For quantum-noise limited detectors such as photoemitters and reverse-biased photodiodes operating in the infrared and optical [7.4–7, 10, 14, 15], assuming that the incident radiation and the coherent LO are polarized in the same plane, the input SNR to the nonlinear device is [see (7.1) and (7.42b)]

$$(\mathrm{SNR})_i = \eta P_r/h\nu\Delta f, \qquad h\nu \gg kT. \tag{7.186}$$

Here $\eta = \eta_1$ is the detector quantum efficiency. P_r is the total received signal radiation power, and kT is the thermal excitation energy (k is Boltzmann's constant and T is the detector temperature). For photovoltaic and photoconductive detectors, the input SNR is generally one-half that given in (7.186) [7.5, 14].

Heterodyne detectors in the microwave and millimeter regions ($h\nu \ll kT$) include square-law mixers such as the crystal diode detector [7.93], the InSb photoconductive detector [7.94–96], the Golay cell [7.95], the pyroelectric detector [7.95], the metal-oxide-metal diode, and the bolometer [7.87]. The latter three types of detectors have also been used successfully in the middle infrared (at 10.6 μm) [7.97–100]. For this type of detector Johnson noise generally predominates, and the input SNR is given by [7.100]

$$(\mathrm{SNR})_i = P_r/kT_{eff}\Delta f . \tag{7.187}$$

For simplicity, we have lumped a number of detector parameters and operating conditions into the receiver effective temperature T_{eff}. Of particular interest in

M. C. Teich, "Nonlinear Heterodyne Detection," in Topics in Applied Physics, vol. 19, Optical and Infrared Detectors, edited by R. J. Keyes (Springer-Verlag, New York, 1st ed.: 1977; 2nd ed.: 1980), ch. 7, pp. 229-300.

the mm and far-infrared regions are the low-noise fast Schottky-barrier diodes recently used in a number of experiments for astronomical observations [7.96, 101].

Inserting (7.186) or (7.187) into (7.185), and letting $(\mathrm{SNR})_0 = 1$, we obtain a minimum detectable total power (MDP) at the output of the three-frequency system given by

$$(\mathrm{MDP})_0 \simeq \frac{h\nu}{\eta}\left\{\frac{1+\xi_G}{\sqrt{\xi_G}}\right\} \cdot \left[\frac{B/[2(\gamma_1^2+\gamma_2^2)^{1/2}]}{2\Phi\{B/[2(\gamma_1^2+\gamma_2^2)^{1/2}]\}-1}\right]^{1/2} f_n^{1/2}(\gamma_1^2+\gamma_2^2)^{1/4} \tag{7.188a}$$

for quantum-noise limited detection, and

$$(\mathrm{MDP})_0 \simeq kT_{\mathrm{eff}}\left\{\frac{1+\xi_G}{\sqrt{\xi_G}}\right\} \cdot \left[\frac{B/[2(\gamma_1^2+\gamma_2^2)^{1/2}]}{2\Phi\{B/[2(\gamma_1^2+\gamma_2^2)^{1/2}]\}-1}\right]^{1/2} f_n^{1/2}(\gamma_1^2+\gamma_2^2)^{1/4} \tag{7.188b}$$

for Johnson-noise limited detection.

The quantities in braces and in square brackets in (7.188) are both typically of order unity. Since $f_n^{1/2}(\gamma_1^2+\gamma_2^2)^{1/4} \sim (v_{||}^{\max}/c)^{1/2}(f\gamma)^{1/2}$ for $\gamma > B$ while it is $\sim (v_{||}^{\max}/c)[f(f_1-f_2)]^{1/2}$ for $\gamma < B$, where $v_{||}^{\max}$ is the maximum expected radial velocity, the system provides increasing advantage at higher radiation frequencies f (since the effective bandwidth $\sim f^{1/2}$) for fixed γ and (f_1-f_2). Small linewidths and close spacing of the lines are also important. For certain choices of parameters, which are determined by the species which it is desired to detect, the SNR at the output of the three-frequency selective system will provide a sufficient confidence level for detection. For situations in which this is not the case, further improvement in the SNR could be obtained by using a multichannel receiver and/or a classical radiometer, as mentioned previously.

7.4.4 Numerical Example: Astronomical Radiation from CN

As an example of the use of the system in the mm region, we calculate the MDP for astronomical radiation arising from the following $N=1\rightarrow 0$, $J=3/2\rightarrow 1/2$ hyperfine transitions of the CN radical: $F=5/2\rightarrow 3/2$ ($f_1 = 113490.9 \pm 0.2$ MHz) and $F=3/2\rightarrow 1/2$ ($f_2 = 113488.1 \pm 0.3$ MHz) [7.102]. Recent radiometric observations of this radiation made use of the simple and sharply defined velocity structure of the Orion-A molecular cloud; a measurement of the $N=1\rightarrow 0$ line of $^{13}C^{16}O$ provided the Doppler effect correction due to the cloud's motion. Using Doppler-independent heterodyne radiometry, on the other hand, requires only a

M. C. Teich, "Nonlinear Heterodyne Detection," in Topics in Applied Physics, vol. 19, Optical and Infrared Detectors, edited by R. J. Keyes (Springer-Verlag, New York, 1st ed.: 1977; 2nd ed.: 1980), ch. 7, pp. 229-300.

bound on the velocity range. A radial velocity within the (substantial) range $-200\ \text{km/s} \leqq v_{\|} \leqq 200\ \text{km/s}$, for example, yields a Doppler shift uncertainty of $2|v_{\|}|f/c \simeq 151.2\ \text{MHz}$. In this case, the detected frequencies would be bounded by $113415.3\ \text{MHz} \leqq f_1' \leqq 113566.5\ \text{MHz}$ and $113412.5\ \text{MHz} \leqq f_2' \leqq 113563.7\ \text{MHz}$. Choosing f_L somewhere between the rest frequencies, e.g., at 113490.0 MHz, we obtain $|f_1' - f_L| \leqq 76.5\ \text{MHz}$ and $|f_2' - f_L| \leqq 77.5\ \text{MHz}$, inducing us to choose $\Delta f = f_n = 78\ \text{MHz}$. Depending on the actual velocity of the cloud, this might allow the beat signal of the LO with other hyperfine lines to be passed to the nonlinear device, which will not impair operation if these other lines are relatively weak. The narrowband filter is centered at the rest difference frequency $f_c = |f_1 - f_2| = 2.8\ \text{MHz}$, with a minimum width $B = 2|v_{\|}|f_c/c \simeq 1.87\ \text{kHz}$. Since $B \ll 2(\gamma_1^2 + \gamma_2^2)^{1/2}$, the MDP is essentially determined by f_n and γ (we choose $\gamma = 1.5\ \text{MHz}$ since $\gamma_1 \simeq \gamma_2 \simeq 1.5\ \text{MHz}$). Inasmuch as $\xi_G \equiv \gamma_2 P_2/\gamma_1 P_1 \simeq 1/2$ for these lines [7.102], the MDP given in (7.188b) becomes MDP $\simeq kT_{\text{eff}}\{2.12\}\,[1.11]\,(8.80 \times 10^3)(1.45 \times 10^3) \simeq kT_{\text{eff}}\delta F$, with $\delta F \simeq 30\ \text{MHz}$ representing the effective bandwidth for the calculation. Using the conventional system with this uncertainty in Doppler shift, and assuming that a one-channel receiver is used, the MDP would be $kT_{\text{eff}}\Delta f$ with $\Delta f \simeq 78\ \text{MHz}$, indicating that improvement is possible with the proposed system.

For situations in which $B > \gamma$, a multichannel receiver using a bank of narrow bandwidth filters could be used in place of the narrow bandpass filter (B), compressing the number of channels below that required in the conventional system. In the infrared and optical, an unknown Doppler shift provides a greater range of uncertainty in the received frequencies than at longer wavelengths; this system should therefore be useful in detecting atomic and molecular radiation at these higher frequencies, particularly in those wavelength regions where atmospheric windows exist. For example, strong CN optical transitions from interstellar sources were first observed in 1940 [7.103, 104]; one could attempt to definitively detect the presence of the CN $R(2)$ line, which would provide an improved estimate for the cosmic blackbody radiation at 1.32 mm [7.104]. Particular attention might also be given to possible infrared emission from CO, which exists in relatively high densities and with a very broad range of velocities in interstellar regions, as determined by its mm-wave emission [7.105, 106]. Clearly, the same considerations apply to the detection of maser radiation from astronomical sources [7.103, 107–109], and to the detection of remote pollutants [7.110, 111].

7.4.5 Discussion

We have described a selective heterodyne radiometer potentially useful in the detection of remote species such as pollutants and interstellar molecules. The system operates on the basis of the difference frequency between two radiated lines which, for closely spaced lines, is relatively insensitive to Doppler shift. This allows for the sensitive detection of known species moving at unknown velocities. The two frequencies may be obtained from individual transitions or

M. C. Teich, "Nonlinear Heterodyne Detection," in Topics in Applied Physics, vol. 19, Optical and Infrared Detectors, edited by R. J. Keyes (Springer-Verlag, New York, 1st ed.: 1977; 2nd ed.: 1980), ch. 7, pp. 229-300.

from two isotopes of the same species. The system introduces little loss over the conventional heterodyne radiometer and has a number of specific advantages. In particular, it requires knowledge only of rest difference frequencies and not of line rest frequencies which are sometimes difficult to determine [7.112], and it requires neither a stabilized nor a tunable LO. Clearly it requires little knowledge of the source velocity and consequently is generally unsuitable for spectroscopy. Changes in the source velocity or direction do not alter system detectability appreciably. This is particularly important in the infrared and optical where Doppler shifts are generally large.

The SNR and MDP at the output of the system have been obtained for a number of cases of interest including sinusoidal signals and Gaussian signals with both Gaussian and Lorentzian spectra. A configuration involving multiple ($n \geqq 2$) signal frequencies has also been considered. Other desirable operating conditions are as follows: 1) The LO frequency should be chosen to be nearly between the signal frequencies, 2) Lines with minimum broadening (low γ) and minimum frequency separation (low B) are most desirable, 3) $\Delta f(f_n)$ should be minimized by bounding the expected Doppler shift as closely as possible, and 4) The strongest pair of lines consistent with the above conditions should be chosen.

The detection of CN radiation provided an example of the use of the technique in the mm region: an indication of possible uses at higher frequencies was provided. For the submillimeter region, it may be possible to use a combination Schottky barrier diode/harmonic mixer which would provide an output at low frequencies as long as the high-frequency beat signals are generated and mixed within the detector. LO harmonics are also readily generated in these devices [7.101] so that harmonic-mixing selective heterodyne radiometry could be performed [7.113]. Josephson junctions, which can sometimes be made to produce their own LO power [7.96], and metal-oxide-metal diodes could also be used. An IMPATT solid state oscillator could conveniently be used as an LO in these regions since frequency stabilization, which is difficult to achieve in these devices [7.96], is not required. At higher frequencies, some fixed-line lasers could possibly be used since the LO frequency need not be tunable.

Disadvantages of the system include the lack of Doppler information, the difficulty of observing absorption lines and continuum radiation, and the added complexity. Use of a calibration load is also more complicated than in the conventional case. Finally, there will be an uncertainty that the detected difference-frequency signal can be properly identified, in analogy with the identification problem for the Doppler shifted signal in the conventional configuration. Thus, the system should be used for the application in which it is most effective: the search for a known emitting weak remote species with an unknown Doppler feature.

Finally, we draw attention to a variation of this scheme, called heterodyne correlation radiometry [7.114] that should be useful for the sensitive detection of radiating species whose Doppler shift is known, but whose presence we wish

M. C. Teich, "Nonlinear Heterodyne Detection," in Topics in Applied Physics, vol. 19, Optical and Infrared Detectors, edited by R. J. Keyes (Springer-Verlag, New York, 1st ed.: 1977; 2nd ed.: 1980), ch. 7, pp. 229-300.

to affirm. Such radiation (which may be actively induced) can arise, for example, from remote molecular emitters, impurities and pollutants, trace minerals, chemical agents, or a general multiline source. A radiating sample of the species to be detected is physically made a part of the laboratory receiver, and serves as a kind of frequency-domain template with which the remote radiation is correlated, after heterodyne detection. This system is expected to be especially useful for the detection of sources whose radiated energy is distributed over a large number of lines, with frequencies that are not necessarily known. Neither a stable nor a tunable local oscillator is required. The minimum detectable power is expressible in a form similar to that for conventional heterodyning (for both quantum-noise-limited and Johnson-noise-limited detectors). The notable distinction is that the performance of the proposed system improves with increasing number of remotely radiating signal lines and increasing locally produced radiation power. Performance degradation due to undesired impurity radiation is not a problem in general.

Acknowledgement. I am grateful to the John Simon Guggenheim Memorial Foundation and to the National Science Foundation for generous financial support. I am also indebted to Rainfield Y. Yen for permitting me to present many of the calculations (in Sec. 7.3) that he carried out as a part of his Ph.D. thesis, and which we later published jointly.

References

7.1 A.T. Forrester, R.A. Gudmundsen, P.O. Johnson: Phys. Rev. **99**, 1691 (1955)
7.2 A. Javan, E.A. Ballik, W.L. Bond: J. Opt. Soc. Am. **52**, 96 (1962)
7.3 B.J. McMurtry, A.E. Siegman: Appl. Opt. **1**, 51 (1962)
A.E. Siegman, S.E. Harris, B.J. McMurtry: Optical heterodyning and optical demodulation at microwave frequencies. In: *Optical Masers*, ed. by J. Fox (Wiley-Interscience, New York 1963) pp. 511–527
7.4 M.C. Teich, R.J. Keyes, R.H. Kingston: Appl. Phys. Lett. **9**, 357 (1966)
7.5 M.C. Teich: Proc. IEEE **56**, 37 (1968) [Reprinted in *Infrared Detectors*, ed. by R.D. Hudson, Jr., J.W. Hudson (Dowden, Hutchinson and Ross, Stroudsburg 1975)]
7.6 B.M. Oliver: Proc. IRE **49**, 1960 (1961)
H.A. Haus, C.H. Townes, B.M. Oliver: Proc. IRE **50**, 1544 (1962)
7.7 A.E. Siegman: Proc. IEEE **54**, 1350 (1966)
7.8 W.S. Read, D.L. Fried: Proc. IEEE **51**, 1787 (1963)
7.8a M.M. Abbas, M.J. Mumma, T. Kostiuk, D. Buhl: Appl. Opt. **15**, 427 (1976)
7.8b E. Jakeman, C.J. Oliver, E.R. Pike: Advances in Phys. **24**, 349 (1975)
7.9 M.C. Teich: Proc. IEEE **57**, 786 (1969)
7.10 M.C. Teich, R.Y. Yen: J. Appl. Phys. **43**, 2480 (1972)
7.11 U.M. Titulaer, R.J. Glauber: Phys. Rev. **140**, B676 (1965); Phys. Rev. **145**, 1041 (1966)
7.12 M.C. Teich: Appl. Phys. Lett. **14**, 201 (1969)
7.13 M.C. Teich: Quantum theory of heterodyne detection. In: *Proc. Third Photoconductivity Conf.*, ed. by E.M. Pell (Pergamon, New York 1971) pp. 1–5
7.14 M.C. Teich: Coherent detection in the infrared. In: *Semiconductors and Semimetals*, ed. by R.K. Willardson and A.C. Beer (Academic, New York 1970) **5**, *Infrared Detectors*, Chap. 9, pp. 361–407
7.15 L. Mandel, E. Wolf: J. Opt. Soc. Am. **65**, 413 (1975)
7.15a G. Lachs: Phys. Rev. **138**, B 1012 (1965)
7.15b J. Peřina: Phys. Lett. **24A**, 333 (1967)

M. C. Teich, "Nonlinear Heterodyne Detection," in Topics in Applied Physics, vol. 19, Optical and Infrared Detectors, edited by R. J. Keyes (Springer-Verlag, New York, 1st ed.: 1977; 2nd ed.: 1980), ch. 7, pp. 229-300.

7.15c J. Peřina, R. Horak: J. Phys. A **2**, 702 (1969)
7.15d E. Jakeman, E. R. Pike: J. Phys. A **2**, 115 (1969)
7.15e J. Peřina, V. Peřinová, L. Mišta: Opt. Acta **19**, 579 (1972)
7.15f M. C. Teich, W. J. McGill: Phys. Rev. Lett. **36**, 754 (1976)
7.16 M. C. Teich: IEEE J. Quant. Electron. **QE-11**, 595 (1975)
7.17 A. Einstein: Ann. Physik **17**, 132 (1905) [translation: Am. J. Physics **33**, 367 (1965)]
7.18 L. Mandel: Proc. Phys. Soc. (London) **74**, 233 (1959); see also
E. M. Purcell: Nature **178**, 1449 (1956)
L. Mandel: Proc. Phys. Soc. (London) **72**, 1037 (1958)
7.19 R. J. Glauber: Phys. Rev. **130**, 2529 (1963); Phys. Rev. **131**, 2766 (1963)
7.20 P. L. Kelley, W. H. Kleiner: Phys. Rev. **136**, A 316 (1964)
7.21 M. C. Teich, G. J. Wolga: J. Opt. Soc. Am. **57**, 542 (1967)
7.22 M. C. Teich, J. M. Schroeer, G. J. Wolga: Phys. Rev. Lett. **13**, 611 (1964)
7.23 H. Sonnenberg, H. Heffner, W. Spicer: Appl. Phys. Lett. **5**, 95 (1964)
7.24 M. C. Teich: Two quantum photoemission and dc photomixing in sodium, Ph.D. thesis (Cornell University 1966) unpublished [also Report no. 453, Materials Science Center, Cornell University, Ithaca, New York, February 1966]
7.25 M. C. Teich, G. J. Wolga: Phys. Rev. **171**, 809 (1968)
7.26 F. Shiga, S. Imamura: Phys. Lett. **25A**, 706 (1967)
7.27 E. M. Logothetis, P. L. Hartman: Phys. Rev. Lett. **18**, 581 (1967)
7.28 E. M. Logothetis, P. L. Hartman: Phys. Rev. **187**, 460 (1969)
7.29 R. E. B. Makinson, M. J. Buckingham: Proc. Phys. Soc. A (London) **64**, 135 (1951)
7.30 R. L. Smith: Phys. Rev. **128**, 2225 (1962)
7.31 H. C. Bowers: Theoretical and experimental considerations of the double-quantum photoelectric effect, M.S. thesis (Cornell University 1964) unpublished
7.32 I. Adawi: Phys. Rev. **134**, A 788 (1964)
7.33 P. Bloch: J. Appl. Phys. **35**, 2052 (1964)
7.34 M. C. Teich, G. J. Wolga: Phys. Rev. Lett. **16**, 625 (1966)
7.35 P. Lambropoulos, C. Kikuchi, R. K. Osborn: Phys. Rev. **144**, 1081 (1966)
7.36 B. R. Mollow: Phys. Rev. **175**, 1555 (1968)
7.37 G. S. Agarwal: Phys. Rev. A **1**, 1445 (1970)
7.38 M. C. Teich, R. L. Abrams, W. B. Gandrud: Opt. Communic. **2**, 206 (1970)
7.39 P. Diament, M. C. Teich: J. Opt. Soc. Am. **59**, 661 (1969)
7.40 C. Freed, H. A. Haus: Phys. Rev. **141**, 287 (1966)
G. Lachs: J. Appl. Phys. **39**, 4193 (1968)
7.41 M. C. Teich, P. Diament: J. Appl. Phys. **40**, 625 (1969)
7.42 P. P. Barashev: Zh. Eksper. i Teor. Fiz. (USSR) **59**, 1318 (1970) [translation: Soviet Phys. JETP **32**, 720 (1971)]
7.43 P. P. Barashev: Phys. Stat. Sol. (a) **9**, 9 (Part I) and 387 (Part II) (1972)
7.44 L. Mandel: J. Opt. Soc. Am. **57**, 613 (1967)
L. Mandel, E. Wolf: Rev. Mod. Phys. **37**, 231 (1965)
7.44a M. J. Beran, J. DeVelis, G. Parrent: Phys. Rev. **154**, 1224 (1967)
7.45 M. C. Teich, D. A. Berkley, G. J. Wolga: Rev. Sci. Instr. **36**, 973 (1965)
7.46 R. A. Fox, R. M. Kogan, E. J. Robinson: Phys. Rev. Lett. **26**, 1416 (1971)
S. Klarsfeld, A. Maquet: Phys. Rev. Lett. **29**, 79 (1972)
7.47 S. J. Ippolito, S. Rosenberg, M. C. Teich: Rev. Sci. Instr. **41**, 331 (1970)
7.48 M. C. Teich: Appl. Phys. Lett. **15**, 420 (1969); U.S. Patent Number 3, 875, 399
7.49 R. L. Abrams, R. C. White, Jr.: IEEE J. Quantum Electron. **QE-8**, 13 (1972)
7.50 M. C. Teich, R. Y. Yen: Appl. Opt. **14**, 666 (1975)
7.51 M. C. Teich, R. Y. Yen: Appl. Opt. **14**, 680 (1975)
7.52 M. C. Teich: Rev. Sci. Instr. **46**, 1313 (1975)
7.53 W. B. Davenport, Jr., W. L. Root: *An Introduction to the Theory of Random Signals and Noise* (McGraw-Hill, New York 1958) p. 112

M. C. Teich, "Nonlinear Heterodyne Detection," in Topics in Applied Physics, vol. 19, Optical and Infrared Detectors, edited by R. J. Keyes (Springer-Verlag, New York, 1st ed.: 1977; 2nd ed.: 1980), ch. 7, pp. 229-300.

7.54 D.J. Angelakos, T.E. Everhart: *Microwave Communications* (McGraw-Hill, New York 1968) p. 204
7.55 Ref. [7.53], pp. 257–259
7.56 Ref. [7.53], p. 255
7.57 M.I. Skolnik: *Introduction to Radar Systems* (McGraw-Hill, New York 1958) p. 185
7.58 W.E. Murray, Jr.: Coherent laser radar Doppler signatures. In: *Optics Research* (MIT Lincoln Lab. 1969) No. 1, p. 6
7.59 R.Y. Yen: Optical communications: An investigation of several techniques, Ph.D. thesis (Columbia University 1972) unpublished
7.60 Ref. [7.53], p. 308
7.61 H.A. Bostick: IEEE. J. Quantum Electron. **QE-3**, 232 (1967)
7.62 H.A. Bostik, L.J. Sullivan: Laser radar and tracking. In: *Optics Research* (MIT Lincoln Lab. 1969) No. 1, p. 21
7.63 Ref. [7.53], p. 193
7.64 Ref. [7.53], p. 356
7.65 R.G. Gallager: *Information Theory and Reliable Communication* (Wiley, New York 1968) p. 365
7.66 R.J. Schwarz, B. Friedland: *Linear Systems* (McGraw-Hill, New York 1965) p. 299
7.67 Ref. [7.53], pp. 93–101
7.68 M. Kac, A.J.F. Siegert: J. Appl. Phys. **18**, 383 (1947)
7.69 R.C. Emerson: J. Appl. Phys. **24**, 1168 (1953)
7.70 V. Voorhis: *Microwave Receivers* (McGraw-Hill, New York 1948) p. 157
7.71 S.O. Rice: Mathematical Analysis of Random Noise. In: *Selected Papers on Noise and Stochastic Processes*, ed. by N. Wax (Dover, New York 1954) pp. 133–294
7.72 S. Stein, J.J. Jones: *Modern Communication Principles* (McGraw-Hill, New York 1967) pp. 138–139
7.73 W.K. Pratt: *Laser Communication Systems* (Wiley, New York 1969) pp. 224–229
7.74 Ref. [7.53], pp. 352–355
7.75 D.L. Fried, G.E. Mevers: J. Opt. Soc. Am. **55**, 740–741 (1965)
7.76 M.C. Teich, S. Rosenberg: Appl. Opt. **12**, 2616 (1973)
7.77 S. Rosenberg, M.C. Teich: Appl. Opt. **12**, 2625 (1973)
7.78 S. Rosenberg, M.C. Teich: IEEE Trans. Inform. Theory **IT-19**, 807 (1973)
7.79 Ref. [7.72], pp. 286–309
7.80 V.I. Tatarski: *Wave Propogation in a Turbulent Medium* (McGraw-Hill, New York 1961)
7.81 P. Diament, M.C. Teich: J. Opt. Soc. Am. **60**, 1489 (1970)
J. Peřina, V. Peřinová, M.C. Teich, P. Diament: Phys. Rev. **A7**, 1732 (1973)
7.82 R.S. Lawrence, J.W. Strohbehn: Proc. IEEE **58**, 1523 (1970)
7.83 D.L. Fried: Appl. Opt. **10**, 721 (1971)
7.84 Ref. [7.53], p. 167
7.85 R.H. Dicke: Rev. Sci. Instr. **17**, 268 (1946)
7.86 J.D. Kraus: *Radio Astronomy* (McGraw-Hill, New York 1966)
7.87 T.G. Phillips, K.B. Jefferts: IEEE Trans. Microwave Theory Tech. **MTT-22**, 1290 (1974)
7.88 J. Gay, A. Journet, B. Christophe, M. Robert: Appl. Phys. Lett. **22**, 448 (1973)
7.89 H. van de Stadt: Astron. Astrophys. **36**, 341 (1974)
7.90 T. de Graauw, H. van de Stadt: Nature (Phys. Sci.) **246**, 73 (1973)
7.91 D.W. Peterson, M.A. Johnson, A.L. Betz: Nature (Phys. Sci.) **250**, 128 (1974)
7.92 N.J. Evans II, R.E. Hills, O.E.H. Rybeck, E. Kollberg: Phys. Rev. **A6**, 1643 (1972)
7.93 C.H. Townes, A.L. Schawlow: *Microwave Spectroscopy* (McGraw-Hill, New York 1955)
7.94 E.H. Putley: Proc. IEEE **54**, 1096 (1966)
7.95 H.A. Gebbie, N.W.B. Stone, E.H. Putley, N. Shaw: Nature (Phys. Sci.) **214**, 165 (1967)
7.96 A.A. Penzias, C.A. Burrus: Ann. Rev. Astronomy Astrophys. **11**, 51 (1973)
7.97 R.L. Abrams, A.M. Glass: Appl. Phys. Lett. **15**, 251 (1969)
7.98 E. Leiba: Compt. Rend. (Paris) **268**, B 31 (1969)
7.99 R.L. Abrams, W.B. Gandrud: Appl. Phys. Lett. **17**, 150 (1970)
7.100 B. Contreras, O.L. Gaddy: Appl. Phys. Lett. **18**, 277 (1971)

M. C. Teich, "Nonlinear Heterodyne Detection," in Topics in Applied Physics, vol. 19, Optical and Infrared Detectors, edited by R. J. Keyes (Springer-Verlag, New York, 1st ed.: 1977; 2nd ed.: 1980), ch. 7, pp. 229-300.

7.101 H.R.Fetterman, B.J.Clifton, P.E.Tannenwald, C.D.Parker, H.Penfield: IEEE Trans. Microwave Theory Tech. **MTT-22**, 1013 (1974)
K. Mizuno, R. Kuwahara, S. Ono: Appl. Phys. Lett. **26**, 605 (1975)
7.102 A.A.Penzias, R.W.Wilson, K.B.Jefferts: Phys. Rev. Lett. **32**, 701 (1974)
7.103 D.M.Rank, C.H.Townes, W.J.Welch: Science **174**, 1083 (1971)
7.104 P.Thaddeus: Ann. Rev. Astronomy Astrophys. **10**, 305 (1972)
7.105 R.W.Wilson, K.B.Jefferts, A.A.Penzias: Astrophys. J. Lett. **161**, L43 (1970)
7.106 P.M.Solomon: Phys. Today **26**, # 3, 32 (1973)
7.107 M.M.Litvak: Ann. Rev. Astronomy Astrophys. **12**, 97 (1974)
7.108 L.E.Snyder, D.Buhl: Astrophys. J. Lett. **189**, L31 (1974)
7.109 L.E.Snyder: IEEE Trans. Microwave Theory Tech. **MTT-22**, 1299 (1974)
7.110 E.D.Hinkley, P.L.Kelley: Science **171**, 635 (1971)
7.111 R.Menzies: Appl. Phys. Lett. **22**, 592 (1973)
7.112 B.Zuckerman, P.Palmer: Ann. Rev. Astronomy Astrophys. **12**, 279 (1974)
7.113 P.F.Goldsmith, R.L.Plambeck, R.Y.Chiao: IEEE Trans. Microwave Theory Tech. **MTT-22**, 1115 (1974)
7.114 M.C.Teich: Proc. Society Photo-Optical Instrumentation Engineers **82**, 132 (1976)

M. C. Teich, "Nonlinear Heterodyne Detection," in Topics in Applied Physics, vol. 19, Optical and Infrared Detectors, edited by R. J. Keyes (Springer-Verlag, New York, 1st ed.: 1977; 2nd ed.: 1980), ch. 7, pp. 229-300.